BETA-LACTAMASE BINDING TO BLIP AND BLIP BASED PEPTIDES

by

Aslıgül Doğan

B.S., Chemical Engineering, Boğaziçi University, 2008

Submitted to the Institute for Graduate Studies in
Science and Engineering in partial fulfillment of
the requirements for the degree of
Master of Science

Graduate Program in Chemical Engineering

Boğaziçi University

2011

ACKNOWLEDGEMENTS

I would like to express my gratitude to my thesis supervisor and co-supervisor, Assist. Prof. Elif Özkırımlı Ölmez and Assoc. Prof. Berna Sarıyar Akbulut, for their invaluable guidance and support during my study.

I would like to thank my thesis committee members Assist. Prof. Demet Akten, Prof. Kutlu Ülgen and Assist. Prof. Nevra Özer for reading my thesis and for their comments on my thesis.

I am grateful to thank, Pınar Kanlıkılıçer and Ahmet Özcan for their helps, suggestions and friendship. I am very grateful to all my friends, especially Kadriye Simay Yalaz, İhsan Ömür Akdağ, Yasemen Güngörmez, Burcu Özkaral, Celal Ceylan for their support and friendship. My sincere thanks to my lab-partners; Deniz Menekşedağ, Begüm Alaybeyoğlu and Seval Aladağ for sharing all the good and bad times. I would like to thank my friends Bahar, Selcen, İpek, Merve, Ünal, Çağlar, Duygu, Şefik, Tarık, Özer, Murat, Nilay, Vasfiye, Ali, Burcu, Okan, Aybüke, Caner, Gülsüm and İrfan. Finally, the biggest thanks to my mother Ayşegül Doğan, my father Atlıhan Doğan and my brother Murat Doğan for their ever-lasting encouragement and support. This thesis is dedicated to them.

TUBITAK Project No. 108M644, Project No. 109M229 and BAP Project No. 09HA504P are gratefully acknowledged for the funding.

ABSTRACT

BETA-LACTAMASE BINDING TO BLIP AND BLIP BASED PEPTIDES

Extensive use of antimicrobial agents has generated selective pressure on bacteria and resulted in development of resistance to beta-lactam antibiotics. The main resistance mechanism in bacteria is the production of beta-lactamase enzymes that can hydrolyze the beta-lactam ring and render the antibiotic inactive before it reaches the target. It is important to find an inhibitor to disable the beta-lactamase enzyme in order to benefit from beta-lactam antibiotics. BLIP is an effective beta-lactamase inhibitor but it exhibits different binding affinities to TEM-1 and SHV-1 beta-lactamases despite their 68 % sequence identity. Molecular Dynamics (MD) simulations were performed in order to investigate the features that lead to the difference in binding affinity of BLIP to these two beta-lactamases. It was found that H10 helix (residues 218 to 230) and omega loop (residues 161 to 179) and especially residue 175, which is aspargine in TEM-1 and glycine in SHV-1, respond differently to BLIP binding in TEM-1 and SHV-1. The relevance of the H10 helix to the difference in binding affinity was further investigated by performing MD simulations on the TEM-1 W229A mutant in the apo and BLIP bound forms. In the second part of the work, peptides based on the BLIP loop (residues 45-52), that inserts into the beta-lactamase active site were used in MD simulations to investigate their binding potential and to study their interaction mechanism. Peptides were designed with different residue mutations. Peptide that was based on 45 to 53 residues of BLIP and that has the G48F mutation is the one that exhibits tightest binding among the designed BLIP based peptides. This peptide can be used as a template for future studies to design new peptides with different residue mutations to enhance the binding affinity.

ÖZET

BETA-LAKTAMAZIN BLIP'E VE BLIP BAZLI PEPTİTE BAĞLANMASI

Antimikrobiyel ajanların yaygın kullanımı bakterilerin mevcut beta-lactam antibiyotiklerine direnç kazanmalarına neden olmuştur. Bakterilerin başlıca direnç mekanizması, beta-laktamaz enziminlerini sentezlemeleri ve sentezlenen enzimlerin beta-laktam halkalarını hidrolize ederek antibiyotiği hedefine ulaşamadan etkisiz hale getirmesidir. Bakterilerle mucadelede antibiyotiklerden etkin olarak yararlanabilmek için beta-laktamaz enzimini etkisiz hale getirecek inhibitör tasarımı büyük önem taşımaktadır. BLIP etkili bir beta-laktamaz inhibitörüdür ancak amino asit dizilimleri açısından % 68 benzerliğe sahip TEM-1 ve SHV-1 beta-laktamazlarına BLIP farklı ilgiler ile bağlanır. BLIP'in bu iki beta-laktamaza karşı farklı bağlanma ilgisine neden olan özellikler, Moleküler Dinamik (MD) simülasyonları ile incelenmiştir. BLIP'e bağlanmada TEM-1 and SHV-1 beta-laktamazlarındaki H10 sarmalı (218'den 230'a olan kalıntılar) ve omega döngüsü (161'den 179'a olan kalıntılar) ile özellikle de TEM-1'de glisin ve SHV-1'de asparajin olan 175. kalıntı farklılık göstermektedir. H10 sarmalının bağlanma ilgisine olan etkisi TEM-1 W229A mutantının apo ve BLIP'e bağlı formları ile yapılan MD simülasyonları ile incelenmiştir. Çalışmanın ikinci kısmında, beta-laktamazın aktif bölgesine bağlanan BLIP'in 45-52 kalıntıları arasındaki dizi temel alınarak tasarlanan peptitlerin MD simülasyonları ile TEM-1 beta-laktamazına bağlanma ve bu enzimi inhibisyon potansiyelleri araştırılmıştır. Farklı peptitler değişik kalıntılara yapılan mütasyonlar ile tasarlanmıştır. BLIP temelli peptitler arasında, G48F mütasyonunu içerecek şekilde BLIP'in 45 ile 53. kalıntıları arasındaki dizi temel alınarak tasarlanan peptidin BLIP ile en kuvvetli bağlanan peptit olduğu bulunmuştur. Bu peptit bağlanma ilgisini arttırmaya yönelik yapılacak çalışmalarda değişik mutasyonlar içeren yeni peptitlerin tasarlanması için bir temel oluşturacaktır.

TABLE OF CONTENTS

LIST OF FIGURES

LIST OF TABLES

LIST OF SYMBOLS

C_α	alpha carbon atom
E_{MM}	Molecular mechanical energy
G_{PB}	Polar salvation energy
G_{np}	Nonpolar salvation energy
k_i^{angle}	angle force constant
k_i^{bond}	bond force constant
k_i^{dihe}	dihedral force constant
q_i	charge of particle
r_{0i}	bond length with minimum energy
r_i	bond length
Å	Angstrom
γ_i	phase shift
ΔG_{bind}	Binding free energy
ε_0	permittivity of free space
ε_{ij}	wall depth
θ_{0i}	bend angle with minimum energy
θ_i	bend angle
σ_{ij}	diameter
$\emptyset_i$	dihedral angle

LIST OF ACRONYMS / ABBREVIATIONS

A	Alanine
Ala	Alanine
Arg	Arginine
Asn	Aspargine
Asp	Aspartic Acid
BLIP	Beta-lactamase Inhibitory Protein
D	Aspartic Acid
E	Glutamic Acid
F	Phenylalanine
G	Glycine
Glu	Glutamic Acid
Gly	Glycine
I	Isoleucine
K	Lysine
L	Leucine
Lys	Lysine
MD	Molecular Dynamics
MMPBSA	Molecular Mechanics Poisson Boltzmann Surface Area
MSF	Mean Square Fluctuation
N	Asparagine
NMR	Nuclear Magnetic Resonance
PDB	Protein Data Bank
Phe	Phenylalanine
Pro	Proline
Q	Glutamine
RMSD	Root Mean Square Deviation
RMSF	Root Mean Square Fluctuation
S	Entropy
Ser	Serine

SPR	Surface Plasmon Resonance
T	Temperature
Trp	Tryptophan
Tyr	Tyrosine
V	potential energy
W	Tryptophan
Y	Tyrosine

1. INTRODUCTION

1.1. Role of Beta-Lactamases in Antibiotic Resistance

All beta-lactam antibiotics are bactericidal agents that inhibit cell wall synthesis of gram-negative bacteria. Penicillins, cephalosporins and carbapenems are among the most frequently used beta-lactam antibiotics. The bacterial cell wall is a complex structure composed of peptidoglycan layers. Peptides in adjacent gylcan strands are cross-linked providing the characteristic net structure of the peptidoglycan in order to maintain cell shape and enable them to withstand large changes in osmotic pressure. Bacterial transpeptidases (detected as penicillin binding proteins, PBPs) are essential enzymes that catalyze this cross-linking step (Buynak, 2007, Ghuysen *et al.*, 1996).

Extensive use of antimicrobial agents has generated selective pressure on bacteria and resulted in development of resistance to beta-lactam antibiotics (Petrosino *et al.*, 1998). Bacteria have three major strategies to avoid the activity of beta-lactam antibiotics: a) alteration of the target site to exhibit low affinity for beta-lactam antibiotics, b) reduction of drug permeation across the bacterial membrane. Lack or diminished expression of outer membrane proteins (OMPs) restricts the entry of beta-lactams into the periplasmic space of gram-negative bacteria, c) production of beta-lactamase enzymes that hydrolyze the beta-lactam ring and render the antibiotic inactive before it reaches the target (Babic *et al.*, 2006, Majiduddin *et al.*, 2002). The last one is the most important resistance mechanism in gram negative bacteria (Bush *et al.*, 1995, Strynadka *et al.*, 1996).

Beta-lactamases are divided into four classes and categorized based on similarity in amino acid sequence and catalytic mechanism. Beta-lactamases contain either a serine residue or a metal ion in their active site to attack and break the amide bond in the beta-lactam ring in order to render the antibiotic inactive. Classes A, C and D use an active-site serine in their mechanism of action, whereas class B beta-lactamases use one of two zinc (Zn^{2+}) atoms for inactivation mechanism (Ambler, 1980).

Class A beta-lactamases known as penicillinases are the major cause of beta-lactam antibiotic resistance. The general inactivation mechanism of class A beta-lactamases involves nucleophilic attack by either Lys73 or Glu166 activated Ser70 on the carbonyl carbon of the beta-lactam ring resulting in the formation of acyl-enzyme intermediate and then hydrolysis (deacylation) of beta-lactam antibiotic (Brasseur *et al.*, 1999, Chen *et al.*, 1996).

TEM-1 and SHV-1 enzymes, belonging to class A beta-lactamases, are the most common plasmid-mediated β-lactamases identified in the 1970s and early 1980s (Matthew *et al.*, 1979, Roy *et al.*, 1983) and ususally found in *E. coli* and *K. pneumoniae* respectively that have resistance to penicillins (ampicillin and piperacillin) (Bush *et al.*, 1995).

TEM-1 beta-lactamase has clinical importance because of its significant contribution to resistance against the beta-lactam antibiotics and became a serious threat (Huang *et al.*, 1996, Wiedemann *et al.*, 1989). This enzyme is able to efficiently hydrolyze most of penicillins and cephalosporins. SHV-1 beta-lactamase exhibits a substrate profile similar to that of TEM-1 (Lee *et al.*, 1991).

In order to overcome the drug resistance arising from TEM-1 and SHV-1, extended spectrum cephalosporins such as cefotaxime and ceftazidime were developed that TEM-1 and SHV-1 are unable to hydrolyze. In addition to developing new drugs, co-administration of a beta-lactamase inhibitor such as sulbactam or clavulanic acid with an existing beta-lactam antibiotic is an effective way in clinical treatment (Parker and Eggleston, 1987). However, both of these methods cause specific mutations in beta-lactamases that either enable them to hydrolyze the extended-spectrum cephalosporins (Medeiros and Crellin, 1997) or allow them to avoid inactivation by the inhibitors (Saves *et al.*, 1995). The emergence of resistance to new antibiotics and beta-lactamase inhibitors is a rising problem and to achieve this problem, new antibiotics and inhibitors must be designed according to evolution of bacterial resistance.

In 1990, the beta-lactamase inhibitor protein (BLIP) was purified from the soil bacterium *S. clavuligerus* (Doran *et al.*, 1990) that also produces beta-lactam antibiotics such as cephamycins as well as a beta-lactamase inhibitor, clavulanic acid (Jensen *et al.*,

1986). BLIP inhibits class A beta-lactamases with a wide range of affinities (Strynadka *et al.*, 1996).

1.2. Structure of TEM-1 and SHV-1 Beta-Lactamases

TEM-1 is a 263-amino-acid protein that is composed of a single polypeptide chain folded into two domains. The first is α/β domain consists of a five stranded β-sheet and three α-helices, the second consists of eight α-helices. The active site is located at the domain interface and comprises residues; Ser70 (the catalytic serine), Lys73, Ser130, Glu166, Asn170 and Lys234 (Fisette *et al.*, 2010, Jelsch *et al.*, 1993). Immediately adjacent to the active site cavity there is a protruding loop-helix region (residues 99 to 112) that has largely negative electrostatic potential in TEM-1 (Strynadka *et al.*, 1996). The omega loop borders the active site and consists of residues 161 to 179 (Fisette *et al.*, 2010). The omega loop is a conserved structural element in all class A beta-lactamases and it is involved in substrate recognition and catalytic function on positioning the catalytic Glu 166. Its conformation is stabilized by a highly conserved salt bridge formed between Arg 164 and Asp 179 (Jelsch *et al.*, 1993, Kuzin *et al.*, 1999).

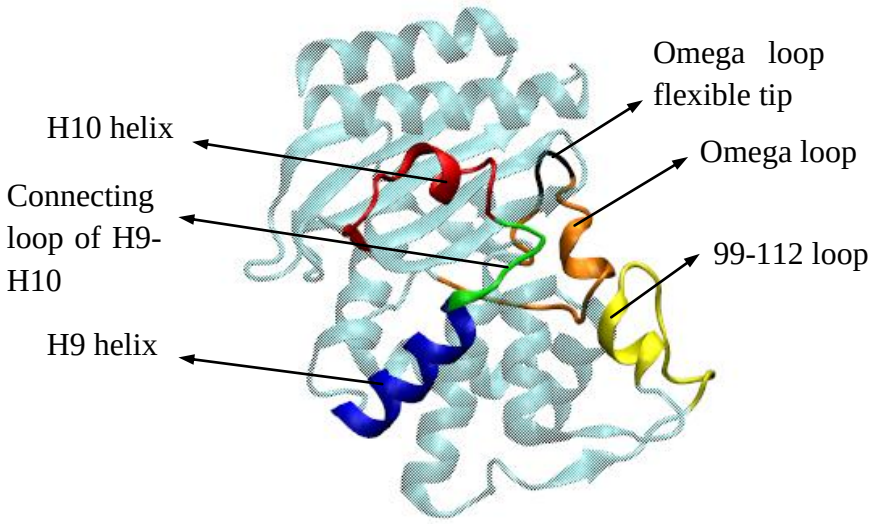

Figure 1.1. Cartoon representation of TEM-1.

Figure 1.1 shows cartoon representation of TEM-1 beta-lactamase as well as its important regions. Orange region represents omega loop (residues 161 to 179) and the black region on omega loop indicates its flexible tip (residues 174 to 176). Yellow region highlights 99-112 loop of beta-lactamase with which the concave beta-sheet region of BLIP interacts. H9 and H10 helices are other important regions of beta-lactamase. Red region highlights H10 helix (residues 218 to 230) and blue region shows H9 helix (residues 201 to 212). These two helixes are connected with a loop (green) and form H9-H10 helix region of beta-lactamase.

SHV-1 beta lactamase is 68% identical with TEM-1 in amino acid sequence and their three dimensional structures are virtually superimposable (Jelsch *et al.*, 1993) with the C_{α} atom overlay within a root mean square deviation of 1.4 Å (Kuzin *et al.*, 1999). Figure 1.2 shows the two superimposed beta-lactamases.

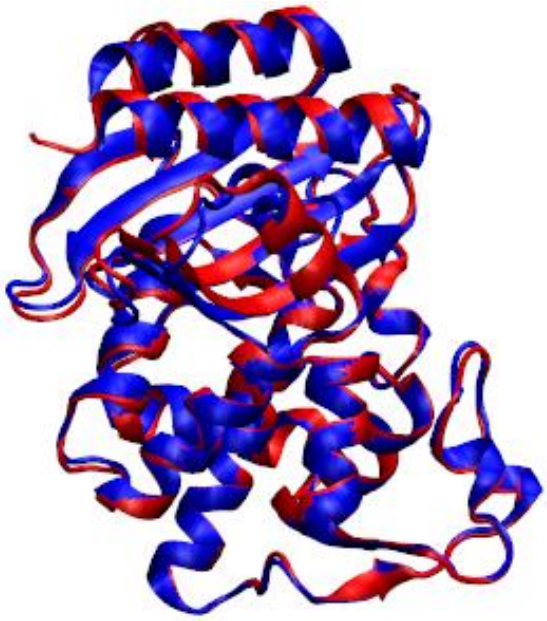

Figure 1.2. Structure of virtually superimposable TEM-1 (blue) and SHV-1 (red).

1.3. Structure of Beta-Lactamase Inhibitory Protein (BLIP) and Its Inhibition Mechanism

BLIP is a 165-amino-acid protein that is an effective inhibitor of TEM-1 beta-lactamase and also able to bind and inhibit other class A beta-lactamases (Petrosino *et al.*,

1999). BLIP composed of a tandem repeat of a 76-amino-acid domain. Each domain consists of a helix-loop-helix motif that packs against four anti-parallel beta-strands. The two domains form a concave surface that is mainly lined with polar, uncharged residues such as serine and tyrosine, also three tryptophan and two phenylalanine residues that contribute to two hydrophobic patches on the concave surface (Strynadka *et al.*, 1996).

The concave beta-sheet region of BLIP sits on top of the negatively charged protruding loop-helix region (99-112) of TEM-1 and SHV-1. In addition, two loops from BLIP inserts into the active site region of beta-lactamase to block substrate binding. Asp49 from the first loop of BLIP aligns itself in the active site and forms four strong hydrogen bonds with four catalytic residues (Ser130, Lys234, Ser235, Arg244). The position of aspartic acid carboxylate mimics that of the carboxylate in the penicillin G. Phe142 side chain from the second loop of BLIP mimics the benzyl group of the beta-lactam antibiotic penicillin G (Strynadka *et al.*, 1996) and further stabilizes the inhibitory complex (Petrosino *et al.*, 1998). Thus, residues Asp49 and Phe142 together form an approximate mimic of the beta-lactamase substrate penicillin G (Strynadka *et al.*, 1996).

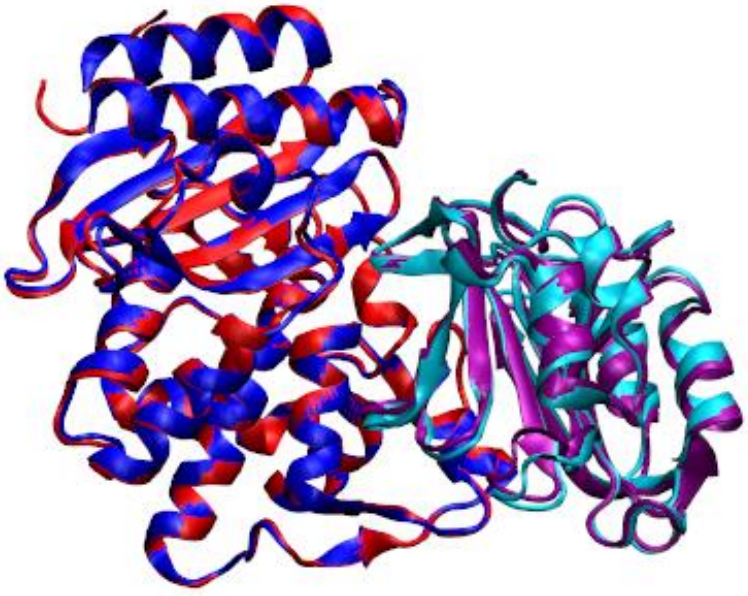

Figure 1.3. TEM-1(blue) BLIP (purple) and SHV-1 (red) BLIP (cyan).

BLIP has affinity to a variety of class A beta-lactamases ranging from micromolar to picomolar. Despite the structural similarity between TEM-1 and SHV-1 beta-lactamases,

BLIP inhibits TEM-1 with nonomolar affinity while it inhibits SHV-1 with only micromolar affinity (Kuzin *et al.,* 1999, Zhang and Palzkill, 2004).

From the Figure 1.3, TEM-1 (blue) in complex with BLIP (purple) and SHV-1 (red) in complex with BLIP (cyan) can be seen. The complex structures were superimposed based on C_α atoms of beta-lactamases.

1.4. BLIP Based Peptides

The three dimensional structures of BLIP and BLIP complex with TEM-1 beta-lactamase indicates that the major interactions in the active site of TEM-1 are from the β-hairpin loop of domain 1 of BLIP, comprising residues 46 to 51 (Rudgers *et al.*, 2001, Strynadka *et al.,* 1996). Asp49 of BLIP is a crucial residue located on the loop that inserts into TEM-1 active site pocket. It makes four strong hydrogen bonds with conserved residues Ser130, Lys234, Ser235, Arg244 in the enzyme that is critical for substrate binding and catalysis. Moreover it mimics the position of the penicillin G (the first beta-lactam antibiotic introduced into clinical practice) carboxylate observed in the acyl-enzyme complex of TEM-1 with substrate. Because of the catalytic importance of the Asp49 residue, β-hairpin loop of BLIP can be used to derive BLIP based peptides (Strynadka *et al.,* 1996).

1.5. Recent Studies on Beta-lactamase Ligand Interaction

The known catalytic mechanism for class A beta-lactamase consists of acylation and deacylation stages. During the acylation stage, a proton of catalytic Ser70 is removed and it is either transferred to the side chain amide group of Lys73 directly or it is transferred to a water molecule that is coordinated by Ser70, Glu166 and Asn170 (Chen *et al.,* 1996). Currently it has been proposed that perhaps both pathways function together to remove the proton from Ser70 (Meroueh *et al.,* 2005). Then the oxygen of Ser70 attacks the carbonyl group of beta-lactam in order to break the amide bond. Immediately an acyl-intermediate is formed and the water molecule that is coordinated by Ser70, Glu166 and Asn170 in acylation is activated to attack the covalent bond formed in the acyl-intermediate structure and the hydrolysis of beta-lactamase happens. Glu166 is known to be crucial for

deacylation and substitution of glutamate to other residues resulted in a stable acyl-enzyme intermediate formation. The crystal structure of TEM-1 E166N enzyme has been determined in the acyl-enzyme form previously (Strynadka *et al.*, 1992). Unlike Ser70 and Glu166, there is limited information about the importance of Asn170, its significance is not well understood. Brown and colleagues investigated the importance of Asn170 for catalysis and substrate specificity of beta-lactam antibiotic hydrolysis with an experiment. In order to do that the codon for position 170 was randomized to create a library containing all 20 possible amino acids then the random library was introduced into *Escherichia coli*, and mutants exhibiting wild type levels of hydrolysis were selected on agar plates that containing ampicillin. Among all mutants of TEM-1 only the mutant with glycine at this position revealed the same level of function as the wild type. According to the analysis for several substrates, TEM-1 N170G very efficiently hydrolyzes substrates that contain a primary amine in the antibiotic side chain such as ampicillin whereas the lack of amino group as in penicillin G resulted in reduction of catalytic efficiency with respect to wild type. These findings showed that the primary amine of the substrate fulfills the role of the amine group of Asn170 in water positioning for TEM-1 beta-lactamase. Thus, TEM-1 can most effectively hydrolyze the beta-lactam antibiotics in the presence of another ligand that coordinates the hydrolytic water in the active site of the enzyme. Figure 1.4 shows the comparison of the wild-type beta-lactamase mechanism with the proposed substrate-assisted catalysis mechanism of the TEM-1 N170G mutant. The amino group provided by the ampicillin substrate serves the role of Asn170 by coordinating the hydrolytic water in the N170G enzyme (Brown *et al.*, 2009).

Catalysis mechanism of the wild-type and the mutant are divided into two stages. In the wild-type mechanism, the hydrolytic water is coordinated by Ser70, Glu166, and Asn170, whereas the hydrolytic water in the N170G mutant is weakly coordinated in the absence of substrate. The primary amine of ampicillin is shown to act as a ligand for the water in the acyl-intermediate step of catalysis instead of the wild-type Asn170 residue side chain to position the catalytic water to be activated by Glu166 for deacylation (Brown *et al.*, 2009).

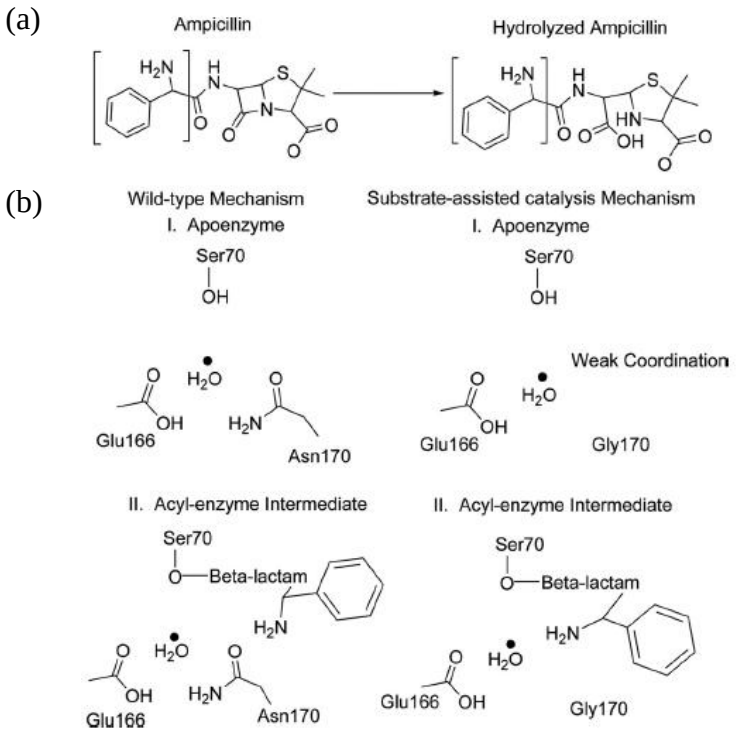

Figure 1.4. Ampicillin as the beta-lactam substrate (a). Schematic representation of catalysis mechanisms of the wild-type beta-lactamase and TEM-1 N170G mutant (b).

Previous molecular dynamics (MD) simulation studies on TEM-1 beta-lactamase revealed that it is a stable enzyme without large structural rearrangements (Diaz *et al.*, 2003, Roccatano *et al.*, 2005). This finding was experimentally confirmed by nuclear magnetic resonance (NMR) study that revealed TEM-1 beta-lactamase is one of the most ordered proteins (Savard and Gagne, 2006). Also in the MD simulation study by Bos and Pleiss, protein flexibility was determined by calculating the root mean square fluctuations (RMSF (Å)). It has been confirmed that residues in secondary structure elements are highly ordered, whereas loop regions are more flexible. Conversely the omega loop is rigid similar to secondary structure elements except its highly flexible tip (Bos and Pleiss, 2009).

The omega loop (residues 161 to 179) is a conserved structural element in all class A beta-lactamases that has a catalytic function by positioning catalytic Glu166 and is involved in substrate binding. Its conformation is stabilized by a highly conserved salt bridge formed between Arg164 and Asp179. The flexible tip (residues 174 to 176) performs an opening and closing motion that was observed on the 50ns timescale of MD study by Bos and Pleiss as shown in the Figure 1.5 (Bos and Pleiss, 2009). The rigidity of

the two hinges of the omega loop was suggested to be due to the presence of water molecules packed between the omega loop and the protein core. These water molecules form highly occupied water bridges and together with their high conservation at well defined positions observed in crystal structures, they stabilize the main part of the omega loop by hydrogen bonding to main chain atoms of the omega loop and the protein core (Bos and Pleiss, 2009).

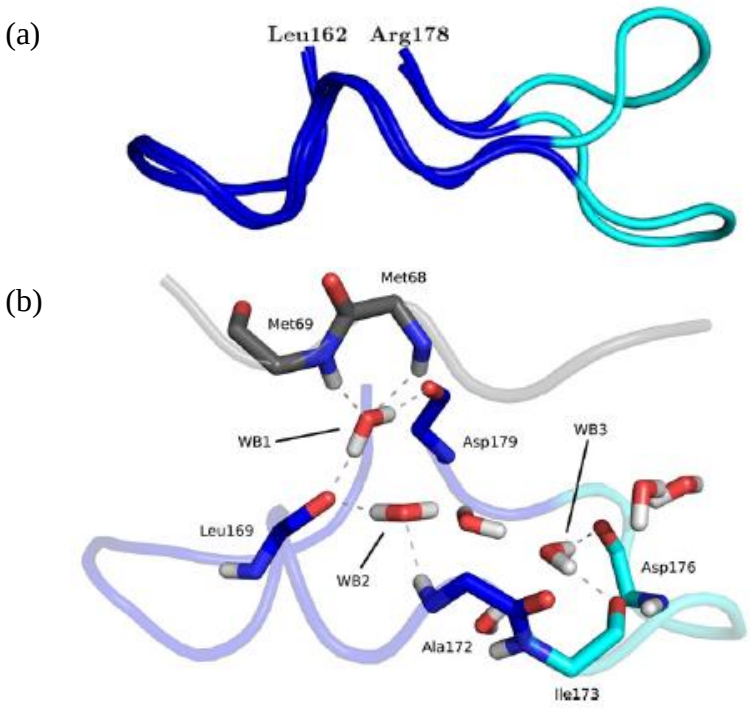

Figure 1.5. Opening and closing motion of the omega loop flexible tip (cyan) (a), water bridges (WB1-WB3) with the main chain atoms of omega loop (blue, cyan for flexible tip) and the protein core (gray).

In a recent experimental study it was suggested that position 104 of beta-lactamase which is glutamate in TEM-1 and aspartate in SHV-1 may result in the differential in binding affinity that BLIP exhibits to TEM-1 and SHV-1, despite their sharing %68 of amino acid identity. In the TEM-1 – BLIP complex, Glu104 forms a salt bridge with BLIP Lys74 and makes favorable vdW interactions with the loop that Phe142 located in due to the large volume of Glu104 which stabilizes its position in the interface. On the other hand, in SHV-1 the smaller side chain of Asp104 cannot form a salt bridge with BLIP Lys74 nor does it make vdW interactions with Phe142. It was found that D104E mutation on SHV-1 resulted in 1000 fold of enhancement in binding affinity between SHV-1 and BLIP. Also

an inverse mutation E104D on TEM-1 has decreased the binding affinity to a similar value that BLIP exhibits for wild type SHV-1. Figure 1.6 shows the 1.6 Å resolution crystallographic structure of the SHV-1 (D104E) - BLIP complex that reveals the interactions responsible for the enhanced affinity (PDB ID: 3N4I) (Hanes *et al.*, 2011).

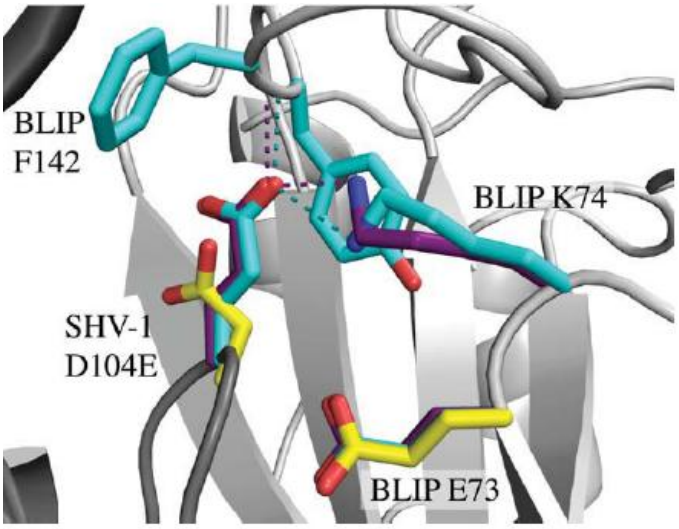

Figure 1.6. E104 participates in a salt bridge (cyan dash) with BLIP K74, similar in the wild type TEM-1 - BLIP structure (purple), the wild type SHV-1 - BLIP co-structure (yellow) was shown for comparison.

In a computational study that EGAD (a physics-based computational design program) software library was used for redesign of BLIP in an attempt to increase affinity for SHV-1. It was found that E73M mutation on BLIP resulted in 400 fold of increase in binding affinity of BLIP revealed to SHV-1. E73M mutation on BLIP enables the formation of salt bridge between Asp104 of SHV-1 and Lys74 of BLIP. Unfortunately, identification of the effect of the E73M mutation on the formation of the salt bridge was failure in the study (Reynolds *et al.*, 2008).

Previously it was shown that the interface between TEM-1 and BLIP is made up of six energetically independent modules each of which comprises a number of closely interacting residues, with few interactions between modules (Reichmann *et al.*, 2008, Reichmann *et al.*, 2005). Mutations in one module do not affect neighboring module residues while a single mutation causes complex energetic and structural consequences within the module. Consequently, the structural and energetic cost of the deletion of an

entire module is small (Reichmann *et al.*, 2005). In another study it was suggested that these modules can be replaced with "ready-made" templates that can be taken from a nonrelated protein found in the Protein Data Bank. In order to redesign the TEM-1 – BLIP interface module 2, which comprises Glu104 and Tyr105 of TEM-1 and Lys74, Phe142 and Tyr143 of BLIP, was substituted with different sets of residues in order to provide high affinity and specificity for the designed complex. The top scoring designed complex was the mutant $E104W_{TEM}$, $Y105K_{TEM}$, $K74Q_{BLIP}$, $F142Y_{BLIP}$, $Y143F_{BLIP}$ in which amino acid composition overlaps the wild type residues but the sequence is different as shown in the Figure 1.7. In order to investigate the cost of the mutations in module 2 on other modules, the binding energy ($\Delta\Delta G_{binding}$) of residues located in neighboring modules was evaluated. Binding energy was calculated by evaluating wild type and mutant proteins in the complex and in the unbound form. The change in module 2 had no effect on residues in module 3 and module 5, but residues $Arg243_{TEM}$ and $Asp49_{BLIP}$ in module 1 have different interaction energy from their interaction in wild type. Still, the new interface closely resembles that of wild type and revealed a similar binding affinity to that of wild type according to the SPR (Surface Plasmon Resonance) that evaluated kinetic constants. This finding suggests that the approach could be generalized to redesign a whole interface with small PDB fragments with increased affinity (Potapov *et al.*, 2008).

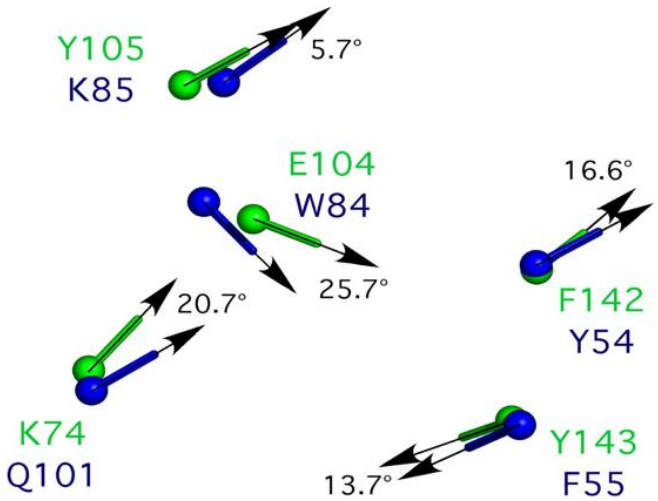

Figure 1.7. Superimposition of the highest-scoring PDB module (PDB ID 1IOO; in blue) and wild-type M2 (in green), all five angles between Cα and Cβ vectors are less than 30°.

The affinity of interacting proteins is affected by surface electrostatic charge which influences the rate of formation of their initial encounter complex as well as their relative positioning within this complex (Albeck and Schreiber, 1999). In a recent study Adaptive Poisson Boltzmann Solver (APBS) plug-in of PyMOL was used in order to calculate electrostatic surfaces (Gretes *et al.*, 2009). In the study, enzyme inhibitor interface between TEM-1 and two BLIP relatives; BLIP-I and BLP were compared with TEM-1 – BLIP in order to investigate the sequence requirements at BLIP residues that contact TEM-1 beta-lactamase. BLIP and BLIP-I with similarly sized binding surfaces are homologous inhibitory proteins that they have 37% amino acid sequence identity. They both revealed nanomolar affinity for TEM-1 however the specific interface formed by each is dissimilar. Despite the apparent homology of BLP to BLIP (32% aa identity) and BLIP-I (42% aa identity) BLP exhibited no binding affinity for TEM-1. The robust and flexible scaffold of the BLIP family fold enables the formation of high-affinity protein-protein interactions while remaining highly selective. The comparison of two naturally occurring, distinct binding interfaces of BLIP and BLIP-I built upon this scaffold showed that there is substantial variation possible in the subnanomolar binding interaction with TEM-1. BLP surface shows that the presence of a few strongly unfavorable interactions especially electrostatic repulsions with a protein partner can negate numerous favorable interactions by decreasing binding affinity (Gretes *et al.*, 2009).

In a recent study a peptide named Pep90 (sequence CYHFLWGPC) was shown to inhibit TEM-1 beta-lactamase within the micromolar range of affinity as well as it can inhibit penicillin binding proteins (PBPs) that involved in cell-wall synthesis of bacteria (Phichith *et al.*, 2010). This study was based on a previous study that a catalytic antibody 9G4H9 which is a functional mimic of beta-lactamase was generated using the internal image properties of anti-idiotypic antibodies (Jerne, 1974) and then a cyclic peptide named Pep90 that inhibited catalytic activity of 9G4H9 was selected (Yribarren *et al.*, 2003). Page displayed variants of Pep90 was generated in order to determine the residues of Pep90 that interacts with the beta-lactamase active site. It was observed that Pep90 has a loop structure similar to that of a BLIP. Pep90 aromatic residues i.e. tryptophan, phenylalanine and tyrosine were mutated and it was found that tryptophan is important for interaction with its target. The replacement of tryptophan with alanine made Pep90 mutant unable to inhibit TEM-1 thus revealing that tryptophan interacts with active site of TEM-1 and the

central tryptophan is necessary for the inhibitory effect of Pep90 on beta-lactamase. Pep90 inhibits TEM-1 with micromolar affinity (Phichith *et al.*, 2010) whereas BLIP inhibits TEM-1 with nanomolar affinity (Kuzin *et al.*, 1999). Although its higher order of magnitude of affinity with respect to other inhibitors, Pep90 has the advantage of combining two functions by both inhibiting enzymes that are the major bacterial resistance mechanism and also enzymes that involved in cell-wall synthesis (Phichith *et al.*, 2010).

1.6. Aims of the Study

In this study TEM-1 and SHV-1 beta-lactamases and their interaction with beta-lactamase inhibitory protein (BLIP) were investigated to better understand the inhibition mechanism of BLIP and beta-lactamase and to identify the features that may be effective in binding affinity. In addition on, the features lead to affinity difference that BLIP exhibits to TEM-1 and SHV-1 beta-lactamases were investigated. Besides, the role of the H10 helix region in TEM-1 that corresponds to residues 218 to 230 was also examined with W229A mutation on TEM-1 to evaluate its probable contribution to binding. TEM-1 binding to peptides based on the BLIP residues 45 to 52 or 45 to 53, which includes the catalytically important Asp49 residue, was examined. Sequence of the peptides was either that in wild type BLIP or included the mutations A46W, D49A, Y50A, Y51A, G48F and G48FY50A. The consequences of the absence of the rest of the BLIP were evaluated.

2. METHODS

2.1. Molecular Dynamics Simulations

Molecular dynamics (MD) simulations calculate the forces on all atoms during each time step and use these forces to update the positions and velocities of atoms (Karplus, 2002) in other words produces the history of positions of the atoms in the system with time. In these simulations motion of the atoms of a system of N interacting atoms with masses m_i is calculated by directly solving the Newtonian equations of motion (Allen, 2004) :

$$F_i(t) = m_i \frac{d^2 r_i(t)}{dt^2} \quad , \quad (i = 1,2, \dots N) \tag{2.1}$$

where r_i and m_i represent the position and mass of atom i and $F_i(t)$ is the force on the atom i at time t. $F_i(t)$ is given by

$$F_i = -\nabla V\,(r_1, r_2 \dots, r_N) \tag{2.2}$$

where $V\,(r_1, r_2 \dots, r_N)$ is the potential energy of the system that depends on the positions of N atoms in the system.

Molecular dynamics simulation algorithm is described with a highly simplified flow chart in the Figure 2.1 (Nordlund, 2007). The simulation proceeds iteratively by calculating forces and solving the equations of motion based on the accelerations obtained from the new forces.

In this study MD simulations were performed with the NAMD program (Phillips *et al.*, 2005). NAMD is a parallel molecular dynamics code utilized for high performance simulation of large bimolecular systems and generated using Charm ++ (Kale and Krishnan, 1993) which is a parallel C++ programming language (Phillips *et al.*, 2005). As mentioned above in these simulations the atoms of the system move according to the Newtonian equation of motion.

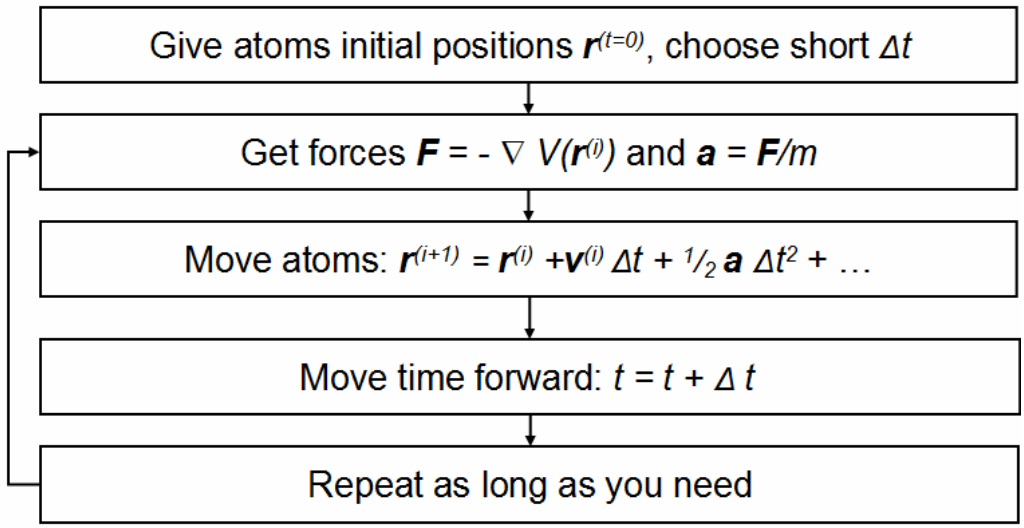

Figure 2.1. Classical molecular dynamics in a nutshell.

The most crucial part of the simulation is the potential energy, represented through the MD "force field" because it must faithfully represent the interaction between atoms. Every atom in the system experiences a force specified by a model force field in order to calculate the interaction of that atom with the rest of the system. NAMD can work both with AMBER and CHARMM force fields (Phillips *et al.*, 2005). CHARMM 22 (MacKerell *et al.*, 1998) force field was used in the present study.

NAMD utilizes a common potential energy function that is divided into two categories that are bonded and non-bonded interactions.

$$V_{total} = V_{bond} + V_{angle} + V_{dihedral} + V_{vdW} + V_{Coulomb} \tag{2.3}$$

The first three terms indicate the bond stretching, angle bending and torsional potential,

$$V_{bond} = \sum_{bonds\, i} k_i^{bond} + (r_i - r_{0i})^2 \tag{2.4}$$

$$V_{angle} = \sum_{angle\, i} k_i^{angle} + (\theta_i - \theta_{0i})^2 \tag{2.5}$$

$$V_{dihedral} = \sum_{dihedral\, i} \begin{cases} k_i^{dihe}[1 + \cos(n_i \emptyset_i - \gamma_i)], & n_i \neq 0 \\ k_i^{dihe}(O_i - \gamma_i)^2 & , n = 0 \end{cases} \tag{2.6}$$

where bond indicates each covalent bond in the system, angle describes angles between each pair of covalent bonds that share a single atom at the vertex, and dihedral describes potential due to the rotation around the middle covalent bond in a sequence of four atoms. An "improper" dihedral term is also included.

The last two terms in the potential energy function represent non-bonded interactions that are van de Waals (Lennard-Jones 6-12 potential) and electrostatic terms :

$$V_{vdW} = \sum_i \sum_{j>i} 4\varepsilon_{ij} \left[\left(\frac{\sigma_{ij}}{r_{ij}} \right)^{12} - \left(\frac{\sigma_{ij}}{r_{ij}} \right)^{6} \right] \tag{2.7}$$

$$V_{coulomb} = \sum_i \sum_{j>i} \frac{q_i q_j}{4\pi\varepsilon_0 r_{ij}} \tag{2.8}$$

For each particle in a given context of bonds, the parameters k_i^{bond}, r_{0i} , etc for the stretching, bending and torsional bonded interactions are laid out in force field parameter files.

A multiple time stepping method is employed by NAMD to improve integration efficiency. The slower varying forces are less frequently computed than the faster varying ones thus three levels of integration loop are implemented in NAMD. The inner loop uses only bonded forces to advance the system, the middle loop uses Lennard Jones and short range electrostatic forces and lastly the outer loop uses long-range electrostatic forces (Phillips *et al.*, 2005). The non-bonded computations comprise between 80% and 95% of the overall computation relying on the cutoff radius used (Kale *et al.*, 1999).

In order to avoid surface effects on the boundary of the simulation system, periodic boundary conditions are used in the MD simulations. According to that the particles are enclosed in a unit simulation cell that is replicated to infinity and edges are given by vectors a_1, a_2, a_3. If a particle leaves the cell from one side of the cell it is replaced by the copy particle that enters the cell from the opposite side. Moreover, each particle is subjected to the potential from all other particles in the system so that entirely eliminating surface effects. On the other hand, computing the long range interactions exactly is impossible because the van der Waals and electrostatic interactions exist between every

non-bonded pair of atoms in the system. In order to achieve this, long-range interactions are truncated with a user-defined cutoff distance. Particle Mesh Ewald (PME) method is used to compute full (nontruncated) electrostatic interactions with minimal additional cost in the simulation systems using periodic boundary conditions (Philips et al., 2005).

In this study, the starting coordinates for the simulation systems were obtained from the X-ray crystal structure of beta-lactamase and beta-lactamase - BLIP complex from the Protein Data Bank with the PDB ID of 1zg4 (TEM-1), 1shv (SHV-1), 1jtg (TEM-1 - BLIP) and 2g2u (SHV-1 - BLIP).

10ns of MD simulations were performed with the NAMD program using the CHARMM22 force field. The simulations were carried out in an explicit solvent of TIP3P water box, the walls of which extended 15 Å from the mass center of the protein under periodic boundary conditions with a grid size of 80Å×72Å×90Å using the Particle Mesh Ewald (PME) method for electrostatic interactions.

Non-bonded forces decrease as the distance between atoms increase. Besides, any given region of space is likely to be charge-neutral, so that reduces its effects on far-away atoms. In order to save computation time, 12 Å of cutoff distance was used to ignore interactions between atoms beyond the cutoff distance.

The SHAKE algorithm (Ryckaert *et al.*, 1977) was applied to constrain bond distances to their equilibrium values. At the beginning of each simulation the solvent box was equilibrated, keeping the protein fixed that allows water molecules to relax to a local minimum (Campanera and Pouplana, 2010). After the whole simulation system was energy minimized for 3000 steps, the system was heated up to the simulation temperature of 300K from the initial temperature of 50 K in 8 ps. A time step of 1fs was used and structures were saved every 250 ps for analyses later.

NAMD can be connected to the molecular visualization package VMD (Humphrey *et al.*, 1996) that allows the user to view running simulation.

2.2. Root Mean Square Deviations

The root mean square deviation (RMSD) of each simulation system was calculated in order to find out the deviations from the initial structure of the coordinates so as to gain an idea about stability of the simulation systems.

On the purpose of obtaining deviation from the initial structure, each structure was averaged according to the equilibrium period of the simulation by using VMD and a Tcl Script in Appendix A. Average simulation structure was aligned on the initial simulation structure based on C_α atoms and the deviation of these atoms from their initial positions was calculated by using RMSD Trajectory Tool of VMD.

For the RMSD calculation of beta- lactamase, average chain A structure of the complex, for ligand RMSD average chain B structure of the complex were aligned to their initial structure and then RMSD for beta-lactamase and ligand were calculated to find the deviation from their initial structure. In order to calculate RMSD of the complex structure, the average complex structure was aligned to the initial complex structure.

2.3. Mean Square Fluctuations

In order to investigate mobility and flexibility of beta-lactamase, ligand and complex in each simulation system, mean square fluctuations (MSF) were calculated which gives fluctuations about the average structure that is obtained from the averaged trajectory of the system. After the alignment of the time averaged structure (beta-lactamase / ligand / complex) from the simulation on the initial simulation structure of itself based on C_α atoms, residue averaged MSF values of the beta-lactamase, ligand and complex were calculated by using Matlab and the script in Appendix B.

2.4. Binding Free Energy Calculations

The MM-PBSA (Molecular Mechanics-Poisson Boltzmann Surface Area) method was used in order to calculate binding free energy thus average interaction energy of each simulation system. Calculation of the binding free energy with MM-PBSA method was

carried out for the snapshots were taken from the MD trajectory (Kollman *et al.*, 2000). In this work calculation of binding free energies were done by using single protein-ligand trajectories that means the snapshot structures for the energy calculations of the protein-ligand complex and separated protein and ligand were taken from the MD trajectory of the protein-ligand complex. Due to previous studies the single trajectory method provides fairly good estimates of relative binding energies than running separate trajectories of complex, protein and ligand (Kollman *et al.*, 2000, Laitinen *et al.*, 2004, Vorontsov and Miyashita, 2011).

In the MM-PBSA method the binding free energy (ΔG_{bind}) is calculated according to the equation (Campanera and Pouplana, 2010, Vorontsov and Miyashita, 2011) :

$$\Delta G_{bind} = G_{complex} - (G_{protein} + G_{ligand}) \quad (2.9)$$

where free energies G correspond to the complex and "dissociated" protein and ligand. Each G value can be decomposed as follows;

$$G = E_{MM} + G_{PB} + G_{np} - TS_{solute} \quad (2.10)$$

where E_{MM} corresponds to molecular mechanical energy of the molecule which is the sum of the internal energy (bonds, angles and dihedrals), electrostatic energy and van der waals term, G_{PB} is the electrostatic (polar) contribution to solvation energy and G_{np} is the nonpolar contribution to solvation that represents the cost of creation a cavity inside the solvent (Campanera and Pouplana, 2010) and proportional to the solvent accessible area of the solute and lastly TS_{solute} is the solute entropy. For the best results ΔG_{bind} should be averaged over a set of snapshots gained through explicit solvent MD simulation (Kollman *et al.*, 2000, Vorontsov and Miyashita, 2011).

After including all energetic terms for complex, protein and the ligand the average binding free energy (ΔG_{bind}) is calculated from the average molecular mechanical gas-phase energies (ΔE_{MM}), solvation free energies ($\Delta\Delta G_{solv}$) and entropy contributions ($-T\Delta S$) of the binding reaction (Laitinen *et al.*, 2003) :

$$\Delta G_{bind} = \Delta E_{MM} + \Delta\Delta G_{solv} - T\Delta S \quad (2.11)$$

In this study the molecular mechanical energy (ΔE_{MM}), of each snapshot was calculated with CHARMM27 (MacKerell *et al.*, 2000) potential energy function. The solvation free energy ($\Delta\Delta E_{solv}$) was calculated as the sum of polar (ΔG_{PB}) and nonpolar (ΔG_{np}) part. The polar part (ΔG_{PB}) is the electrostatic contribution to solvation that is obtained by solving the Poisson Boltzmann equation and calculated by APBS (Baker *et al.*, 2001). Nonpolar solvation free energy (ΔG_{np}) is calculated from solvent accessible surface area (SASA) and MSMS program (Sanner *et al.*, 1996) was used to calculate SASA (Sitkoff *et al.*, 1994) for the estimation of the nonpolar solvation free energy. Finally, Wordom (Seeber *et al.*, 2007) was used in order to calculate entropic contributions to the binding free energy.

3. BETA-LACTAMASE BINDING TO BLIP

TEM-1 and SHV-1 beta-lactamases in apo forms and in complex with BLIP and BLIP (D49A), TEM-1 (W229A) in apo form and in complex with BLIP and free BLIP and BLIP (D49A) were examined by MD simulations to decipher the interaction of beta-lactamase with beta-lactamase inhibitory protein BLIP. For the initial coordinates of the simulation systems X-ray crystal structures were taken from Protein Data Bank. PDB codes of unbound TEM-1 and SHV-1 are 1zg4 and 1shv respectively. 1jtg and 2g2u are PDB codes of TEM-1 – BLIP and SHV-1 – BLIP complexes. The simulations were performed for 10 ns at constant T = 300K and P = 1 atm using NAMD simulation program.

3.1. Simulation Systems and Stability of the Simulations

Root mean square deviation (RMSD) of each simulation system was calculated in order to find out the deviation from the initial structure and to verify the stability of the simulation systems. So as to obtain deviation from the initial structure, each structure was averaged according to the equilibrium period of the simulation and each averaged structure aligned on the initial simulation structure of itself based on C_α atoms and the deviation of these atoms from their initial positions was calculated. For the RMSD calculation of beta-lactamase, chain A of the complex which is TEM-1 or SHV-1, for ligand RMSD, chain B of the complex which is BLIP or BLIP (D49A), were aligned to their initial structure and then RMSD was calculated to find the deviation from initial structure. In order to calculate RMSD of the complex structure, the average complex structure was aligned to the initial complex structure. Table 3.1 gives a list of the simulation systems and the RMSD values between the initial structure and the average structure for beta-lactamase, ligand and the complex. Also the residue averaged MSF values for the equilibrium period are in parenthesis. Equilibrium period of each simulation was written under the simulation system in nanosecond.

Considering the RMSD values of the simulation systems, Apo TEM-1 deviated from its initial structure by 0.78 Å, which is less than its deviation in Apo TEM-1 (W229A) and Apo SHV-1 beta-lactamases that have 0.95 Å and 0.99 Å of RMSD values respectively.

Table 3.1. RMSD values (Å) of beta-lactamase, ligand and complex in each simulation system and MSF values ($Å^2$) are in parenthesis.

Simulation System	Beta-Lactamase	Ligand	Complex
TEM-1 (4-10 ns)	0.78 (0.39)		
TEM-1 (W229A) (4-10 ns)	0.95 (0.35)		
TEM-1 – BLIP (2-10 ns)	0.82 (0.28)	1.44 (0.45)	1.89 (0.48)
TEM-1 - BLIP (D49A) (1.5-10 ns)	0.89 (0.25)	0.95 (0.34)	1.39 (0.37)
TEM-1 (W229A) – BLIP (2.5-10 ns)	0.86 (0.28)	0.90 (0.44)	1.60 (0.51)
SHV-1 (1.5-10 ns)	0.99 (0.32)		
SHV-1 – BLIP (5-10 ns)	0.82 (0.33)	0.84 (0.49)	1.13 (0.54)
SHV-1 - BLIP (D49A) (5-10 ns)	0.85 (0.31)	0.79 (0.37)	1.28 (0.48)
BLIP (2-10 ns)		0.77 (0.57)	
BLIP (D49A) (3-10 ns)		0.87 (0.58)	

In the BLIP bound form, RMSD with respect to initial structure for TEM-1 stayed close to its value in the apo form (0.78 Å) at 0.82 Å. On the other hand, BLIP binding decreased deviation of TEM-1 (W229A) from 0.95 Å in unbound form to 0.86Å in BLIP bound form. Also it decreased SHV-1 deviation from 0.99 Å in unbound form to 0.82 Å in BLIP bound form.

In the BLIP (D49A) bound form, D49A mutation on BLIP increased TEM-1 deviation from its initial position with a RMSD value of 0.89 Å while its RMSD value is 0.82 Å in the wild type structure. However, SHV-1 did not reveal a high change as TEM-1 had due to D49A mutation on BLIP. It has a RMSD of 0.85 Å in BLIP (D49A) bound form, while its RMSD is 0.82 Å in BLIP bound form.

BLIP has a RMSD of 0.77 Å in its apo form but its average deviation from the initial structure increased due to beta-lactamase binding. BLIP, deviated by 1.44 Å from its initial

position upon TEM-1 binding, by 0.90 Å upon TEM-1 (W229A) binding and by 0.84 Å upon SHV-1 binding.

D49A mutation on Apo BLIP increased RMSD value to 0.87 Å while its RMSD value is 0.77 Å in the wild type structure. BLIP (D49A), deviated by 0.95 Å from its initial position upon TEM-1 binding and by 0.79 Å upon SHV-1 binding.

TEM-1 – BLIP complex has the highest RMSD value (1.89 Å) because of the high deviation in the BLIP structure. TEM-1 (W229A) – BLIP complex deviated from its initial structure by 1.60 Å. RMSD value of SHV-1 – BLIP complex is 1.13 Å. TEM-1-BLIP (D49A) complex has 1.39 Å of RMSD which is significantly less than RMSD of wild type complex, also RMSD value of SHV-1 – BLIP (D49A) is less than its wild type complex with an RMSD of 0.79Å.

RMSD profiles of the simulation systems were examined in order to better understand of their behaviors during the 10 ns length simulation.

3.1.1. Stability of TEM-1 Beta-lactamase During the Simulations

In order to examine behavior of TEM-1 beta-lactamase during the simulations both unbound and ligand bound forms and also its W229A mutated form in unbound and ligand bound structure were investigated. Figure 3.1 shows RMSD profile of beta-lactamase in each simulation system that reveals its stability in the simulations.

The unbound TEM-1 simulation reached equilibrium in about 4 ns and TEM-1 in complex with BLIP reached equilibrium in 2 ns of 10 ns simulation (Figure 3.1a and Figure 3.1b) with RMSD values of 0.78 Å and 0.82 Å between the initial TEM-1 structure in apo form and in BLIP bound form and the time averaged structure of TEM-1 in the two simulations respectively (Table 3.1), suggesting that BLIP binding did not change the TEM-1 structure remarkably.

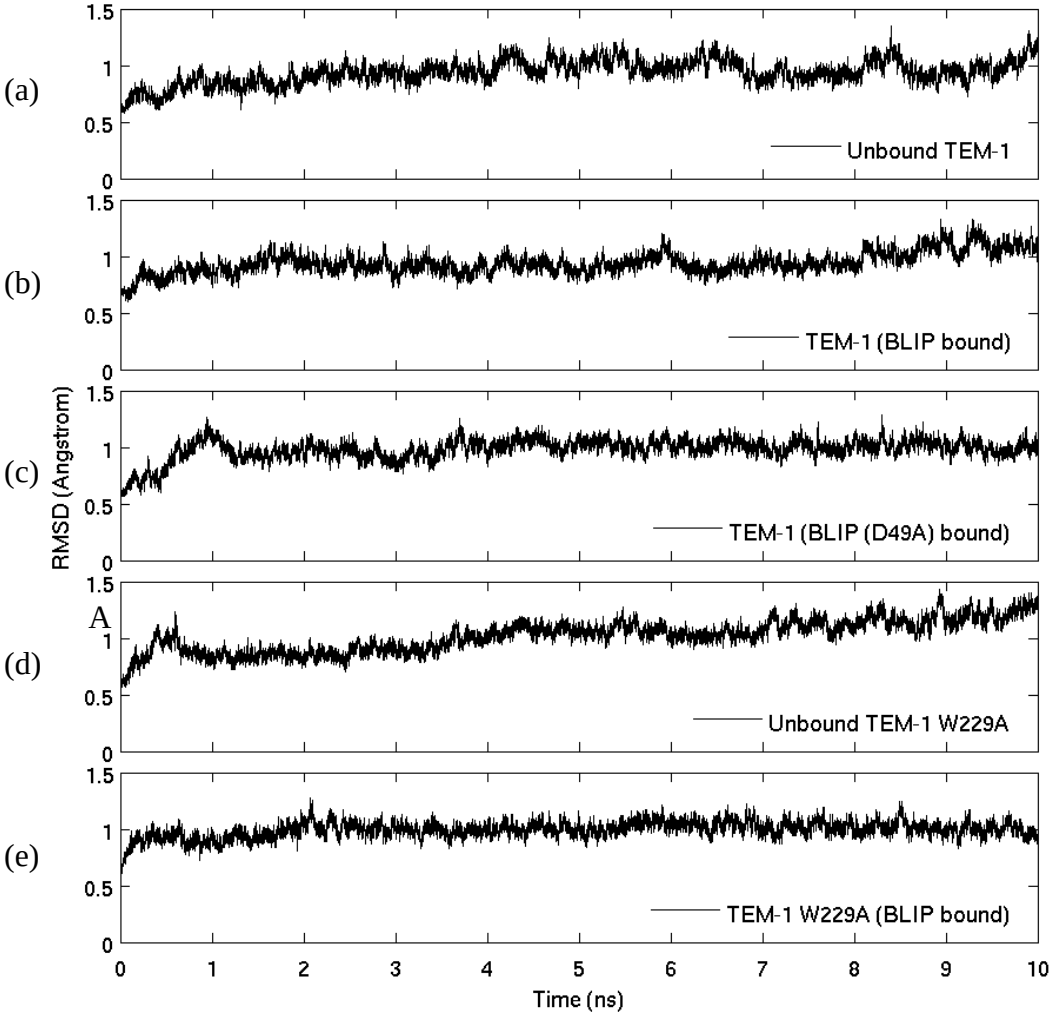

Figure 3.1. RMSD of apo TEM-1, BLIP and BLIP (D49A) bound TEM-1, apo TEM-1 W229A mutant and BLIP bound TEM-1 W229A with respect to initial structure of beta-lactamase in the simulations.

Simulation for TEM-1 in complex with BLIP (D49A) reached equilibrium in about 1.5 ns of 10 ns simulation (Figure 3.1c). After reaching equilibrium both TEM-1 in complex with BLIP and BLIP (D49A) revealed stable behavior with little fluctuations. The RMSD value of TEM-1 in complex with BLIP (D49A) is 0.89 Å which is close to RMSD value of TEM-1 in wild type bound form (0.82 Å).

Simulation on TEM-1 W229A mutant reached equilibrium in 4 ns of 10 ns simulation in its unbound form while, its BLIP bound form needed 2.5 ns in order to be stable (Figure 3.1d and Figure 3.1e). The RMSD of TEM-1 (W229A) in its unbound and BLIP bound forms are 0.95 Å and 0.86 Å respectively (Table 3.1). Apo TEM-1 (W229A)

deviated from its initial structure more than wild type Apo TEM-1 deviated from its initial structure (0.78 Å).

For each simulation system, stability of the beta-lactamase was assessed by calculating RMSD with respect to the initial simulation structure of beta-lactamase. TEM-1 or its W229A mutant was stable and showed only a small deviation from the initial simulation structure that stayed around 0.83 Å for TEM-1 and around 0.91 Å for TEM-1 W229A mutant in the simulations.

3.1.2. Stability of SHV-1 Beta-lactamase During the Simulations

Stability of SHV-1 beta-lactamase was investigated by examining its behavior during the simulations. Figure 3.2 reveals RMSD profile of SHV-1 in its unbound and ligand bound forms.

Simulation on unbound SHV-1 reached equilibrium in about 1.5 ns on the other hand, SHV-1 in complex with BLIP needed about 5 ns in order to reach equilibrium (Figure 3.2a and Figure 3.2b). While unbound SHV-1 stayed stable with few fluctuations, SHV-1 in complex with BLIP revealed more fluctuations. Nevertheless, unbound SHV-1 deviated from its initial structure more than SHV-1 in complex with BLIP. The RMSD of unbound SHV-1 is 0.99 Å and the RMSD of SHV-1 in complex with BLIP is 0.82 Å. The significant difference between RMSD values of SHV-1 in unbound and BLIP bound forms arising from the H10 helix (218 to 230) of SHV-1 that has different conformations in unbound and BLIP bound forms. H10 in unbound SHV-1 structure deviated by 2.67 Å from its initial position which is significantly greater than H10 deviation in BLIP bound SHV-1 structure with a RMSD value of 1.29 Å (Table 3.2).

In the initial simulation structure H10 helix in the SHV-1 – BLIP structure had a position similar with the H10 helix of both unbound and BLIP bound TEM-1 and H10 helix of the unbound SHV-1 had a different position with respect to them. However during the simulation, H10 helix in unbound SHV-1 changed its position significantly and at the end of the simulation it stayed nearly similar position with the final H10 position in SHV-1-BLIP structure. These findings were gained from the observation of the unbound and

BLIP bound TEM-1 and unbound and BLIP bound SHV-1 simulation systems in VMD. Before the observation of simulation systems, these four simulation structure were aligned based on C_α atoms of beta-lactamase structure and then simulation systems were observed to compare the H10 helix position in each simulation system.

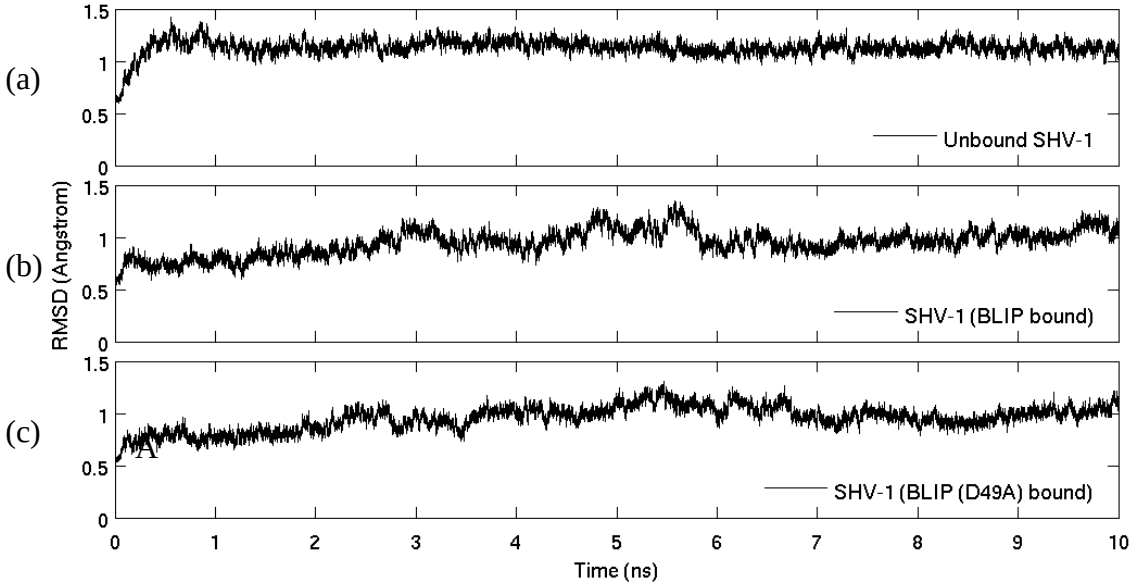

Figure 3.2. RMSD to initial structure for SHV-1 in the unbound SHV-1, BLIP and BLIP (D49A) bound SHV-1 simulations.

SHV-1 in complex with BLIP (D49A) needed 5 ns to reach equilibrium as SHV-1 in complex with BLIP. SHV-1 in both simulation systems showed similar RMSD profiles (Figure 3.2b and Figure 3.2c). The RMSD of SHV-1 in complex with BLIP (D49A) is 0.85 Å which is close to RMSD value of SHV-1 in complex with BLIP (0.82 Å).

Stability of SHV-1 beta-lactamase in each simulation system was determined according to the RMSD calculation. SHV-1 was stable and showed only a small deviation from the initial simulation structure that stays around 0.89 Å in the simulations.

3.1.3. Stability of Beta-lactamase Inhibitory Protein (BLIP) During the Simulations

In order to examine the behavior of BLIP during the simulations, both unbound and beta-lactamase bound forms of BLIP and BLIP (D49A) were investigated.

Comparison of RMSD profiles to initial BLIP structure in the different simulations (Figure 3.3) showed that BLIP stayed within 1.2 Å to its initial structure for most simulations except in the TEM-1 bound case.

According to the Figure 3.3 unbound BLIP and BLIP (D49A) revealed fluctuating profiles throughout the 10 ns simulations nonetheless, unbound BLIP deviated from its initial structure less than unbound BLIP (D49A) and their average RMSD values are 0.77 Å and 0.87 Å respectively.

BLIP moves away from its initial structure when it is bound to TEM-1; when BLIP is in complex with TEM-1, BLIP has an RMSD of 1.44 Å which is significantly more than RMSD of unbound BLIP (0.77 Å). However; binding of TEM-1 did not affect BLIP (D49A) remarkably; the RMSD of BLIP (D49A) is 0.95 Å in TEM-1 bound form while it is 0.87 Å in unbound form.

The RMSD profiles of unbound and SHV-1 bound BLIP simulations showed that BLIP structure was not affected from SHV-1 binding as significantly as it was affected from TEM-1 binding. BLIP has an RMSD of 0.84 Å in SHV-1 bound form which is very close to RMSD of unbound BLIP (0.77 Å) and notably less than RMSD value of BLIP in TEM-1 bound form (1.44 Å). Also, D49A mutation did not affect BLIP significantly in the presence of SHV-1; it has an RMSD of 0.79 Å which is close to RMSD value of unbound form (0.87 Å).

BLIP in TEM-1 W229A mutant bound form revealed similar RMSD profile to unbound BLIP rather than BLIP in TEM-1 bound form. Also, with 0.90 Å of RMSD value BLIP in TEM-1 (W229A) bound form is more stable than BLIP in TEM-1 bound form (1.44 Å).

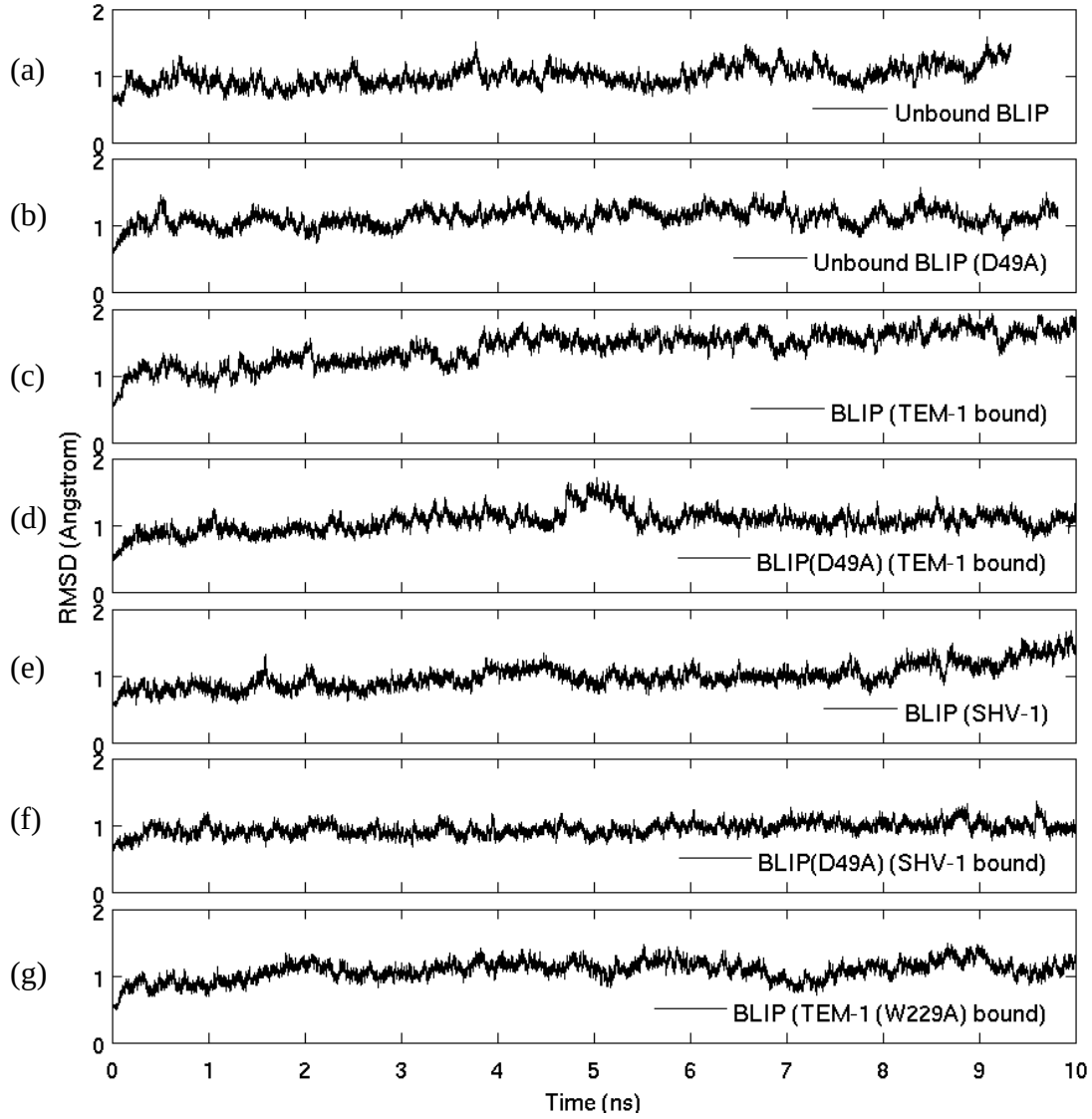

Figure 3.3. RMSD of apo BLIP and BLIP (D49A), TEM-1 bound BLIP and BLIP (D49A), SHV-1 bound BLIP and BLIP (D49A) and TEM-1 (W229A) bound BLIP with respect to initial structure in the simulations.

3.2. Mobility and Flexibility of Simulation Systems

In order to investigate mobility and flexibility of beta-lactamase, ligand and complex in each simulation system, mean square fluctuations (MSF) were calculated which gives fluctuations about the average structure. Table 3.1 indicates residue averaged MSF values of TEM-1 and SHV-1 beta-lactamases, BLIP and BLIP (D49) and their complexes, as well as those of TEM-1 W229A mutant and its complex with BLIP.

3.2.1. Mobility of TEM-1 Beta-lactamase in Unbound and BLIP Bound Forms

Mean square fluctuations were calculated in order to gain an idea about average mobility of TEM-1 (Table 3.1) and also mobility of its important regions (Table 3.2) in its unbound and BLIP bound forms. MSF graphs show mobility of residues and the peaks highlight the most mobile and flexible parts.

In order to calculate MSF values, Matlab and the script in Appendix B was used. Simulation trajectory file that comprises whole motion of the beta-lactamase throughout the equilibrium period of the simulation was used as the input. After the alignment of the time averaged beta-lactamase structure from the simulation on the initial simulation structure of beta-lactamase based on C_α atoms, MSF value of each residue on beta-lactamase was calculated. Then MSF graphs that reveal MSF value of each residue were gained. Figure 3.4 shows the MSF graphs of unbound TEM-1 (a), BLIP bound TEM-1 (b) and also their difference by subtracting residue based MSF values of BLIP bound TEM-1 from unbound TEM-1 (ΔMSF) (c).

The structure of TEM-1 (Figure 3.4d) was colored according to the residue based MSF value difference (ΔMSF). Residues that gain or lose mobility due to BLIP binding were highlighted with colors. In order to generate colored structure figure, residue based MSF value difference data obtained by the Matlab script in Appendix B was used and the MSF values were mapped onto the structure in VMD using the Tcl script in Appendix A. Residues were highlighted with colors ranging from blue to green to red that correspond to range in MSF value difference from low to high. For example if the difference is a positive value, i.e. the residue has higher mobility in the apo simulation, it is colored red to green and when the difference is negative it is colored green to blue.

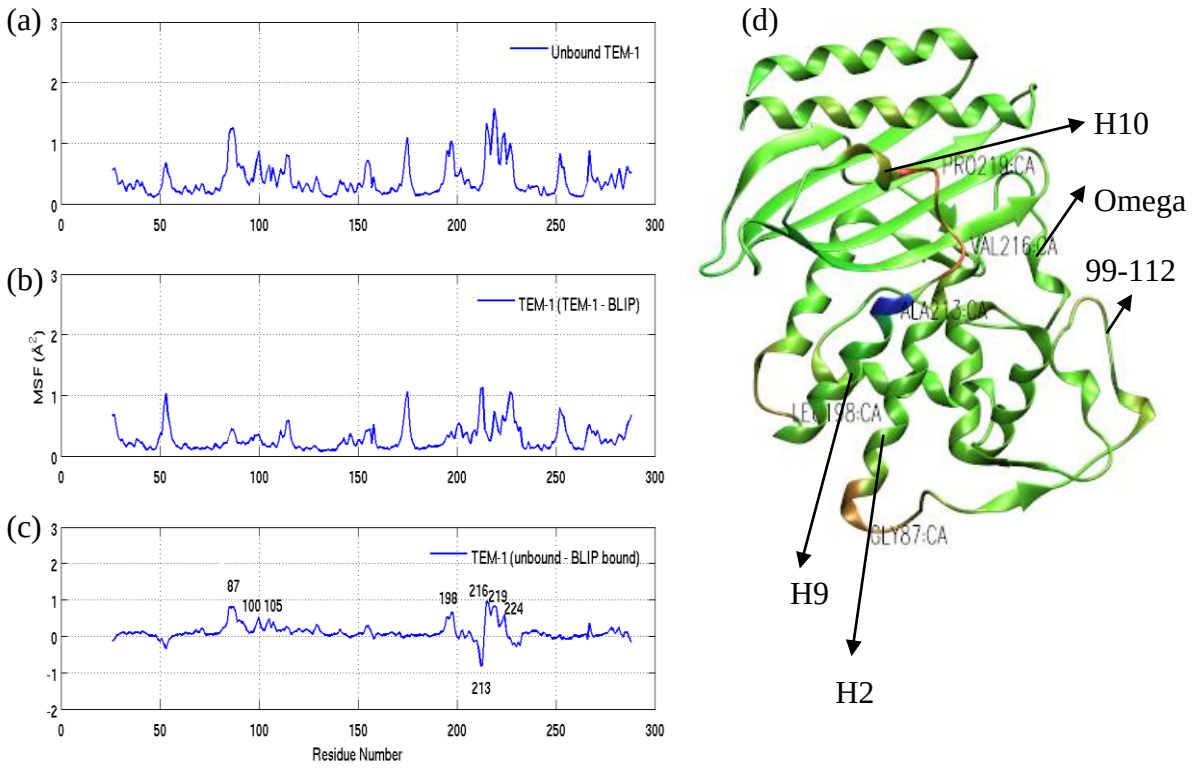

Figure 3.4. Residue based MSF of unbound TEM-1 (a), TEM-1 in the presence of BLIP (b) and their difference (c), TEM-1 structure colored by MSF value difference of unbound and BLIP bound TEM-1 (d).

The most mobile region of unbound TEM-1 is H10 helix (218 to 230) with 0.95 $Å^2$ of average MSF value. Also with 0.84 $Å^2$ of MSF value, omega loop flexible tip (174 to 176) is very mobile. However, omega loop is not very flexible it has a MSF value of 0.35 $Å^2$ which is less than average MSF value of unbound TEM-1 structure (0.39 $Å^2$). Also 99-112 loop is not very mobile with 0.49 $Å^2$ of MSF value. The active site of TEM-1, corresponding to Ser70, Lys73, Ser130, Glu166, Asn170 and Lys234 is almost rigid and its MSF value is 0.23 $Å^2$ (Table 3.2).

BLIP binding made TEM-1 less mobile and average mobility of TEM-1 decreased to 0.28 $Å^2$ due to BLIP binding while its 0.39 $Å^2$ in unbound form (Table 3.1).

According to the ΔMSF profile of TEM-1 (Figure 3.4c) binding of BLIP mostly affects H10 helix region of TEM-1. While H10 helix of unbound TEM-1 has an average MSF value of 0.95 $Å^2$, it became 0.64 $Å^2$ after BLIP binding (Table 3.2). The average MSF value of H9-H10 helix region (201 to 230) was also lower in the presence of BLIP

(from 0.70 to 0.54) but the decrease is not as significant as it was for the H10 helix region, because Ala213 on the loop connecting H9 and H10 increased its mobility after BLIP binding. Apart from that, Leu198 near the N-terminus of the H9 helix has decreased mobility after BLIP binding (Figure 3.4c).

BLIP binding reduced the mobility of low flexible omega loop (161-179) and 99-112 loop to 0.29 and 0.23 $Å^2$ respectively. On the other hand, omega loop flexible part as indicated in its name has high flexibility and BLIP binding did not affect its motion much.

The active site of TEM-1, corresponding to Ser70, Lys73, Ser130, Glu166, Asn170 and Lys234, has lowest flexibility among other regions and after BLIP binding decreased to nearly half of its unbound structure value which is 0.23 $Å^2$.

Figure 3.4d reveals the regions that show large differences between the unbound and BLIP bound forms of TEM-1 include the H10 helix (218 to 230), H9 helix (201 to 212) and Gly87 on the loop connecting H2 helix (69 to 84) to b2 strand (94 to 97) that lost mobility after BLIP binding while omega loop and the 99-112 loop did not change their mobilities significantly upon BLIP binding.

3.2.2. The Effect of BLIP D49A Mutation on TEM-1 Mobility

Mean square fluctuations were calculated in order to gain an idea about average mobility of TEM-1 (Table 3.1) and also mobility of its important regions (Table 3.2) in the presence of BLIP (D49A).

The average mobility of TEM-1 beta-lactamase in BLIP bound form slightly decreased from 0.28 to 0.25 $Å^2$ with D49A mutation on BLIP (Table 3.1). To identify the regions that lost or gained mobility due to the D49A mutation, residue based MSF values were calculated and compared for the BLIP bound (Figure 3.5a) and BLIP (D49A) bound (Figure 3.5b) TEM-1, also the difference was calculated (Figure 3.5c) and mapped onto the structure (Figure 3.5d) as described for Figure 3.4.

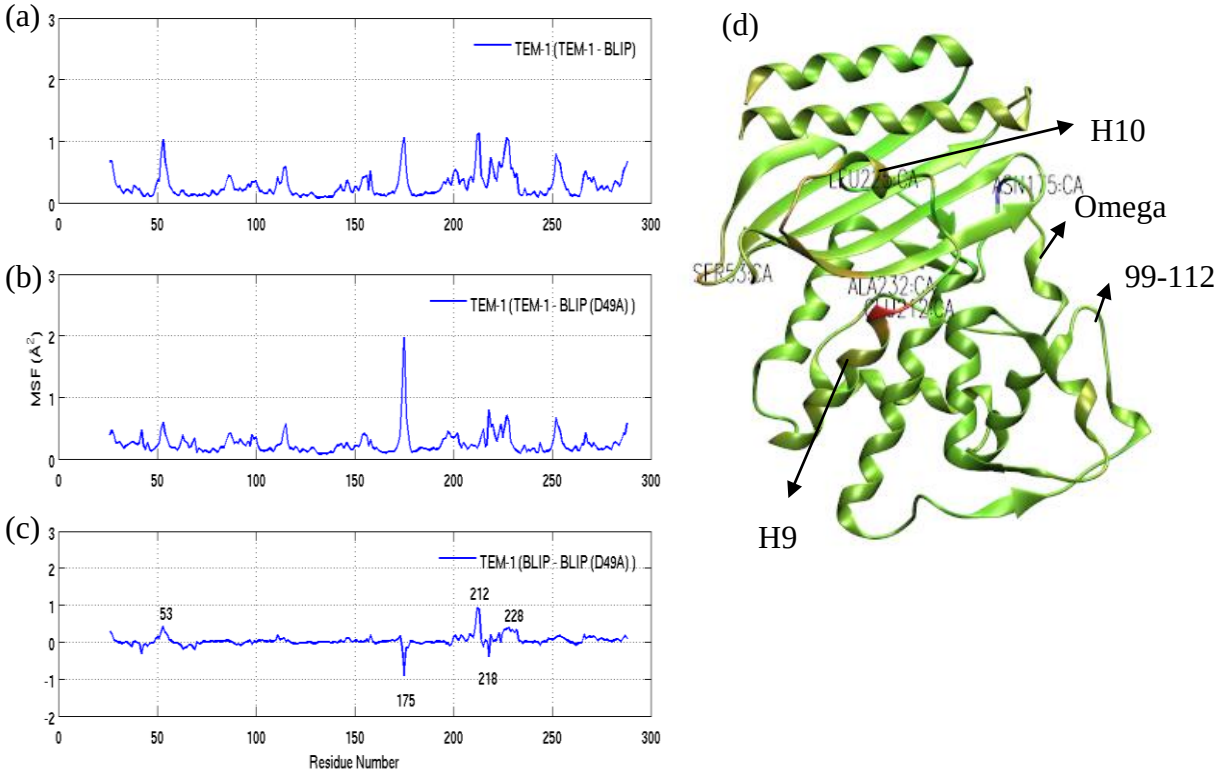

Figure 3.5. Residue based MSF of TEM-1 in the presence of BLIP (a) and BLIP (D49A) (b) the change in mobility of TEM-1 due to D49A mutation (c), TEM-1 structure colored by MSF value difference (d).

H9-H10 region (201 to 230) of TEM-1, lost mobility due to D49A mutation on BLIP and MSF value of this region decreased from 0.54 to 0.35 $Å^2$. Glu212 of the H9 helix lost significant mobility due to mutation and it is colored red. Moreover, residues 225 to 232 on the H10 helix and near the C-terminus of it lost some mobility after D49A mutation as highlighted with orange (Figure 3.5d). Ser53 on the loop connecting B1 (43 to 50) and B2 (55 to 60) also lost some mobility and it is orange in Figure 3.5d.

On the contrary, omega loop (161 to 179) especially the flexible part (174 to 176) gained significant flexibility after mutation as represented the peak of residue Asn175 (Figure 3.5c) and colored blue (Figure 3.5d). The MSF values of omega loop and omega loop flexible part became 0.34 and 1.22 $Å^2$ after the mutation while they were 0.29 and 0.81 $Å^2$ respectively before mutation. The flexibility of active site region of TEM-1 that is bound to BLIP (D49A) increased to 0.24 from 0.11 $Å^2$ in the BLIP bound state.

3.2.3. Mobility of TEM-1 Beta-Lactamase with W229A Mutation in Unbound and BLIP Bound Forms and the Effect of Mutation on Binding

Pro252, on the loop connecting B4 and B5 beta-strands, is a highly mobile residue of TEM-1 beta-lactamase and also another class A beta-lactamase SHV-1. This proline residue composes a stacking structure with Pro226 and Trp229 of H10 helix (Figure 3.6).

As mentioned previously H10 helix is a highly mobile region of TEM-1 beta-lactamase and after BLIP binding, its average MSF value decreased to 0.64 from 0.95 $Å^2$ in unbound form. Regarding residue based MSF values of these three stacking residues 252, 226 and 229 it was observed that among them only Trp229 MSF value has changed upon BLIP binding. Pro226 has a MSF value of 0.89 and 0.88 $Å^2$ in unbound and BLIP bound TEM-1 respectively. Also Pro252 has a MSF value of 0.78 and 0.79 $Å^2$ in unbound and BLIP bound forms.

On the other hand, MSF value of Trp229 increased from 0.35 $Å^2$ in unbound form to 0.56 $Å^2$ in BLIP bound form. In order to examine the relevance of Trp229 on H10 to overall flexibility and binding, it was substituted with alanine and simulations for both unbound and BLIP bound TEM-1 W229A mutant structures were performed for 10ns.

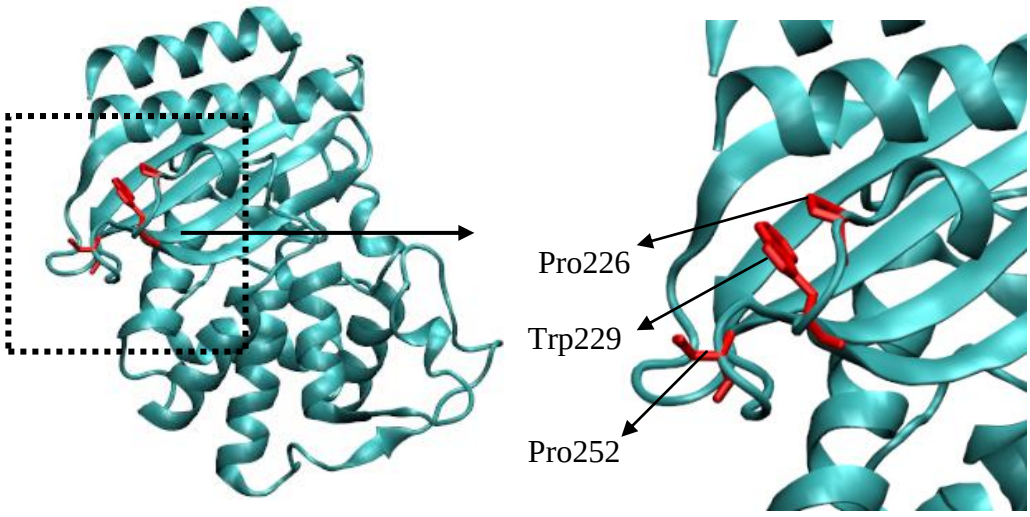

Figure 3.6. Cartoon representation of TEM-1 average simulation structure (TEM-1 – BLIP simulation) that highlights stacking composition of Pro226, Trp229 and Pro252.

TEM-1 and TEM-1 with mutation W229A were compared in their unbound forms in order to find out the effect of W229A mutation on TEM-1 (Figure 3.7). The average mobility of TEM-1 is around 37 $Å^2$ both in wild type and mutated form. In order to identify the regions that lost or gained mobility due to mutation, residue based MSF values were calculated and compared for TEM-1 (Figure 3.7a) and TEM-1 W229A mutant (Figure 3.7b), also the difference was calculated (Figure 3.7c) and mapped onto the structure (Figure 3.7d) as described for Figure 3.4. According to the Figure 3.7d the biggest differences are in the H10 helix region and Ala86 located on the loop connecting H2 helix (69 to 84) to b2 strand (94 to 97).

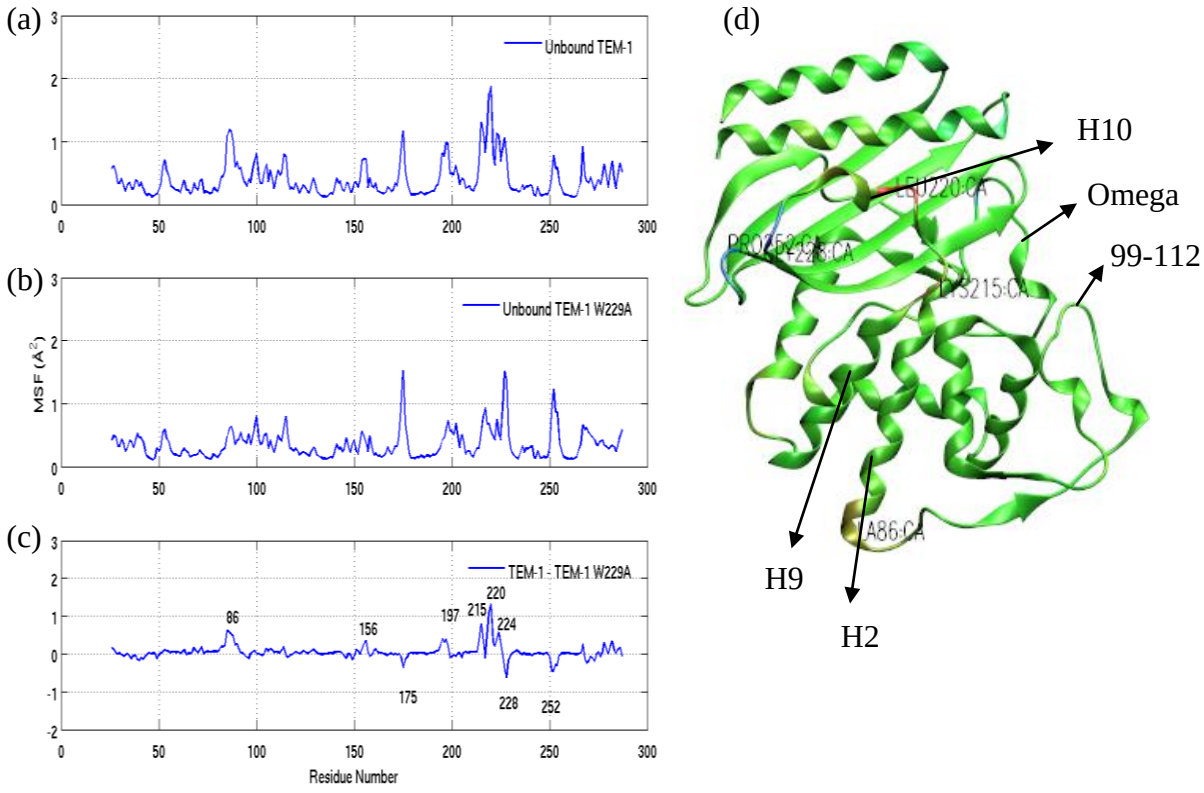

Figure 3.7. Residue based MSF of unbound TEM-1 (a) and TEM-1 W229A mutant (b) and the change in mobility of TEM-1 due to W229A mutation (c), TEM-1 structure colored by MSF value difference (d).

Flexibility of H10 helix (218 to 230) decreased from 0.95 to 0.70 $Å^2$ with W229A mutation (Table 3.1). Leu220 of H10 lost mobility very significantly after W229A mutation on TEM-1 and colored red because of the high MSF value of wild type TEM-1. On the other hand, Gly228 of H10 gained mobility due to W229A mutation (blue). Lys215 on the loop connecting H9 and H10 helices lost mobility and colored orange and also

Glu197 on the loop near the N-terminus of H9 helix lost some mobility (Figure 3.7c and Figure 3.7d).

Omega loop flexible part mobility increased from 0.84 to 1.04 $Å^2$ due to the mutation (Table 3.1). However, Gly156 on the loop connecting omega loop to H6 (145 to 154) lost some mobility.

Pro252 on the loop connecting B4 (243 to 251) and B5 (259 to 266) beta-strands which is also in the stacking structure with Pro226 and Trp229 of H10 helix, colored blue that represents high increase in mobility due to mutation (Figure 3.7d).

TEM-1 and TEM-1 W229A mutant was also compared in the presence of BLIP in order to find out the effect of W229A mutation on binding (Figure 3.8).

The overall mobility of both TEM-1 and TEM-1 (W229A) decreased to 0.28 $Å^2$ about from 0.37 $Å^2$ upon BLIP binding. Comparison of the BLIP bound TEM-1 with BLIP bound TEM-1 (W229A) (Figure 3.8) indicates that certain structural elements respond differently in the wild type and the mutant. The most significant differences between wild type and mutated TEM-1 in the presence of BLIP are at residues Leu198 and Ala213 that are located near the N and C terminuses of H9 helix (201 to 212) respectively, where blue indicates the increase upon mutation and red for the decrease after the mutation (Figure 3.8d).

In the BLIP bound form, H10 helix of TEM-1 lost some flexibility with W229A mutation and its MSF value decreased from 0.64 to 0.45 $Å^2$ while 99-112 loop and omega loop did not reveal change in flexibility due to mutation. On the other hand, Gly156 on the loop connecting omega loop to H6 helix (145 to 154) enhanced its mobility slightly.

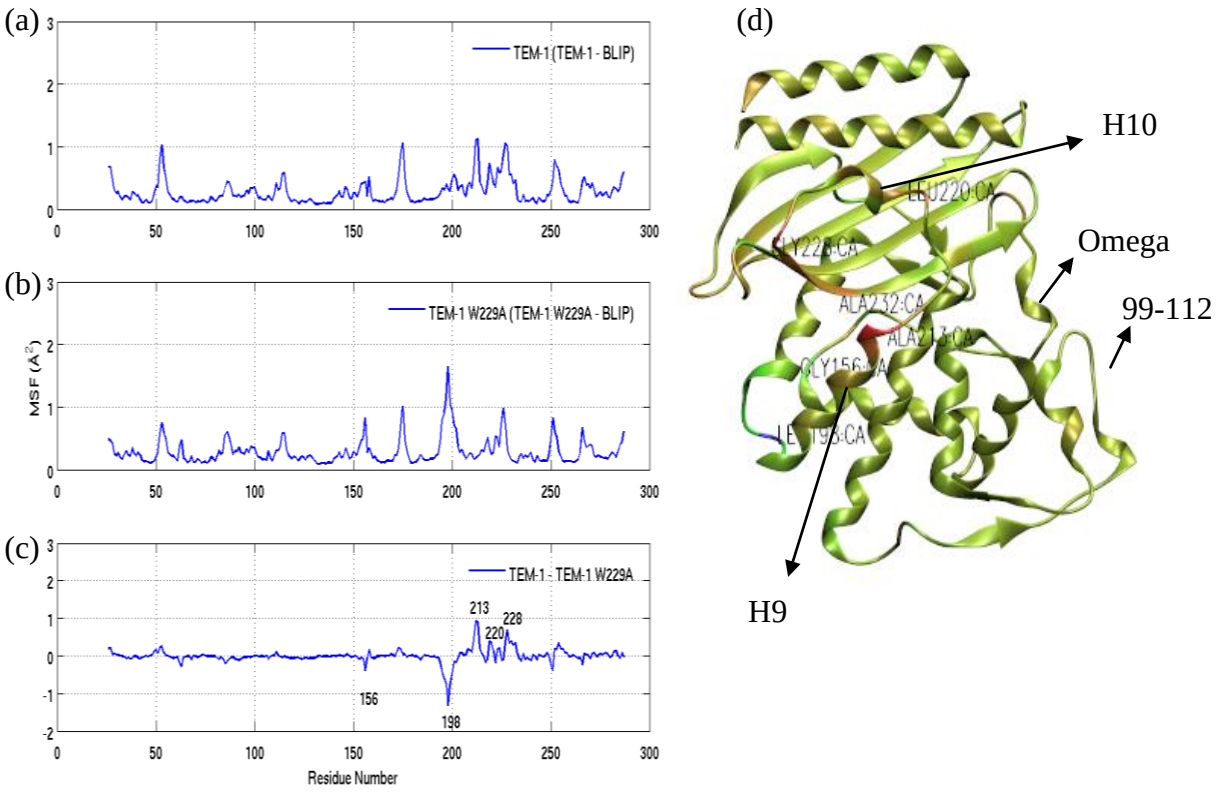

Figure 3.8. Residue based MSF of TEM-1 (a) and TEM-1 W229A mutant (b) in the presence of BLIP, the change in mobility of TEM-1 due to mutation (c), TEM-1 structure colored by MSF value difference (d).

3.2.4. Mobility of SHV-1 Beta-lactamase in Unbound and BLIP Bound Forms

Mean square fluctuations were calculated in order to gain an idea about average mobility of SHV-1 (Table 3.1) and also mobility of its important regions (Table 3.2) in its unbound and BLIP bound forms.

The average mobility of SHV-1 beta-lactamse stayed around 0.30 $Å^2$ in the presence or absence of BLIP (Table 3.1). To identify the regions that lost or gained mobility due to BLIP binding, residue based MSF values were calculated and compared for the unbound (Figure 3.9a) and BLIP bound (Figure 3.9b) SHV-1, also the difference between unbound and BLIP bound SHV-1 was calculated (Figure 3.9c) and mapped onto the structure (Figure 3.9d) as described for Figure 3.4.

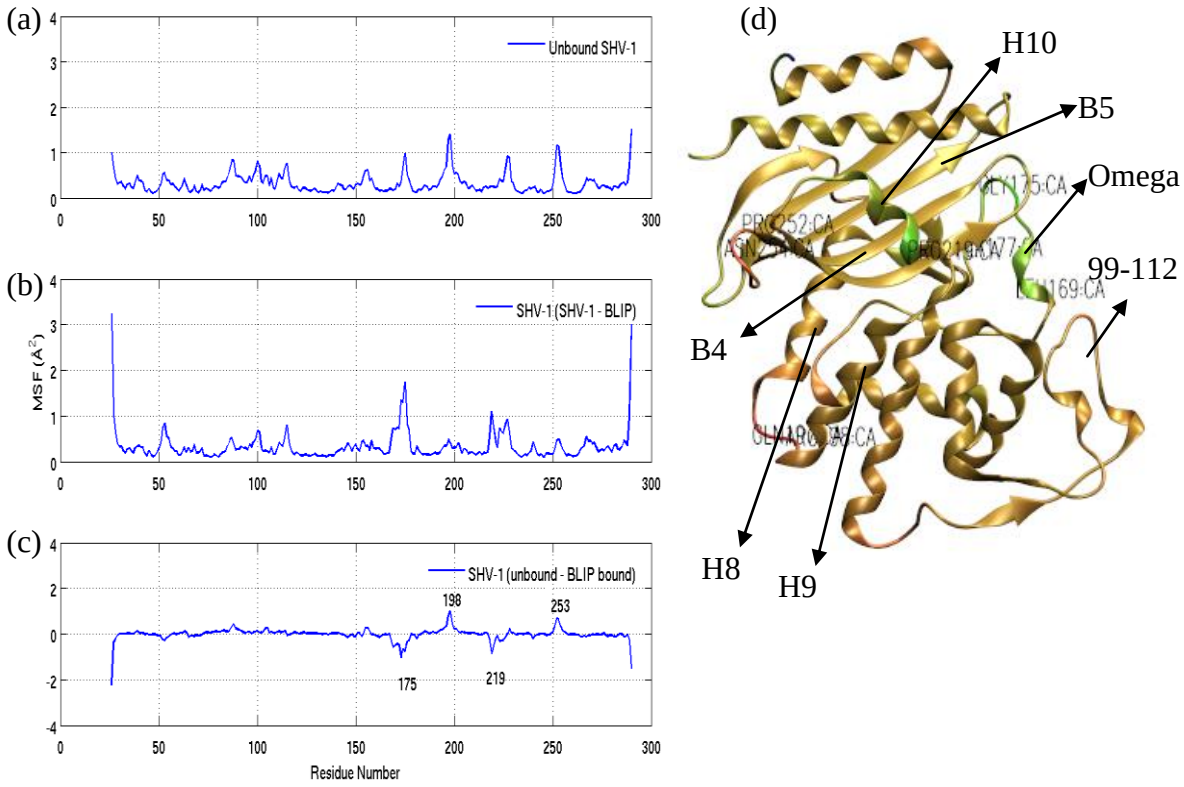

Figure 3.9. Residue based MSF of unbound SHV-1 (a), BLIP bound SHV-1 (b) and the change in mobility due to BLIP binding (c), SHV-1 structure colored by residue based MSF value difference (d).

Unbound SHV-1 has a low flexible H10 helix with 0.42 $Å^2$ of MSF value. However BLIP binding increased its MSF value to 0.62 $Å^2$ and H10 helix became more mobile (Table 3.2).

Omega loop (161 to 179) of unbound SHV-1 is almost rigid with 0.29 $Å^2$ of MSF value. The flexible tip of omega loop has a MSF value of 0.71 $Å^2$. However, omega loop especially its flexible part (174 to 176) gained mobility due to BLIP binding and their MSF values increased to 0.59 and 1.29 $Å^2$ respectively (Table 3.2).

Figure 3.9d represents most significant differences between unbound and BLIP bound SHV-1. While H10 helix and omega loop gaining mobility due to BLIP binding (green), residues 196 to 198 on the loop connecting H8 (183 to 195) and H9 (201 to 212) helixes, and 252 to 254 on the loop connecting B4 (243 to 251) and B5 (259 to 266) beta-strands lost mobility arising from BLIP binding (red). However, 99-112 loop did not reveal

a significant change due to BLIP binding its MSF value slightly decreased from 0.45 to 0.34 $Å^2$ in the presence of BLIP (Table 3.2).

3.2.5. The Effect of BLIP D49A Mutation on SHV-1 Mobility

The overall mobility of SHV-1 was not affected due to D49A mutation with MSF value of 0.33 $Å^2$ in BLIP bound form and 0.32 $Å^2$ in BLIP (D49A) bound form. A similar comparison showed that TEM-1 mobility also stayed constant at around 0.26 $Å^2$ in the wild type or mutant BLIP bound states (Table 3.1).

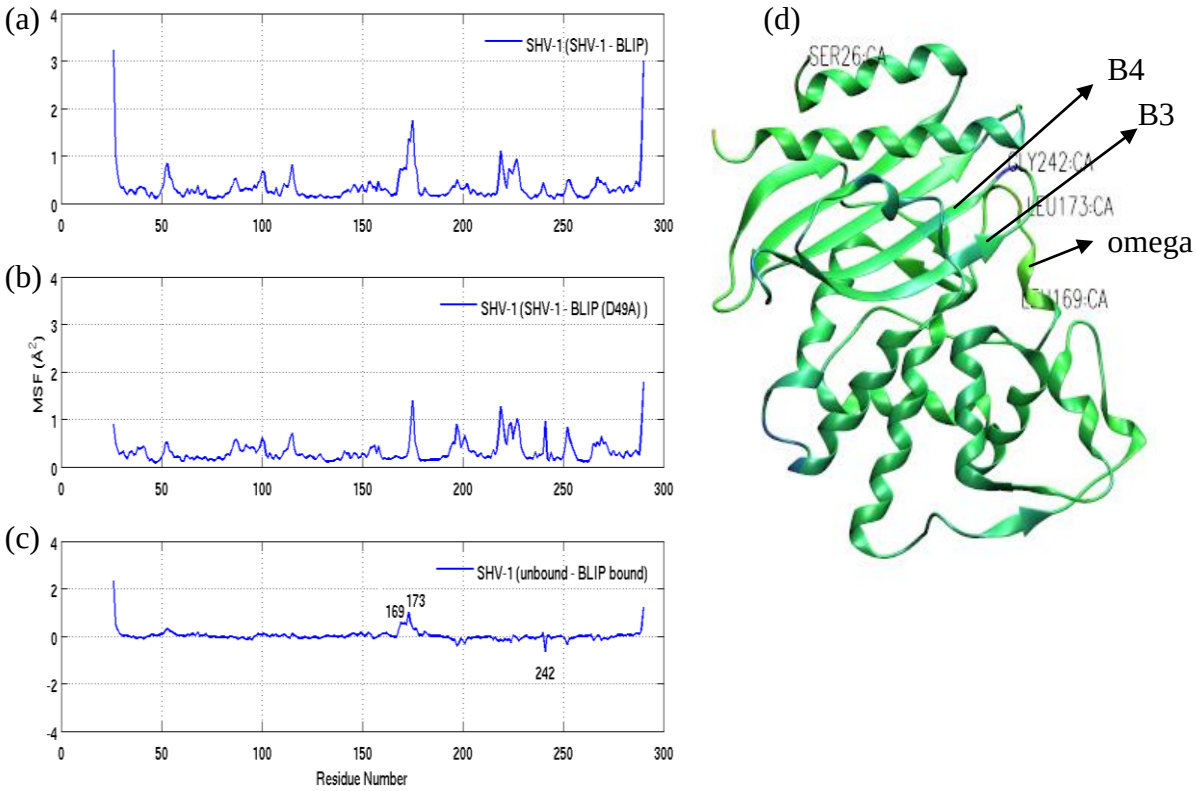

Figure 3.10. Residue based MSF of SHV-1 in the presence of BLIP (a) and BLIP (D49A) (b), the change in mobility of SHV-1 due to D49A mutation (c), SHV-1 structure colored by residue based MSF value difference (d).

To identify the regions that lost or gained mobility due to the mutation, residue based MSF values were calculated and compared for the BLIP bound (Figure 3.10a) and BLIP (D49A) bound (Figure 3.10b) SHV-1, also the difference was calculated (Figure 3.10 C) and mapped onto the structure (Figure 3.10d) as described for Figure 3.4. According to

that the residue based MSF values revealed only slight changes due to the mutation (Figure 3.10c and d).

Omega loop (161 to 179) lost some mobility after D49A mutation and its MSF value decreased to 0.32 from 0.59 $Å^2$ in the wild type and also omega loop flexible part mobility decreased to 0.90 from 1.29 $Å^2$. On the other hand, Gly242 on the loop connecting B3 (230 to 238) and B4 (243 to 251) beta-strands gained some mobility due to D49A mutation on BLIP.

3.2.6. Comparison of TEM-1 Beta-lactamase with SHV-1 Beta-lactamase

TEM-1 and SHV-1 beta-lactamases are 68% identical in amino acid sequence and their three dimensional structures are virtually superimposable (Jelsch *et al.*, 1993, Kuzin *et al.*, 1999). Also, TEM-1 and SHV-1 beta-lactamases share similar substrate profiles that both hydrolyze the older beta-lactam antibiotics such as penicillin, ampicillin, and cephalosporin C (Heritage *et al.*, 1999). Nevertheless beta-lactamase inhibitor protein (BLIP) binds and inhibits TEM-1 1000 times more than it inhibits SHV-1. BLIP binds to TEM-1 with nanomolar affinity but binds to SHV-1 with micromolar affinity (Kuzin *et al.*, 1999).

According to this study it has been found that TEM-1 beta-lactamase is more mobile than SHV-1 beta-lactamase in the unbound form with average MSF values of 0.39 $Å^2$ and 0.32 $Å^2$ respectively (Table 3.1). Residue based MSF values were calculated and compared for the unbound TEM-1 (Figure 3.11a) and unbound SHV-1 (Figure 3.11b), also the difference between them was calculated (Figure 3.11c) and mapped onto the structure (Figure 3.9d) as described for Figure 3.4.

The main difference arises from a more mobile H9-H10 region (201 to 230), MSF value of which is 0.70 $Å^2$ in TEM-1 and 0.34 $Å^2$ in SHV-1 structure. Especially H10 helix of TEM-1 is very mobile with a MSF value of 0.95 $Å^2$ while it is 0.42 $Å^2$ in SHV-1 structure (Figure 3.11c). Also, Leu198 near the N-terminus of the H9 helix and residues 253 to 255 on the connecting loop of B4 and B5 beta-strands revealed significant difference but in this case flexibility is high in SHV-1 (Figure 3.11d).

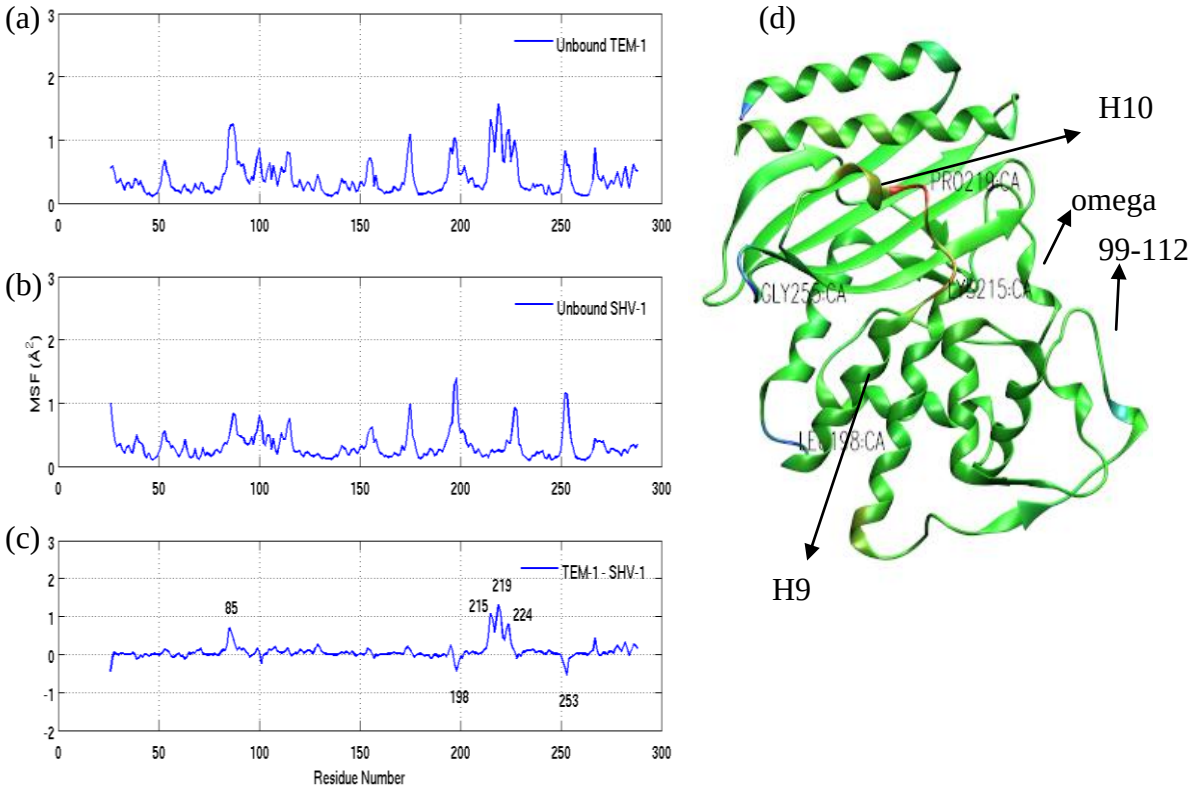

Figure 3.11. Residue based MSF of TEM-1 (a) and SHV-1 (b) and the difference between TEM-1 and SHV-1 (c), beta-lactamase structure colored by MSF value difference between TEM-1 and SHV-1(d).

The active site of TEM-1 is less stable than that of SHV-1 and MSF value of SHV-1 active site is 0.11 $Å^2$ which is nearly half of the MSF value of active site residues of TEM-1 with a MSF value of 0.23$Å^2$ (Table 3.1).

On the other hand, flexibilities of 99-112 loop, omega loop and omega loop flexible part did not present a significant variation between unbound TEM-1 and SHV-1.

TEM-1 and SHV-1 structures were also compared in the presence of BLIP in order to evaluate the difference between TEM-1 and SHV-1 and also to investigate the probable reasons of difference in affinity that BLIP revealed to them.

According to the Table 3.1, BLIP binding decreased mobility of TEM-1 from 0.39 $Å^2$ in unbound structure to 0.28 $Å^2$ in BLIP bound structure whereas SHV-1 did not affected from BLIP binding and both unbound and BLIP bound SHV-1 has MSF value

around 0.30 $Å^2$. The larger difference in mobility of TEM-1 upon BLIP binding is due to the drop in flexibility of H10 helix from 0.95 to 0.64 $Å^2$ MSF value. The flexibility of this region is very low (0.42) in apo SHV-1 and increased to 0.62 $Å^2$ upon BLIP binding (Table 3.2).

On the other hand, omega loop and particularly its flexible tip did not affected in TEM-1 upon BLIP binding, but their flexibility increased significantly in SHV-1 due to BLIP binding. The MSF values of omega loop and its flexible tip are 0.29 and 0.81 $Å^2$ in TEM-1 in the presence of BLIP whereas their MSF values are 0.59 and 1.29 $Å^2$ in SHV-1 in the presence of BLIP.

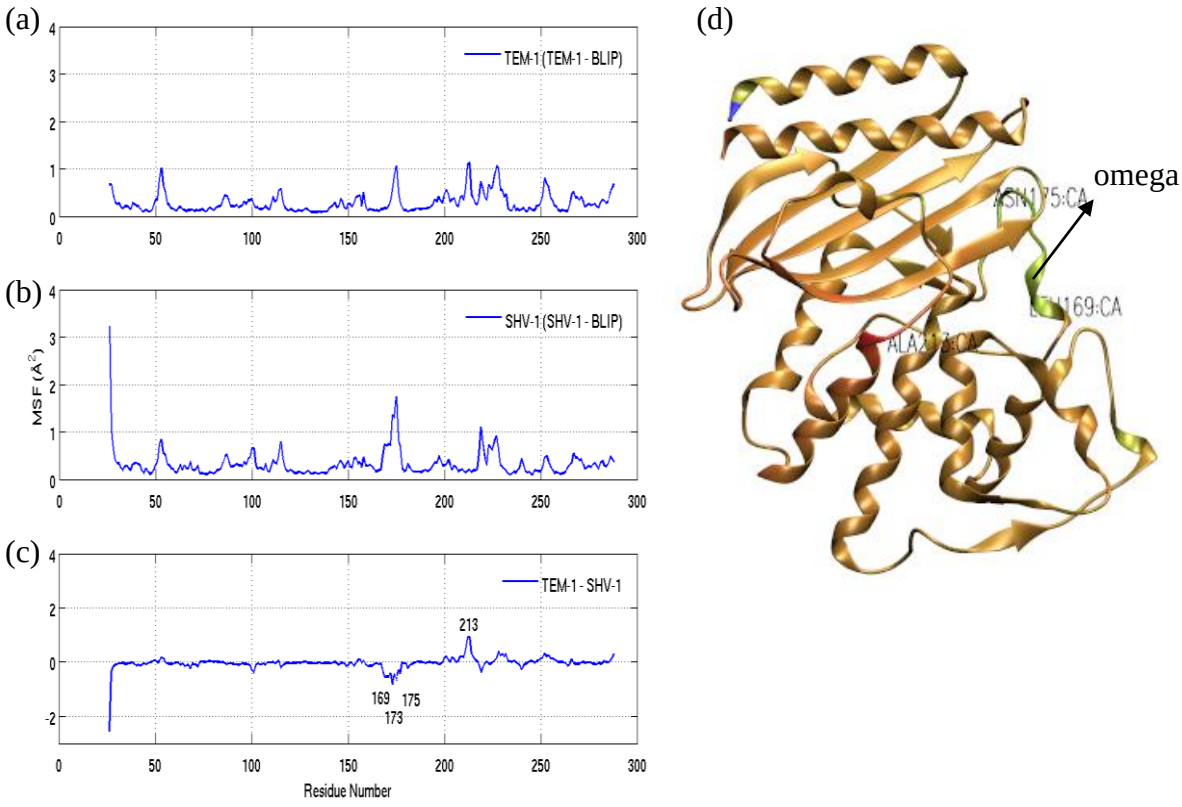

Figure 3.12. MSF of TEM-1 (a) and SHV-1 (b) in the presence of BLIP, the difference between BLIP bound TEM-1 and BLIP bound SHV-1 (c) beta-lactamse structure colored by MSF value difference.

Residue based MSF values were calculated and compared for TEM-1 (Figure 3.12a) and SHV-1 (Figure 3.12b) in the presence of BLIP, also the difference between them was

calculated (Figure 3.12c) and mapped onto the structure (Figure 3.12d) as described for Figure 3.4.

According to the Figure 3.12d, the residue based MSF value difference between TEM-1 and SHV-1 in their BLIP bound structures is very significant in the region corresponds to 169 to 175 of omega loop that is highlighted with green which indicates low flexibility in TEM-1 compared to SHV-1. Among these residues 173 and 175 are different which is Ile173 and Asn175 in TEM-1 and Leu173 and Gly175 in SHV-1. The difference between the mobility of omega loop of TEM-1 and SHV-1 in BLIP bound structures may be causing the difference in affinity to BLIP.

Previous studies have also suggested that omega loop is a structural motif of class A beta-lactamases that contributes to the substrate specificity profile of these enzymes (Matagne *et al.*, 1998, Petrosino and Palzkill, 1996). In addition, the difference in the response of H10 helix to BLIP binding may contribute to the variation in BLIP binding affinity for the two enzymes.

A comparison of the residue averaged MSF values for beta-lactamase in different simulations showed that most of them stayed around 0.30 $Å^2$, except Apo TEM-1 for which the residue averaged MSF value is highest at 0.39 $Å^2$ (Table 3.1). BLIP binding to TEM-1 reduced the average MSF value of TEM-1 (0.28 $Å^2$), but BLIP binding to SHV-1 did not change the MSF value of SHV-1. Average mobility of Apo TEM-1 (0.39 $Å^2$) slightly decreased upon W229A mutation (0.35 $Å^2$). TEM-1 (W229A) was affected by BLIP binding; similar to the decrease in MSF value for TEM-1, the MSF value of TEM-1 (W229A) decreased from 0.35 $Å^2$ to 0.28 $Å^2$ after BLIP binding.

The MSF values for BLIP in the different simulations were higher at around 0.45 $Å^2$ than the MSF values for the beta-lactamases at around 0.30 $Å^2$. The apo forms of BLIP and BLIP (D49A) had the highest MSF values at 0.57 and 0.58 $Å^2$. Beta-lactamase binding reduced the MSF values of BLIP to 0.45 $Å^2$ (TEM-1 binding) and 0.49 $Å^2$ (SHV-1 binding) while beta-lactamase binding to BLIP (D49A) resulted in lower MSF values at 0.34 $Å^2$ (with TEM-1) and 0.37 $Å^2$ (with SHV-1). W229A mutation on TEM-1 had similar effect on BLIP mobility, with a decrease to 0.44 $Å^2$ from 0.57 $Å^2$.

When the average mobility of the complexes are compared, one can see that the MSF values are all around 0.50 $Å^2$, except for TEM-1 – BLIP (D49A) complex, for which the MSF value is 0.37 $Å^2$. This reduction is due to the reduction lower BLIP (D49A) mobility in the complex simulations.

In an effort to determine the structural elements contributing to the change in RMSD and change in MSF for different simulation systems, RMSD and MSF values for these regions were calculated (Table 3.2). These important regions of beta-lactamase were highlighted in Figure 1.1.

The RMSD values on Table 3.2 were calculated with VMD RMSD Trajectory Tool and the script in Appendix A by using the initial simulation structure file and also trajectory file obtained during each simulation to find the deviation from the initial structure. To calculate RMSD values of H10 helix, H9-H10 region, 99-112 loop, omega loop, omega loop flexible tip and also active site residues, average structure of beta-lactamase that was obtained from the trajectory file according to the equilibrium period of the simulation was aligned to the initial simulation structure of beta-lactamase based on C_α atoms and the deviation of each region between its conformation in the average structure and its initial conformation was calculated. The MSF values were calculated from the trajectory file of each simulation system by using Matlab and the script in Appendix B. After the alignment of the time averaged beta-lactamase structure from the simulation on the initial simulation structure of beta-lactamase based on C_α atoms, residue averaged MSF values of these regions were calculated for the equilibrium period of the simulations.

In the apo form, H9-H10 helices and the omega loop flexible part are the most mobile in TEM-1 with average MSF values higher than 0.70 $Å^2$ (Table 3.2) compared to the overall average MSF value of 0.39 $Å^2$ (Table 3.1). For SHV-1, on the other hand, the overall average MSF value is 0.32 $Å^2$ (Table 3.1) and structural elements that were examined exhibited fluctuations close to this value except for the omega loop flexible part, whose average MSF value is 0.71 $Å^2$ (Table 3.2).

Table 3.2. RMSD (Å) and MSF (Å^2) values of important regions on beta-lactamase in each simulation system (MSF values are in parenthesis).

Simulation System	H10	H9-H10	99-112 loop	Ω loop	Ω loop flexible part	Active Site Residues
TEM-1 (4-10 ns)	1.77 (0.95)	1.34 (0.70)	0.64 (0.49)	0.59 (0.35)	1.19 (0.84)	0.55 (0.23)
TEM-1 (W229A) (4-10 ns)	2.15 (0.70)	1.94 (0.54)	0.91 (0.44)	0.71 (0.38)	1.46 (1.04)	0.56 (0.21)
TEM-1 – BLIP (2-10 ns)	0.92 (0.64)	1.06 (0.54)	0.62 (0.23)	0.88 (0.29)	1.38 (0.81)	0.58 (0.11)
TEM-1 - BLIP (D49A) (1.5-10 ns)	1.21 (0.48)	1.53 (0.35)	0.50 (0.19)	0.84 (0.34)	1.59 (1.22)	0.73 (0.24)
TEM-1 (W229A) – BLIP (2.5-10 ns)	1.30 (0.45)	1.47 (0.37)	0.64 (0.24)	0.92 (0.26)	1.62 (0.72)	0.71 (0.14)
SHV-1 (1.5-10 ns)	2.67 (0.42)	2.03 (0.34)	0.64 (0.45)	0.52 (0.29)	0.61 (0.71)	0.56 (0.12)
SHV-1 – BLIP (5-10 ns)	1.29 (0.62)	0.98 (0.40)	0.68 (0.34)	1.03 (0.59)	0.89 (1.29)	0.57 (0.15)
SHV-1 - BLIP (D49A) (5-10 ns)	1.16 (0.75)	1.35 (0.50)	0.69 (0.30)	0.70 (0.32)	0.86 (0.90)	0.61 (0.18)

BLIP binding to TEM-1 decreased flexibility of H10 helix from 0.95 Å^2 in unbound structure to 0.64 Å^2. Mutation at position 49 of BLIP from aspartic acid to alanine reduced mobility of H10 helix further to 0.48 Å^2 but its deviation from the initial structure increased to 1.21 Å due to mutation. In other words D49A mutation on BLIP decreased mobility of H10 helix in TEM-1 but it deviated from its initial structure more because of the loss of interactions between BLIP 49 and active site residues of TEM-1.

H10 helix is less flexible in SHV-1 (0.42 Å^2) than TEM-1 (0.95 Å^2). BLIP binding increased its mobility to 0.62 Å^2 in SHV-1 while BLIP binding decreased the mobility of H10 in TEM-1 (0.64 Å^2). The difference in the response of H10 helix to BLIP binding may contribute to the variation in BLIP binding affinity for the two enzymes.

Despite its low flexibility, H10 helix of SHV-1 deviated from its initial structure with a RMSD value of 2.67 Å which is significantly higher than the RMSD values for H10 in the other simulations with RMSD values around 1.50 Å. This high deviation of H10 in

SHV-1 structure arising from its alternate conformation. In the initial simulation structure, H10 helix in the SHV-1 – BLIP structure had a position similar with the H10 helix of both unbound and BLIP bound TEM-1 but H10 helix of the unbound SHV-1 had a different conformation with respect to them, this finding was also obtained in a previous study which suggested that H10 helix of SHV-1 – BLIP structure partially unravels at N-terminus, assuming a structure similar to the H10 helix as observed in both the unbound and bound forms of TEM-1 (Reynolds *et al.*, 2006). However during the simulation, H10 helix in unbound SHV-1 changed its position and at the end of the simulation it stayed nearly similar position with the H10 position in SHV-1-BLIP structure.

Simulation of W229A mutant of TEM-1 was performed in order to examine the relevance of Trp229 on H10 to overall flexibility and binding by substituting it with alanine. In the W229A mutant of TEM-1, H10 helix became less mobile than its counterpart in the wild type with a MSF value of 0.70 $Å^2$ while MSF value of H10 of wild type is 0.95 $Å^2$. When the individual MSF values of each residue of the H10 helix was calculated it was observed that Ala229 of mutant (0.50 $Å^2$) is more mobile than Trp229 of wild type (0.35 $Å^2$) with a bulkier side chain. Nevertheless, neighboring residues became less mobile due to the W229A mutation and as a result average mobility of H10 in the TEM W229A mutant has decreased. On the other hand it deviated from initial structure more, with a RMSD value of 2.15 Å, while its RMSD is 1.77 Å in TEM-1. BLIP binding reduced both MSF (0.45 $Å^2$) and RMSD (1.30 Å) values of H10 in mutant TEM-1 similar to wild type TEM-1.

The omega loop flexible part is a very mobile and flexible region of both beta-lactamases in apo and BLIP bound forms. The MSF value of omega loop flexible part is 0.84 $Å^2$ in unbound TEM-1 and BLIP binding did not affect its flexibility (0.81 $Å^2$). On the other hand, BLIP (D49A) binding increased the flexibility to 1.22 $Å^2$ due to the significant increase in mobility of Asn175 from 1.10 $Å^2$ in wild type to 1.97 $Å^2$ after D49A mutation on BLIP. Binding of BLIP to SHV-1 increased mobility of omega loop flexible part significantly from 0.71 $Å^2$ in unbound structure to 1.29 $Å^2$ in BLIP bound structure arising from the significant increase in mobility of Gly175 (from 1.00 to 1.74 $Å^2$). On the other hand with D49A mutation on BLIP mobility of the flexible tip decreased to 0.90 $Å^2$ due to the decrease in mobility of Gly175 (from 1.74 to 1.40 $Å^2$). Due to W229A mutation on

TEM-1, the flexibility of omega loop flexible part increased to 1.04 $Å^2$ from 0.84 $Å^2$ in wild type TEM-1 structure. When BLIP bound to TEM-1 (W229A), MSF value of flexible part decreased to 0.72 $Å^2$.

Unlike its flexible tip omega loop is slightly flexible feature of beta-lactamases. Its MSF value in TEM-1 is 0.35 $Å^2$ while it is 0.38 $Å^2$ in TEM-1 (W229A) and also 0.29 $Å^2$ in SHV-1. While BLIP binding decreased mobility of omega loop in TEM-1 and TEM-1 W229A mutant slightly (0.29 and 0.26 $Å^2$), BLIP binding increased mobility of omega loop in SHV-1 significantly from 0.29 to 0.59 $Å^2$ due to the significant increase in mobility of its flexible tip which increased from 0.71 to 1.29 $Å^2$ as a result of BLIP binding. Residue 175 located in the tip of the omega loop varies between TEM-1 and SHV-1 which is aspargine with bulkier side chain in TEM-1 and glycine in SHV-1. Both in unbound and BLIP bound forms of TEM-1, Asn175 has a MSF value of 1.10 $Å^2$ while Gly175 of SHV-1 increased from 1.00 to 1.74 $Å^2$ after BLIP binding. The significant increase in mobility of Gly175 in SHV-1, lead the high mobile omega loop in SHV-1 – BLIP structure unlike the low mobile omega loop in other simulation systems. The difference between residue 175 of omega loop in TEM-1 (Asn175) and SHV-1 (Gly175) may be a probable reason that BLIP reveals different affinity to them which is higher for TEM-1. The previous studies have also suggested that omega loop is a structural motif of class A beta-lactamases that contributes to the substrate specificity profile of these enzymes (Matagne *et al.*, 1998, Petrosino and Palzkill, 1996).

BLIP binding increased the deviation of omega loop from its initial structure in each beta-lactamase. The deviation of omega loop in TEM-1 increased from 0.59 to 0.88 Å while it increased from 0.52 to 1.03 Å in SHV-1 and from 0.71 to 0.92 in TEM-1 (W229A) due to the BLIP binding. While D49A mutation did not affect the deviation of omega loop in TEM-1, it reduced RMSD value of omega loop in SHV-1 to 0.70 from 1.03 Å.

The 99-112 loop is not as mobile and flexible as H10 and omega loop flexible part. The mobility of 99-112 loop in the apo forms of TEM-1, TEM-1 (W229A) and SHV-1 are very close to each other with MSF values of 0.49, 0.44 and 0.45 $Å^2$ respectively. Each beta-lactamase revealed same pattern to BLIP binding by decreasing the flexibility of 99-112 loop (0.23 in TEM-1, 0.24 in TEM-1 (W229A) and 0.34 in SHV-1) but this decrease

is less significant in SHV-1. The concave beta-sheet region of BLIP sits on top of the 99-112 loop and the presence of BLIP may restricts 99-112 loop mobility. Arising from D49A mutation on BLIP, flexibility of 99-112 loop decreased some more both in TEM-1 (0.19 $Å^2$) and SHV-1 (0.30 $Å^2$). Because $Ala49_{BLIP}$ lost its strong interactions with the active site pocket residues of TEM-1 so it moved away from the active site pocket some while it came close to 99-112 loop and this motion restricts mobility of 99-112 loop more.

According to the RMSD values of 99-112 loop, BLIP and BLIP (D49A) binding did not change its deviation from initial structure both in TEM-1 and SHV-1 and it deviated around 0.60 Å. On the other hand, due to W229A mutation on unbound TEM-1, 99-112 deviated from its initial structure with a RMSD of 0.91 Å. However BLIP binding to TEM-1 W229A mutant decreased mobility of 99-112 loop to the same value in the wild type TEM-1 complex. In the initial simulation structure 99-112 loop in TEM-1 and TEM-1 W229A mutant were at the same position in both the bound and unbound forms. However during the simulation 99-112 loop of other three nearly stayed at the same position with respect to each other, while 99-112 of the unbound TEM-1 W229A mutant revealed some deviation with respect to counterpart in the other simulation systems.

According to these findings H10 helix and omega loop are the important features of beta-lactamases and the configuration and mobility of these features can affect the beta-lactamase response to BLIP binding.

3.3. Energy Calculations of the Simulation Systems

3.3.1. Intermolecular Interaction Energy

The intermolecular interaction energy between the beta-lactamase and the ligand is important to understand binding mechanism. For this purpose, non-bonded interactions between the beta-lactamase and the ligand were examined. Interaction energy between the beta-lactamase and the ligand was calculated from the simulation trajectory file by using NAMD Energy Plugin of VMD and an output file that comprises interaction energies every 0.1 ns of time step was gained for each simulation system. Examination of energy profiles can give a clue about binding affinity of each complex and also their behaviors

during the simulation whether the beta-lactamase and the ligand move away from each other or they come close.

Figure 3.13 reveals the electrostatic interaction energy profiles of simulation systems in which electrostatic interaction energy value ranges between -200 and -700 kcal/mol in different simulations while Figure 3.14 shows vdW interaction energy profiles whose value ranges between -70 and -130 kcal/mol. The non-bonded interaction energy which is totaling of electrostatic and vdW interactions between beta-lactamase and the ligand was showed in Figure 3.15 for each simulation system in which non-bonded interaction energy value ranges between -300 and -800 kcal/mol for different simulations. Thus electrostatic interaction is the major contribution to the non-bonded interaction energy between beta-lactamase and the ligand.

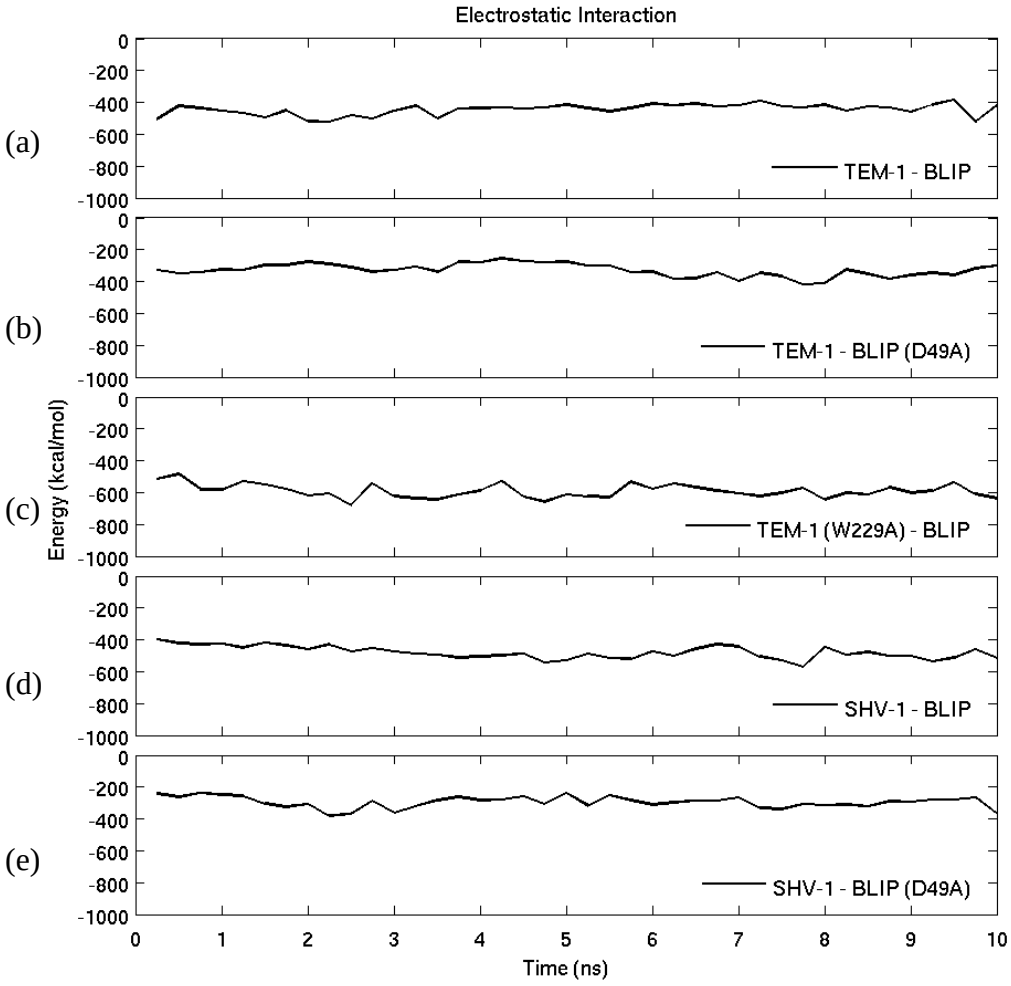

Figure 3.13. Electrostatic interaction profile of simulation systems.

The electrostatic interaction energy value in TEM-1 - BLIP complex ranges between -380 and -550 kcal/mol during the simulation (Figure 3.13a). W229A mutation on TEM-1 made electrostatic interactions between beta-lactamase and BLIP more favorable in which energy value varies -480 to -700 kcal/mol during the TEM-1 (W229A) – BLIP simulation (Figure 3.13c). On the other hand, D49A mutation on BLIP disfavors the electrostatic interactions and in TEM-1 – BLIP (D49A) simulation electrostatic energy value varies between -270 and -420 kcal/mol (Figure 3.13b). Electrostatic interactions in SHV-1 – BLIP complex with ranging value between -400 and -600 (Figure 3.13d) are close to electrostatic interactions between TEM-1 and BLIP. D49A mutation on BLIP disfavors the electrostatic interactions for SHV-1 ligand complex (-230 to -390) (Figure 3.13e) as it did for TEM-1 ligand complex (Figure 3.13b).

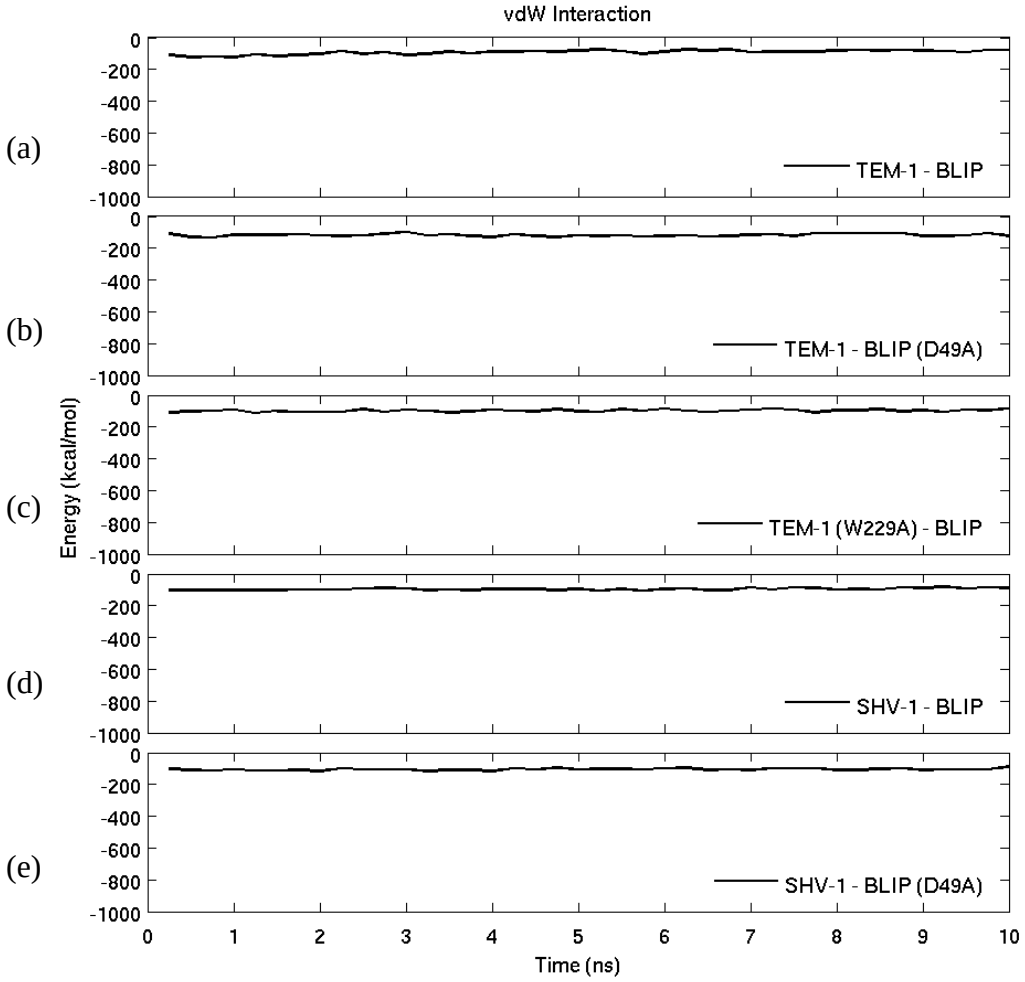

Figure 3.14. vdW interaction profile of simulation systems.

While electrostatic interactions reveal significant differences in each beta-lactamase and ligand complex, vdW intearaction energy profile change around -70 to -130 kcal/mol for each simulation system (Figure 3.14) and vdW interaction has a minor contribution to total energy.

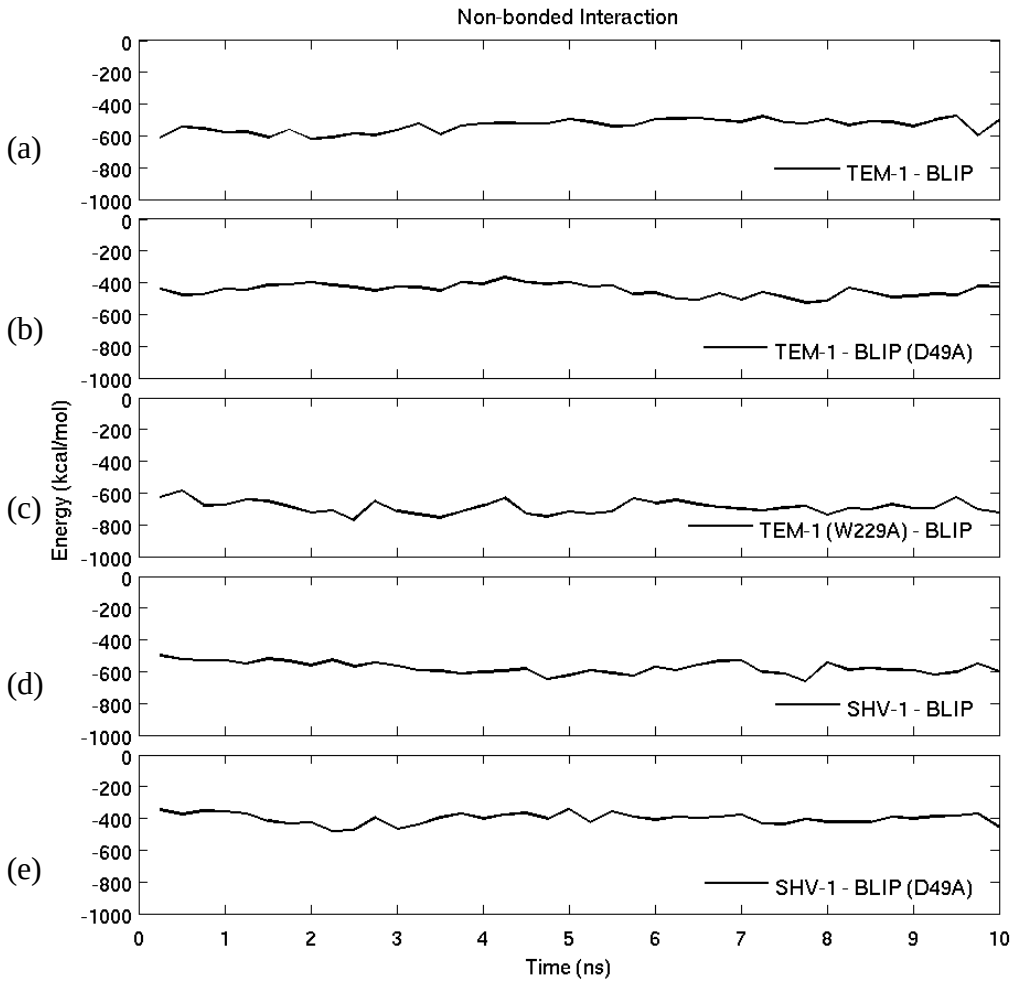

Figure 3.15. Non-bonded interaction (electrostatic + vdW) profile of simulation systems.

Non- bonded interaction energy for TEM-1 – BLIP complex varies between -470 and -620 kcal/mol (Figure 3.15a) throughout the simulation due to the mobility of the beta-lactamase and the ligand. Also TEM-1 (W229A) – BLIP complex revealed a similar energy profile with more favorable energy values ranging between -580 and -770 kcal/mol (Figure 3.15c). The average non-bonded interaction energy of the wild type and the mutant complexes are -514.23 (25.24) kcal/mol and -691.20 (30.34) kcal/mol respectively and standard deviation of the energy values are in parenthesis. According to that, W229A

mutation made non-bonded interactions between beta-lactamase and the ligand stronger. For the SHV-1 – BLIP complex non-bonded interactions (Figure 3.15d) are close to non-bonded interactions of TEM-1 - BLIP complex (Figure 3.15a) with -590.32 (32.68) kcal/mol average non-bonded interaction energy value.

D49A mutation on BLIP disfavors non-bonded interaction for both TEM-1 and SHV-1 beta-lactamases. Also, the fluctuating energy profile of both TEM-1 – BLIP (D49A) and SHV-1 – BLIP (D49A) indicate that BLIP (D49A) was not stable and either moved away from the beta-lactamase or moved towards to it (Figure 3.15b and e). Non-bonded energy profile of TEM-1 – BLIP (D49A) (Figure 3.15b) compared with RMSD profile of BLIP (D49A) in the presence of TEM-1 (Figure 3.3d) and both figures revealed that BLIP (D49A) moved away from TEM-1 during first 5 ns and then moved towards to TEM-1 after 5 ns with some fluctuations. Also non-bonded energy profile of SHV-1 – BLIP (D49A) (Figure 3.15e) was compared with RMSD profile of BLIP (D49A) in the presence of SHV-1 (Figure 3.3f). BLIP (D49A) moved towards to SHV-1 in first 2ns of simulation then did not reveal a significant movement but revealed some fluctuations. The average non-bonded interaction energy between BLIP (D49A) and TEM-1 and SHV-1 beta-lactamases are -465.87 (36) and -400.14 (27.54) kcal/mol respectively.

The binding interface of beta-lactamase and ligand is divided into six clusters which represent crucial interactions between TEM-1 (or SHV-1) beta-lactamase and BLIP (Reichmann *et al.*, 2007). A list of interface cluster residues of TEM-1 – BLIP and SHV-1 – BLIP complexes were given in Table 3.3.

Table 3.3. Cluster residues of TEM-1, SHV-1 and BLIP.

Cluster	**TEM-1 or SHV-1 Residues**	**BLIP Residues**
C1	Ser130, Lys234, Ser235 (TEM), Thr235 (SHV) Arg243(TEM) or Arg244(SHV)	Asp49
C2	Glu104 (TEM), Asp104(SHV), Tyr105, Asn170	Lys74, Phe142 Tyr143
C3	Gln99, Asn100 (TEM), Gln100 (SHV)	His148, Trp150, Arg160
C4	Val103, Pro167, Glu168	Trp162
C5	Met129, Val216	Phe36 , Tyr50
C6	Glu110	Ser71, Ser113

Table 3.4. Intermolecular interaction energy between cluster residues of beta-lactamase and ligand (kcal/mol), standard deviations are in parenthesis.

Cluster	TEM-1 - BLIP	TEM-1 - BLIP (D49A)	TEM-1 (W229A) - BLIP	SHV-1 - BLIP	SHV-1 - BLIP (D49A)
C1	-189.08 (5.24)	-14.23 (2.08)	-178.64 (14.66)	-158.50 (13.16)	-11.81 (2.09)
C2	-104.00 (4.93)	-109.65 (3.88)	-99.5 (3.46)	-87.30 (4.90)	-84.73 (13.98)
C3	-27.57 (4.58)	-39.17 (2.61)	-26.04 (9.12)	-21.27 (4.40)	-20.46 (3.23)
C4	-7.66 (1.47)	-6.39 (1.35)	-6.42 (1.42)	-6.79 (1.89)	-7.32 (3.49)
C5	-4.73 (0.75)	-5.14 (1.30)	-6.45 (0.88)	-5.49 (1.02)	-6.46 (0.94)
C6	-10.20 (6.37)	-29.66 (3.94)	-36.4 (8.73)	-31.31 (3.49)	-29.96 (4.31)

Intermolecular interaction energy represents nonbonded (vdW and electrostatic energy) interaction energy levels between residues. Comparison of intermolecular interaction energy of each cluster in beta-lactamase ligand complexes, can give an idea about binding affinity of complexes. Interaction energy between the clusters was calculated from the simulation trajectory file for each simulation system by using NAMD Energy Plugin of VMD (Table 3.4).

As previously mentioned, Asp49 from the first loop of BLIP is a crucial residue; it aligns itself in the active site and forms four strong hydrogen bonds with four catalytic residues (Ser130, Lys234, Ser235, Arg244). Due to the mutation of aspartic acid to alanine at position 49, the interaction within the cluster 1 of both TEM-1 and SHV-1 complexes were affected significantly and changes from -189.08 kcal/mol in TEM-1 – BLIP to -14.23 in TEM-1 – BLIP (D49A) structure. Likewise interaction energy changed from -158.50 kcal/mol in SHV-1 – BLIP to -11.81 in SHV-1 – BLIP (D49A). This increase in energy indicates reduction of interaction between beta-lactamase and the ligand. Interaction energy of other clusters in SHV-1 – BLIP complex was not affected from D49A mutation. However, cluster 3 and cluster 6 in TEM-1 – BLIP complex revealed some change in energy due to mutation (Table 3.4).

The intermolecular interaction energy difference between cluster 1 of TEM-1 (-189.08) and SHV-1 (-158.50) complexes was mainly due to interaction difference of Asp49 of BLIP with Lys234 of TEM-1 rather than residues Ser130, Ser235 and Arg243 (or Arg244 for SHV-1) of TEM-1 in cluster 1. The electrostatic interaction energy of $Lys234_{TEM}$ - $Asp49_{BLIP}$ in TEM-1 – BLIP complex is -95.37 while it is -48.29 kcal/mol for SHV-1 – BLIP complex. The electrostatic interaction energies of BLIP 49 with Ser130, Ser235 and Arg243 (or Arg244 for SHV-1) are nearly the same for both TEM-1 - BLIP and SHV-1 - BLIP complexes.

While intermolecular interaction energy of cluster 3 in TEM-1 – BLIP complex is -27.57 kcal/mol, it became -39.17 due to BLIP D49A mutation. None of the cluster 3 residues (Gln99, Asn100, His148, Trp150, Arg160) has an electrostatic or vdW interaction with residue 49 and their distance from residue 49 is around 20 to 25 Å. The intermolecular interaction energy of cluster 3 residues were calculated as interacting pairs in which each pair consists of one residue from TEM-1 and other from BLIP or BLIP(D49A) to examine individual contribution of each residue to interaction energy. 99_{TEM}-160_{BLIP} pair has intermolecular interaction energy of -4.2 kcal/mol and after D49A mutation it became -14.13 kcal/mol. Other interacting residue pairs; 99_{TEM}-148_{BLIP}, 99_{TEM}-150_{BLIP}, 100_{TEM}-148_{BLIP}, 100_{TEM}-150_{BLIP} and 100_{TEM}-160_{BLIP} revealed no significant change in interaction energy value due to mutation. So it can be inferred that the change in interaction energy of cluster 3 from -27.57 kcal/mol in wild type to -39.17 kcal/mol in mutated complex is mainly due to change in interaction energy of Gln99 from TEM-1 with Arg160 from BLIP. Based on this, D49A mutation makes interaction energy of cluster 3 more favorable by enhancing the electrostatic interactions between Gln99 and Thr160. The distance between 99_{TEM} and 160_{BLIP} is about 9Å in both wild type and mutated complex.

The electrostatic interaction is more significant than vdW interaction for cluster 6 with -9.7 kcal/mol and -0.51 kcal/mol respectively for wild type TEM-1 – BLIP complex. D49A mutation changed interaction energy of cluster 6 from -10.20 to -29.66 kcal/mol. None of the cluster 6 residues (Glu110, Ser71, Ser113) has an electrostatic or vdW interaction with Asp49 or Ala49 and residue 49 is about 16 Å away from $Glu110_{TEM}$ and about 20 Å away from $Ser71_{BLIP}$ and $Ser113_{BLIP}$. Intermolecular interaction energy of

$Glu110_{TEM}$-$Ser71_{BLIP}$ changed from -5.77 to -17.8 kcal/mol and that of $Glu110_{TEM}$-$Ser113_{BLIP}$ changed from -4.43 to -11.86 kcal/mol due to BLIP D49A mutation. The distance between C_α atoms of $Glu110_{TEM}$ and $Ser71_{BLIP}$ is 10.5 Å and C_α atom of $Glu110_{TEM}$ is 11 Å away from that of $Ser113_{BLIP}$ in the average simulation structure of complex. Due to D49A mutation, the distance between C_α atoms of $Glu110_{TEM}$-$Ser71_{BLIP}$ and Glu110TEM-$Ser113_{BLIP}$ interacting pairs became 8 and 9 Å respectively in the average simulation structure of complex. The decrease in distance between interacting pairs of cluster 6 led to an increase in intermolecular interaction between them in the TEM-1 – BLIP (D49A) complex.

Mutation of tryptophan at position 229 to alanine has changed intermolecular interaction energy of cluster 6 significantly, whereas interaction energies of other clusters revealed slight change. The main interaction in the cluster 6 comes from electrostatic interaction with an interaction energy of -37.33 kcal/mol while vdW interaction energy is only 0.92 kcal/mol and total non-bonded interaction energy of cluster 6 in TEM(W229A) - BLIP complex is -36.4 kcal/mol while it is -10.2 kcal/mol in TEM-1 – BLIP complex. None of the cluster 6 residues have an electrostatic and vdW interaction with Trp229 of wild type TEM-1 or Ala229 of mutated TEM-1 and also residue 229 is about 35Å away from cluster 6 residues. The C_α atom of Glu110 of TEM-1 is about 11 Å away from C_α atoms of Ser71 and Ser113 of BLIP in the average simulation structure of TEM-1 – BLIP complex. After W229A mutation the distance revealed a slight change and became about 9 Å in the average simulation structure of TEM-1 (W229A) – BLIP complex, but this slight approach of residues may be the reason of the enhancing electrostatic interaction energy in cluster 6.

3.3.2. Binding Free Energy

Binding free energy was calculated by using MM-PBSA (Molecular Mechanics-Poisson Boltzmann Surface Area) method thus reveals tightness of binding. Calculation of the binding free energy with MM-PBSA method was carried out for the snapshot structures taken from MD trajectory of the system. In MM-PBSA, MM represents average molecular mechanical gas-phase energies (electrostatic, van der Waals and bonded interaction energy) that were calculated in VMD with a Tcl script in Appendix A, PB represents polar

solvation energy that was calculated by APBS (Baker *et al.*, 2001) and SA is for non-polar salvation energy that was calculated by using MSMS program (Sanner et al., 1996).

Table 3.5. Binding free energy (kcal/mol) of simulation systems and energy types that contribute to free energy.

Energy Term (kcal/mol)	TEM-1 - BLIP	TEM-1	BLIP	Δ Energy
$E_{electrostatic}$	-8755	-6536	-1795	-424
E_{vdW}	-1826	-1174	-568	-84
E_{bonded}	6421	4075	2346	0
E_{MM}	-4160	-3635	-17	-508
Gpb	-2061	-1393	-782	114
Gsa	98	64	49	-15
MMPBSA	-6123	-4964	-750	-409
Entropy	700	417	285	-2
G	-6823	-5381	-1035	-407

Energy Term (kcal/mol)	TEM-1 - BLIP (D49A)	TEM-1	BLIP (D49A)	Δ Energy
$E_{electrostatic}$	-8487	-6432	-1703	-352
E_{vdW}	-1867	-1189	-562	-116
E_{bonded}	6416	4070	2346	0
E_{MM}	-3938	-3551	81	-468
Gpb	-2503	-1716	-944	157
Gsa	95	64	47	-16
MMPBSA	-6346	-5203	-816	-327
Entropy	695	416	281	-2
G	-7041	-5619	-1097	-325

Energy Term (kcal/mol)	TEM-1 (W229A) - BLIP	TEM-1 (W229A)	BLIP	Δ Energy
$E_{electrostatic}$	-8786	-6349	-1831	-606
E_{vdW}	-1841	-1172	-572	-97
E_{bonded}	6389	4044	2348	-3
E_{MM}	-4238	-3477	-55	-706
Gpb	-1956	-1379	-769	192
Gsa	94	63	47	-16
MMPBSA	-6101	-4793	-778	-530
Entropy	764	459	306	-1
G	-6865	-5252	-1084	-529

Table 3.5. Binding free energy (kcal/mol) of simulation systems and energy types that contribute to free energy (continues).

Energy Term (kcal/mol)	SHV-1 - BLIP	SHV-1	BLIP	Δ Energy
$E_{electrostatic}$	-9538	-7334	-1713	-491
E_{vdW}	-1842	-1187	-561	-94
E_{bonded}	6411	4068	2343	0
E_{MM}	-4969	-4453	69	-585
Gpb	-2341	-1555	-1001	215
Gsa	97	65	48	-16
MMPBSA	-7213	-5943	-884	-386
Entropy	686	412	277	-3
G	-7899	-6355	-1161	-383

Energy Term (kcal/mol)	SHV-1 - BLIP (D49A)	SHV-1	BLIP (D49A)	Δ Energy
$E_{electrostatic}$	-9562	-7439	-1831	-292
E_{vdW}	-1838	-1168	-566	-104
E_{bonded}	6415	4070	2345	0
E_{MM}	-4985	-4537	-52	-396
Gpb	-1807	-1261	-724	178
Gsa	96	66	47	-17
MMPBSA	-6696	-5732	-729	-235
Entropy (T*S)	520	316	208	-4
G	-7216	-6048	-937	-231

Table 3.5 shows binding free energy value of each simulation system as well as all the energy contributions to binding free energy. Binding free energy for each simulation system was calculated by subtracting entropy contributions (-TΔS) from ΔMMPBSA. ΔEnergy represents change in related energy term due to the binding calculated by subtracting the beta-lactamase and ligand energy terms from energy term of the complex.

Considering the energy values in the Table 3.5, the main contribution to binding free energy for each simulation system comes from the change in electrostatic energy due to binding. Polar and non-polar solvation energies have minor contribution to binding free energy also entropy contributions are slight with respect to other energy types.

Table 3.6. Binding free energy (kcal/mol) of simulation systems and change in binding free energy due to mutation.

Simulation System	**Δ G (kcal/mol)**	**Δ Δ G[a] (kcal/mol)**
TEM-1 - BLIP	-407	0
TEM-1 - BLIP (D49A)	-325	82
TEM-1 (W229A) - BLIP	-529	-122
SHV-1 - BLIP	-383	0
SHV-1 - BLIP (D49A)	-231	152

[a] $\Delta\Delta G = \Delta G_{mutant} - \Delta G_{wildtype}$

BLIP revealed a tighter binding for TEM-1 than SHV-1 with -407 and -383 kcal/mol of ΔG values. Because of the catalytic importance of Asp49, mutation of aspartic acid to alanine increased binding free energy thus indicating decrease in binding affinity. TEM-1 – BLIP (D49A) and SHV-1 – BLIP (D49A) have -325 and -231 kcal/mol of ΔG values (Table 3.6).

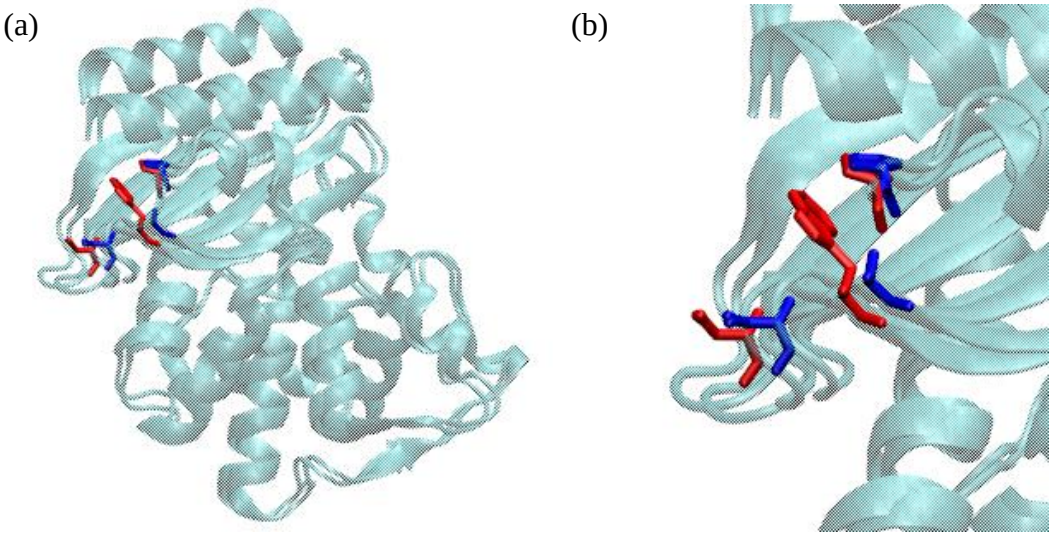

Figure 3.16. Average simulation structures of TEM-1 and TEM-1 W229A mutant aligned based on C_α atoms (a) and Pro226, Trp229, Pro252 (red) in TEM-1 and Pro252, Ala229, Pro226 (blue) in TEM-1 W229A (b).

As mentioned before the importance of Trp229 of H10 on binding was investigated. In order to do that tryptophan at position 229 was substituted with alanine. According the binding free energy value of TEM-1 (W229A) – BLIP complex, it was found that removal

of tryptophan side chain due to W229A mutation significantly increased binding affinity for BLIP and binding free energy decreased from -407 kcal/mol in wild type complex to -529 kcal/mol in TEM-1 (W229A) - BLIP complex. This finding reveals the importance of Trp229 and also H10 helix that it harbors on binding. As previously mentioned a stacking structure is formed by Pro252 on the loop connecting B4 and B5 beta-strands with Pro226 and Trp229 of H10 helix. Also, MSF value of Trp229 has changed upon BLIP binding from 0.35 $Å^2$ in unbound form to 0.56 $Å^2$ in BLIP bound form, while Pro226 and Pro252 reveal the same MSF value in the presence or absence of BLIP. It was thought that the ring structure of Trp229 on H10 helix may be important for binding besides the positions of these three stacking residues to each other. The stacking of these three residues did not change with respect to each other upon W229A mutation (Figure 3.16) but the loss of cylic side chain of tryptophan due to substitution with alanine increased binding affinity on the contrary to expectations.

3.4. Correlation between the Beta-lactamase and the Ligand

In order to determine the communication pathway between beta-lactamase and the ligand, the correlation between them was investigated. First, correlation values for residues of the interface clusters that were described in Section 3.3.1 were calculated by using Matlab script in Appendix B. Results showed that correlations between cluster residues of beta-lactamase and ligand are all less than 0.5, indicating that low or no correlation exist between the clusters (Table 3.7).

To calculate the correlation between beta-lactamase and the ligand, trajectory file that was gained from each simulation system was loaded to Matlab. After the aligment of the structure on the average simulation structure based on C_α atoms, correlation map that reveals the correlation between residues of beta-lactamase and the ligand was plotted for each simulation system which was colored according to correlation values (Figure 3.17, Figure 3.19, Figure 3.21, Figure 3.23, Figure 3.25). In VMD, these correlated residues of which correlation values more than 0.5 were visualized and labeled with black lines between correlated residue pairs for each simulation system with the help of a Tcl script in Appendix A (Figure 3.18, Figure 3.20, Figure 3.22, Figure 3.24, Figure 3.26).

Table 3.7. Correlation between residues of beta-lactamase and ligand within each cluster.

Cluster	TEM-1 - BLIP	TEM-1 - BLIP (D49A)	TEM-1 (W229A) - BLIP	SHV-1 - BLIP	SHV-1 - BLIP (D49A)
C1	0.19	0.18	0.19	0.32	0.39
C2	0.32	0.35	0.35	0.13	0.23
C3	0.23	0.19	0.07	0.05	0.11
C4	0.07	0.09	0.02	-0.10	0.23
C5	0.13	0.10	0.13	0.18	0.25
C6	-0.20	0.18	-0.13	0.13	0.08

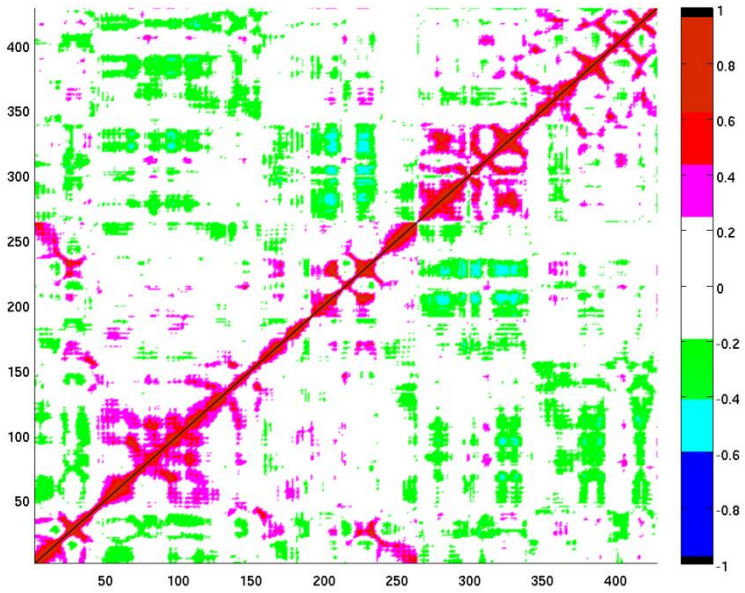

Figure 3.17. All the correlations between TEM-1 and BLIP.

All the correlations between TEM-1 and BLIP were shown in Figure 3.17. The correlation plot is diagonally symmetric and 1 to 263 corresponds to TEM-1 residues and 264 to 428 represents BLIP residues of the TEM-1 – BLIP complex. The rectangular area, edges of which correspond to TEM-1 residues (1 to 263) and BLIP residues (264 to 428) reveals the correlations between the beta-lactamase and the ligand. Color scale goes from white to red for positive correlation values between residues of beta-lactamase and the ligand whereas negative correlation values were shown in white to blue. Also regions that correlation does not exist were colored white. Red regions on the rectangular area that defined above correspond to the correlations highlighted with black lines in Figure 3.18 which have correlation with higher than 0.5 correlation value. TEM-1 – BLIP complex has

few correlations with value higher than 0.5, also it has few correlations that correlated with -0.4 to -0.6 correlation values. However most of the correlations have correlation value that range between 0.2 and -0.4.

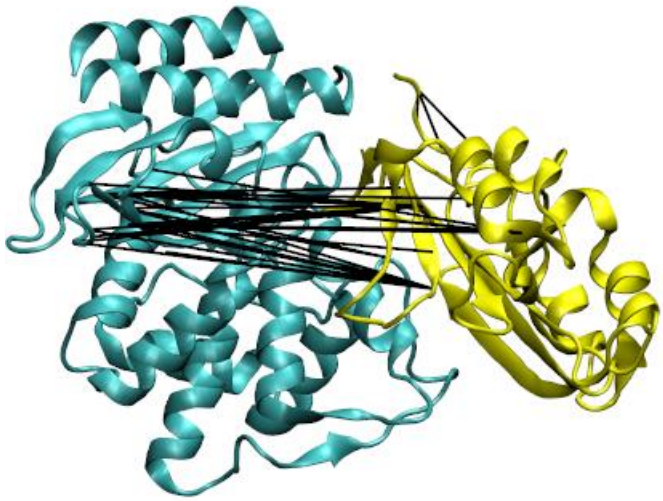

Figure 3.18. Correlations between TEM-1 (cyan) and BLIP (yellow) higher than 0.5 correlation value shown as black lines.

Considering the Figure 3.18 residues of TEM-1 and BLIP that are correlated with a correlation value of more than 0.5 were shown as black lines. The correlation values are lower than 0.5 for the interface residues as mentioned in Table 3.7 but long range correlations exist between the hinge region formed by H10 helix and B3 strand (230-238) with BLIP. Also, residues of the loop connecting B4 (243-251) and B5 (259-266) correlated with BLIP.

Mutation of tryptophan at position 229 of TEM-1 to alanine created new correlations with higher than 0.5 correlation value in addition to the correlations between BLIP and hinge region formed by H10 helix and B3 strand (230-238), and the loop connecting B4 (243-251) and B5 (259-266) of TEM-1. Due to W229A mutation, also H8 helix (183 to 195) and B1 strand (43-50) correlated with BLIP with more than 0.5 correlation value (Figure 3.20).

Negative correlations between the beta-lactamase and the ligand whose correlation value range between -0.2 and -0.6 increased with W229A mutation on TEM-1 as it seems

from the rectangular area that shows the correlations between the beta-lactamase (1 to 263) and the ligand (264 to 428) in Figure 3.19.

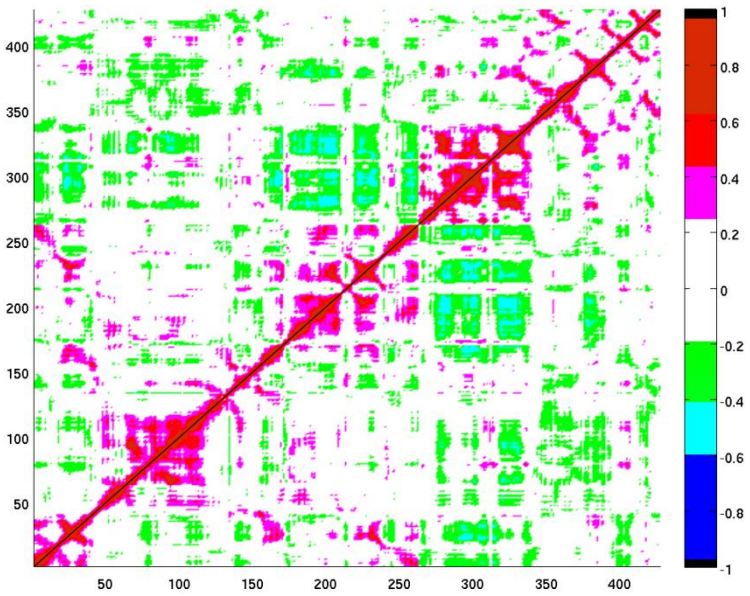

Figure 3.19. All the correlations between TEM-1(W229A) and BLIP.

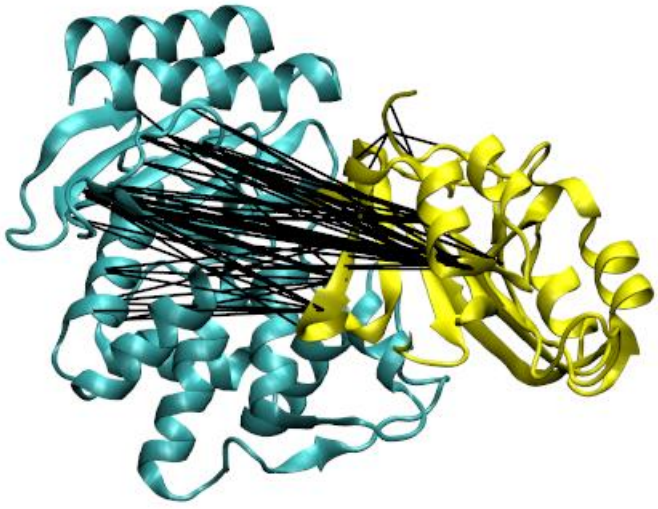

Figure 3.20. Correlation between TEM-1(W229A) (cyan) and BLIP higher than 0.5 correlation value shown as black lines.

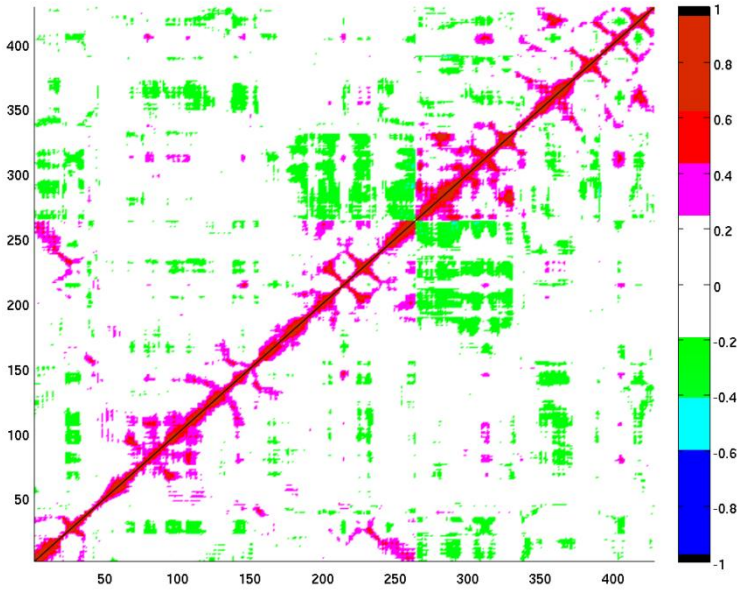

Figure 3.21. All the correlations between TEM-1 and BLIP (D49A).

Figure 3.21 shows all the correlations between TEM-1 and BLIP (D49A) mutant. According to the comparison of correlation plot of TEM-1 – BLIP(D49A) complex (Figure 3.21) with correlation plot of TEM-1 – BLIP complex (Figure 3.17), D49A mutation on BLIP eliminated some of the correlations between the beta-lactamase and the ligand that were highlighted with white in the Figure 3.21 which represents very low or no correlation (0.2 to -0.2).

Mutation of aspartic acid at position 49 of BLIP to alanine destroyed the correlations between BLIP and hinge region formed by H10 helix and B3 strand (230-238), and also the loop connecting B4 (243-251) and B5 (259-266) of TEM-1. Moreover, there is no correlation between TEM-1 residues and BLIP (D49A) with a correlation value more than 0.5. However, some regions of TEM-1 correlated with BLIP (D49A) with correlation value between 0.4 and 0.5 (Figure 3.22). According to that H11 helix (276-286) of TEM-1 is the region that is correlated with BLIP (D49A) with correlation value between 0.4 and 0.5.

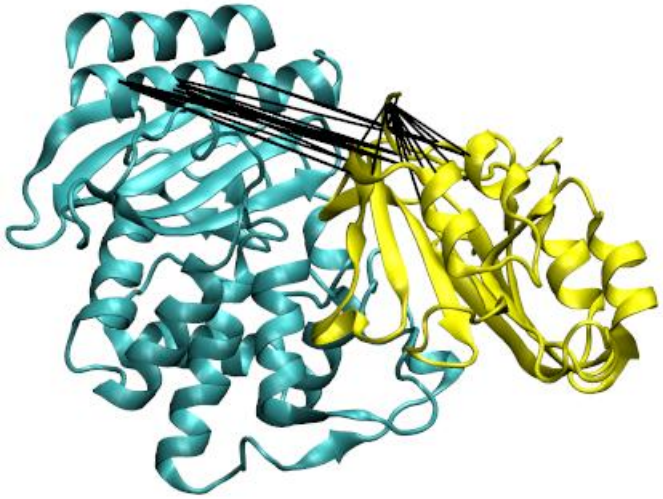

Figure 3.22. Correlation between TEM-1 (cyan) and BLIP (D49A) higher than 0.4 correlation value shown as black lines.

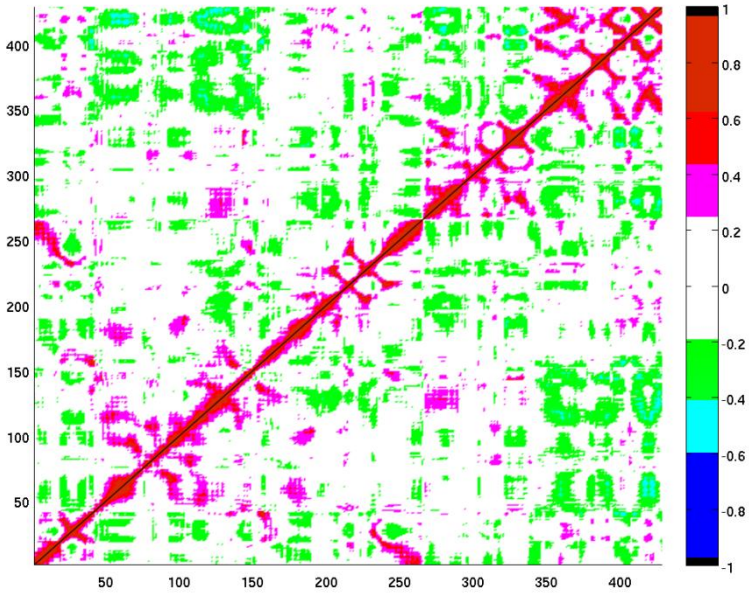

Figure 3.23. All the correlations between SHV-1 and BLIP.

In the SHV-1 – BLIP complex, SHV-1 and BLIP correlated with few positive correlations but they mainly have negative correlations that vary 0 to -0.6 correlation value (Figure 3.23). Nevertheless SHV-1 – BLIP complex has some correlations with higher than 0.5 correlation value (Figure 3.24). According to the Figure 3.24 BLIP is correlated with b1 (66-67) strand of SHV-1 and also residues of the loop connecting b1 to B2 (55-60). Moreover, BLIP is correlated with H7 (168-170) helix and some residues from H6 (145-154) helix of SHV-1 with correlation values higher than 0.5.

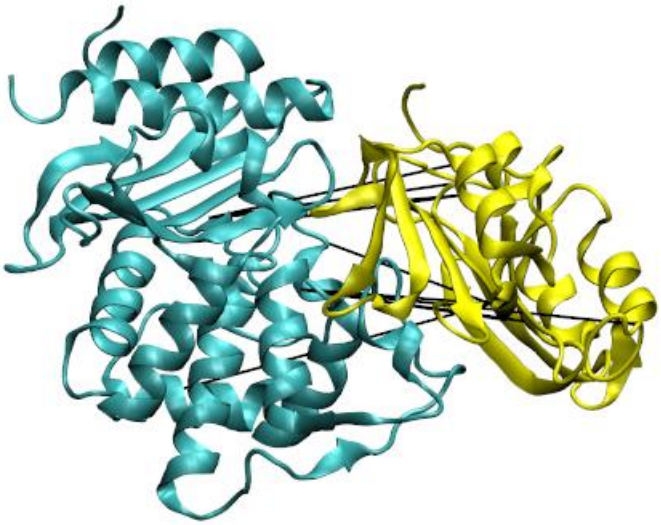

Figure 3.24. Correlation between SHV-1(cyan) and BLIP (yellow)) higher than 0.5 correlation value shown as black lines .

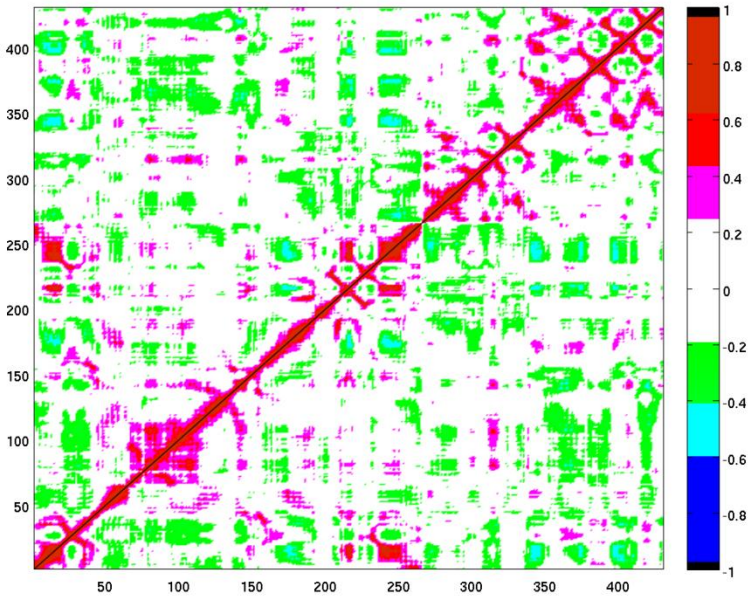

Figure 3.25. All the correlations between SHV-1 and BLIP (D49A).

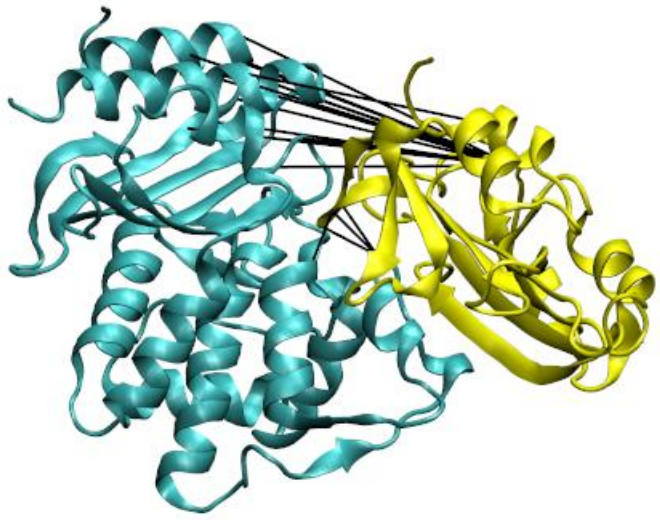

Figure 3.26. Correlation between SHV-1 and BLIP (D49A), higher than 0.5 correlation value shown as black lines.

All the correlation between SHV-1 and BLIP (D49A) mutant showed in Figure 3.25. When the correlation plot of mutant complex compared with the correlation plot of wild type complex it seems that correlations did not affected significantly by D49A mutation on BLIP as D49A mutation affected the correlations between TEM-1 and BLIP by eliminating most of the correlations.

Whereas correlations of BLIP with b1 (66-67) strand of SHV-1 and also residues of the loop connecting b1 to B2 (55-60), H7 (168-170) helix and some residues from H6 (145-154) helix of SHV-1 reduced and their correlation values decreased under 0.5.

Despite some changes in correlated residues of SHV-1 and BLIP due to D49A mutation on BLIP, still many correlations exist between SHV-1 and BLIP (D49A) unlike TEM-1 – BLIP (D49A) complex in which all the correlations with higher than 0.5 correlation value disappeared due to D49A mutation.

Figure 3.26 reveals the correlations between SHV-1 and BLIP (D49A) with correlation value higher than 0.5. According to that BLIP (D49A) is correlated with H1 (29-40) helix of SHV-1 and also the loop connecting H1to B1 strand (43-50). Moreover it is correlated with Gln277 and Gln278 of H11 (276-286).

4. TEM-1 BETA-LACTAMASE BINDING TO BLIP BASED PEPTIDES

In this study 10ns of TEM-1 – Peptide complex simulations were carried out in order to investigate TEM-1 beta-lactamase binding to BLIP based peptides. Initial peptide coordinates were based on the BLIP 45 to 52 or 45 to 53 loop, which includes the catalytically important Asp49 residue of BLIP. Sequence of the peptides was either that in wild type BLIP or included the mutations A46W, D49A, Y50A, Y51A, G48F and G48FY50A. LLIIL are hydrophobic residues and have the ability to get into the cell spontaneously therefore LLIIL can be used to increase cellular uptake of peptides (Elmquist et al., 2006). LLIIL residues were added to wild type peptide 45-53 to investigate whether it affects binding of peptide to TEM-1.

Table 4.1. Simulation systems and amino acid sequence of peptides.

Simulation	TEM-1 - Peptide Complex	Peptide Sequence
P1	TEM-1 - Peptide 45-52 (wt)	COO-HAAGDYYA-NH2
P2	TEM-1 - Peptide 45-52 (D49A)	COO-HAAG**A**YYA-NH2
P3	TEM-1 - Peptide 45-52 (Y50A)	COO-HAAGD**A**YA-NH2
P4	TEM-1 - Peptide 45-52 (Y51A)	COO-HAAGDY**A**A-NH2
P5	TEM-1 - Peptide 45-52 (A46W)	COO-H**W**AGDYYA-NH2
P6	TEM-1 - Peptide 45-53 (wt)	COO-HAAGDYYAY-NH2
P7	TEM-1 – Peptide LLIIL-45-53	COO-**LLIIL**-HAAGDYYAY-NH2
P8	TEM-1 - Peptide 45-53 (G48F)	COO-HAA**F**DYYA-NH2
P9	TEM-1 – Peptide 45-53 (G48F Y50A)	COO-HAA**F**D**A**YA-NH2

4.1. Stability of the Simulation Systems

Root mean square deviation (RMSD) of each simulation system was calculated in order to find out the deviation from the initial structure and to verify the stability of the simulation systems. In order to obtain deviation from the initial structure, each simulation structure was averaged according to the equilibrium period of the simulation and each averaged structure aligned on the initial simulation structure of itself based on C_α atoms and the deviation of these atoms from their initial positions was calculated. For the RMSD

calculation of beta- lactamase, average TEM-1 structure and for ligand RMSD, average peptide structure were aligned to its respective initial structure and then RMSD values of beta-lactamase and peptide were calculated. These RMSD values give information about internal changes in beta-lactamase or peptide. In order to calculate RMSD of complex structure, the average complex structure was aligned to its initial state. Also, to determine deviation of peptide with respect to beta-lactamase, the alignment was performed on beta-lactamase and RMSD of the peptide was calculated. Table 4.2 shows average RMSD values of beta-lactamase, peptide and complex for each simulation system. In the Ligand[a] column, peptide RMSD that was calculated after the alignment of average peptide structure to the initial structure of peptide that represents the peptide deviation according to its initial position were listed; Ligand[b] column shows peptide RMSD that was calculated after the alignment of average beta-lactamase structure to the initial structure of beta-lactamase to reveal deviation of peptide with respect to beta-lactamase.

Table 4.2. RMSD values of TEM-1 beta-lactamase, peptide and complex in each simulation system.

Simulation	**RMSD (Å)**			
	Beta-Lactamase	**Ligand[a]**	**Complex**	**Ligand[b]**
P1 (1.5 -10ns)	0.72	1.63	0.92	3.45
P2 (2.5-10ns)	1.02	2.71	1.50	6.59
P3 (2.5-10ns)	0.76	1.25	0.89	2.88
P4 (1.5-10ns)	0.80	2.78	0.99	3.49
P5 (2.5-10ns)	0.68	0.54	0.78	2.33
P6 (1.5-10ns)	0.67	1.18	0.73	1.76
P7 (2-10ns)	1.10	1.30	1.28	3.33
P8 (3-10ns)	1.04	1.93	1.27	4.18
P9 (2-10ns)	0.81	1.01	0.99	3.24

a peptide deviation with respect to itself

b peptide deviation with respect to beta-lactamase

According to the Table 4.2 RMSD values of TEM-1 beta-lactamase stayed between 0.67 and 1.10 Å. Peptide RMSD, when it is aligned on peptide reveal a variety between 0.54 and 2.78 Å of RMSD values. Also, when alignment is based on TEM-1, peptide has RMSD value ranging from 1.76 to 6.59 Å. Complex RMSD values varied between 0.73 and 1.50 Å.

TEM-1 beta-lactamase was less deviated when bound to P5 and P6 among other peptides. Moreover, P5 deviated from its initial structure less than other peptides deviated from their initial structure. On the other hand, P6 deviated from TEM-1 beta-lactamase with a RMSD value of 1.76 Å which is pretty slight deviation from TEM-1 with respect to other peptides.

Deviation of beta-lactamase, peptide and complex in each simulation system were examined in the following parts in detail by considering the RMSD profiles of TEM-1, peptide and complex for each simulation system. RMSD profile of TEM-1 in peptide bound form was calculated after the alignment of average TEM-1 structure on the initial simulation structure of itself. Also, RMSD profile of peptide in TEM-1 bound structure was calculated after the alignment of average TEM-1 structure on the initial simulation structure of TEM-1 in order to determine the deviation of peptide with respect to TEM-1. Besides, RMSD profile of the whole complex structure was calculated in order to examine the deviation of complex from the initial simulation structure.

Also, to examine whether the peptide moved away from TEM-1, the change in distance between peptide and TEM-1 during 10 ns simulation was measured in VMD for each simulation system, by considering the distance of catalytic Asp49 C_α atom of peptide to the C_α atoms of active site residues of TEM-1 that correspond to Ser70, Lys73, Ser130, Glu166, Asn170 and Lys234.

4.1.1. Stability of TEM-1 - Peptide 45-52 (wild type) During the Simulation

RMSD profiles of TEM-1, peptide 45-52 wt and their complex were shown in the Figure 4.1. TEM-1, in complex with peptide that is based on 45 to 52 of BLIP (P1) reached equilibrium in about 1.5 ns of 10 ns simulation (Figure 4.1a) and revealed slight

fluctuations throughout the simulation. The average RMSD value of TEM-1 is 0.72 Å, while P1 and complex have 1.63 Å and 0.92 Å of RMSD values respectively (Table 4.2).

The RMSD profile of P1 that was calculated after the alignment of TEM-1 revealed that peptide reached equilibrium at about 2.5 ns but deviated away from TEM-1 after 7ns (Figure 4.1b). TEM-1 – Peptide 45-52 complex reached equilibrium at about 2 ns and revealed somewhat stable behavior except through the end of the simulation (Figure 4.1c).

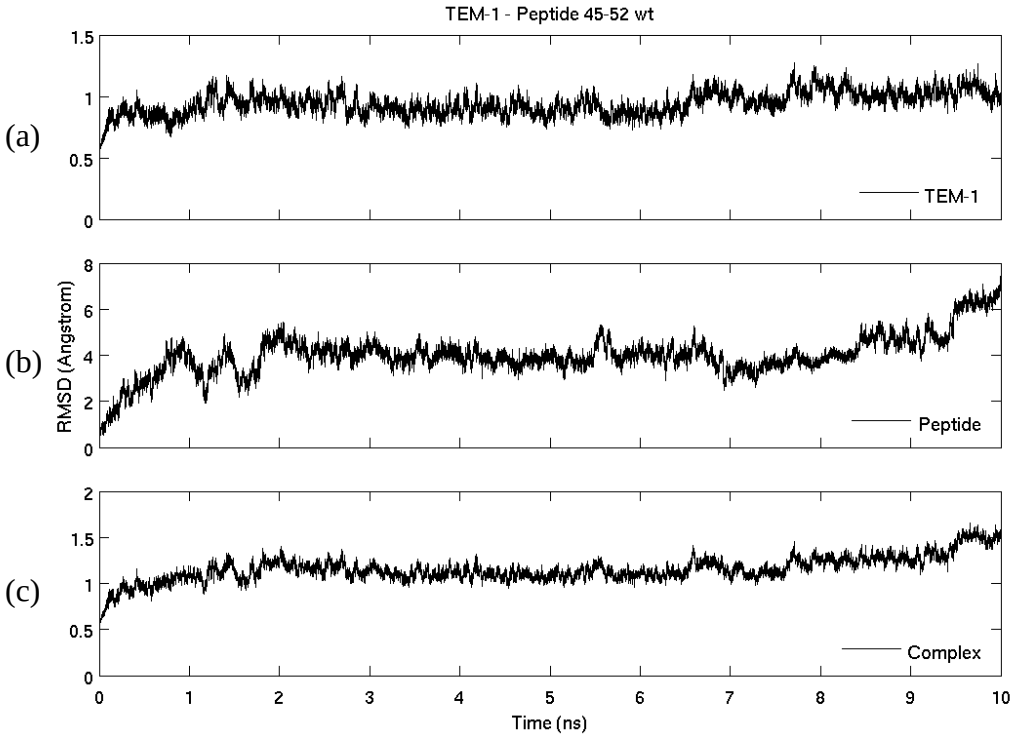

Figure 4.1. RMSD of beta-lactamase, peptide and complex in TEM-1- Peptide 45-52 wt simulation.

In the initial simulation structure the distance of $Asp49_{BLIP}$ C_α atom to the C_α atoms of TEM-1 active site residues Ser70, Lys73, Ser130, Glu166, Asn170 and Lys234 was 8, 12, 7, 13, 11 and 10 Å respectively. The peptide seemed that it inserted itself into the active site pocket of TEM-1. Catalytic Asp49 stayed nearly at the same distance to active site of TEM-1 and only 1Å of movements occur about Lys73 and Glu166 in 7ns of the simulation but at 7^{th} ns the distance of Asp49 to active site residues became the same with initial simulation distance. After 7ns, Asp49 approached 1 Å to Ser70, Ser130 and Glu166 first and then moved away again. At the end of the simulation, Asp49 came the same

distance to active site residues that it is in the initial simulation structure. Thus, Asp49 preserved its distance from the active site residues, only around 0 to 1Å of changes during the simulation. However, N and C terminuses of the peptide were very mobile and their distance to Asp49 ranged between 10 to 13 Å during the simulation which indicate deviation from TEM-1 (Figure 4.1b). Arising from the high fluctuation of N and C terminuses (change around 3 Å) and the change in distance of Asp49 to active site pocket around 1 Å, peptide deviated from TEM-1 with an average RMSD of 3.45 Å (Table 4.2).

4.1.2. Stability of TEM-1 - Peptide 45-52 (D49A) During the Simulation

In the presence of Peptide 45-52 (D49A) (P2), TEM-1 reached equilibrium in about 2.5 ns (Figure 4.2a) and the RMSD value between the average structure and the initial structure is 1.02 Å. The RMSD between the average structure of P2 and its initial structure is 2.71 Å while complex has 1.50 Å of RMSD value (Table 4.2).

According to the RMSD profile of P2 that was calculated after the alignment of average TEM-1 structure on the initial simulation structure of TEM-1 (Figure 4.2b), P2 reached equilibrium in 0.5 ns but after 3ns it revealed significant fluctuations. The change in distance between TEM-1 and P2 was examined in VMD to figure out whether the peptide moved away from TEM-1.

In the initial simulation structure the distance between C_α of $Ala49_{BLIP}$ and TEM-1 active site residues Ser70, Lys73, Ser130, Glu166, Asn170 and Lys234 was 8, 12, 7, 13, 11 and 10 Å respectively as in the wild type complex. Until 3ns Ala49 stayed at the same distance to TEM-1 active site pocket. In this position the peptide seems like it inserted itself into TEM-1 active site pocket and fluctuates there. Then the distance between Ala49 and active site residues increased and became 11, 13, 11, 17, 17 and 11 at 5ns. During 5 to 10 ns the peptide moved away from TEM-1 some more and it revealed an oscillating movement between active site pocket of TEM-1 and 99-112 loop. Ala49 became 21, 21, 14, 24, 26, 20 Å away from the active site residues Ser70, Lys73, Ser130, Glu166, Asn170 and Lys234 respectively at 8.5 ns. An immediate approach had happened after 9ns for a short time and at the end of the simulation the distance of Ala49 from active site residues became 17, 19, 12, 22, 22 and 16Å respectively. RMSD profile of the peptide reveals the

deviation of the peptide during the simulation (Figure 4.2b). P2 deviated from TEM-1 with an average RMSD of 6.59 Å (Table 4.2).

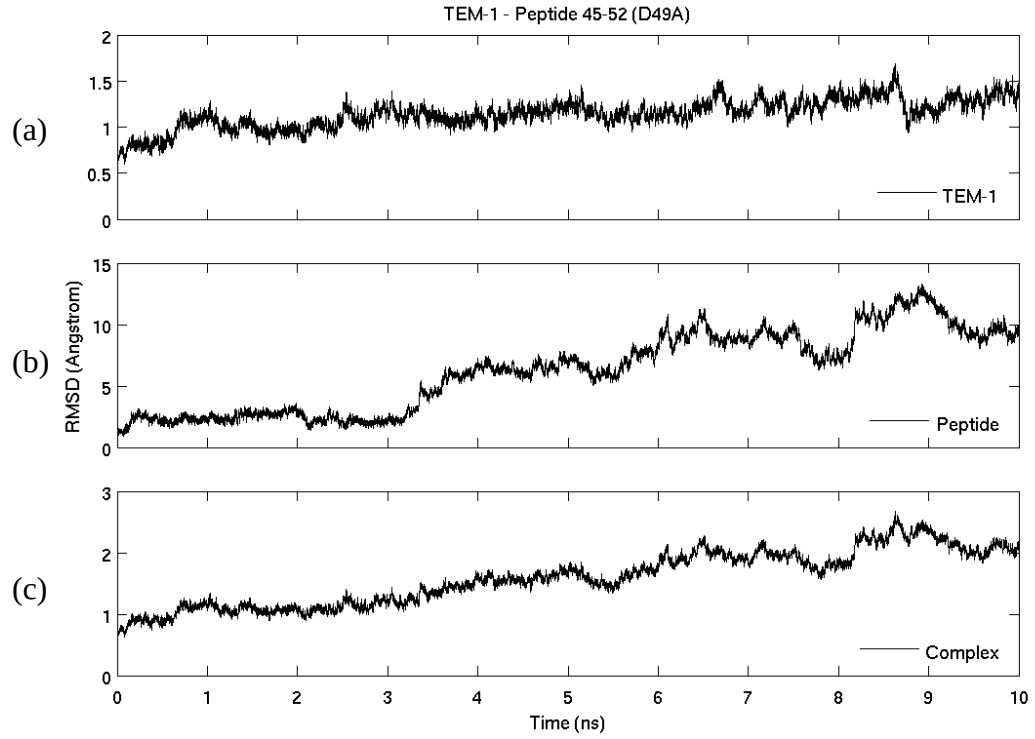

Figure 4.2. RMSD of beta-lactamase, peptide and complex in TEM-1 - Peptide 45-52 (D49A) simulation.

TEM-1 – P2 complex reached equilibrium in about 1ns but after 3 ns significant fluctuations happened (Figure 4.2c) due to the movement of peptide from TEM-1.

TEM-1 in the presence of P2 (Figure 4.2a) is less stable than TEM-1 in the presence of wild type peptide P1 (Figure 4.1a). Moreover, fluctuations at P2 and TEM-1 – P2 complex are notable with respect to wild type. Also the RMSD profile of P2 that revealed its deviation with respect to TEM-1 indicates that D49A mutation on BLIP affected the stability of peptide significantly due to the loss of interaction between catalytic Asp49 and TEM-1 active site residues.

4.1.3. Stability of TEM-1 - Peptide 45- 52 (Y50A) During the Simulation

A previous experimental study on TEM-1 – BLIP suggests that Y50A mutation on BLIP increases binding affinity for TEM-1 by 50-fold (Zhang and Palzkill, 2003). In order to investigate whether the peptide 45-52 has an increase in binding affinity with Y50A mutation, tyrosine at position 50 substituted with alanine.

In this simulation system TEM-1 is in complex with P3 that corresponds to 45 to 52 loop of BLIP with Y50A mutation. TEM-1 reached equilibrium in 2.5 ns (Figure 4.3a) and its average RMSD value is 0.76 Å (Table 4.2). Its deviation from the initial structure is close to the wild type deviation from the initial structure which is 0.72 Å. Also TEM-1 in complex with P3 is almost as stable as when it is in complex with wild type peptide P1. P3 has an RMSD of 1.25 Å when in complex with TEM-1 and RMSD between average structure and initial structure for the complex is 0.89 Å.

Figure 4.3b reveals that P3 reached equilibrium in about 2 ns of the simulation but its stability disappeared after 5.5 ns. The change in distance between TEM-1 and peptide during the simulation was investigated in VMD as described before. According to that, $Asp49_{BLIP}$ stayed at 8, 12, 7, 13, 11 and 10 Å distant respectively from TEM-1 active site residues Ser70, Lys73, Ser130, Glu166, Asn170 and Lys234 only with little changes around 1Å to some residues and revealing slight fluctuations. Nevertheless, N-terminus and C-terminus of the P3 were very mobile and had significant fluctuations during the simulation. Supposing the Asp49 is stable in its place, the distance of N-terminus and C-terminus from Asp49 were calculated based on C_α atoms in order to understand the deviation of two from TEM-1. At the beginning of the simulation, N and C terminuses were 11 and 10 Å away from Asp49. In 6.5 ns the distances became 12 and 8 Å and accordingly average P3 structure seems to deviate away from TEM-1 due to their mobility (Figure 4.3b). However, according to the figure, deviation of P3 decreased after 7.5 ns due to the decrease in distance of N and C terminuses from Asp49 which became 8Å for both. The average deviation of P3 from TEM-1 has a RMSD of 2.88 Å. Despite the fluctuating RMSD profile considering the average RMSD values, P3 is more stable than wild type P1.

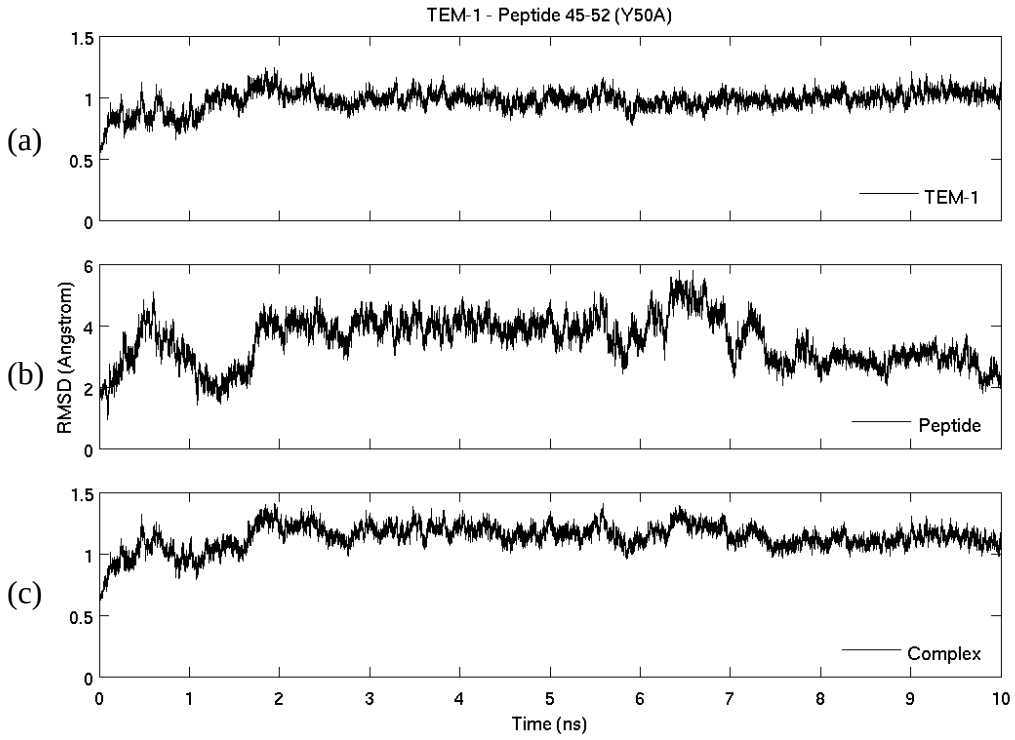

Figure 4.3. RMSD of beta-lactamase, peptide and complex in TEM-1 - Peptide 45- 52 (Y50A) simulation.

4.1.4. Stability of TEM-1 - Peptide 45 -52 (Y51A) During the Simulation

In a previous study it was found that Y51A mutation on BLIP did not affect the tightness of binding significantly and revealed only a slight decrease in binding affinity for TEM-1 (Wang *et al.,* 2009). Considering this finding the effect of Y51A mutation on binding of peptide 45-52 to TEM-1 was carried out.

In order to reach equilibrium, TEM-1 needed 1.5 ns (Figure 4.4a) in the presence of peptide 45-52 (Y51A) and average RMSD values of beta-lactamase, peptide and complex are 0.80 Å, 2.78 Å, and 0.99 Å respectively.

TEM-1 in the presence of P4 (0.80 Å) is nearly as stable as it is in the presence of P1 (0.72 Å) and P3 (0.76 Å). Thus, Y50A and Y51A mutations on peptide did not affect stability of beta-lactamase as remarkable as D49A mutation.

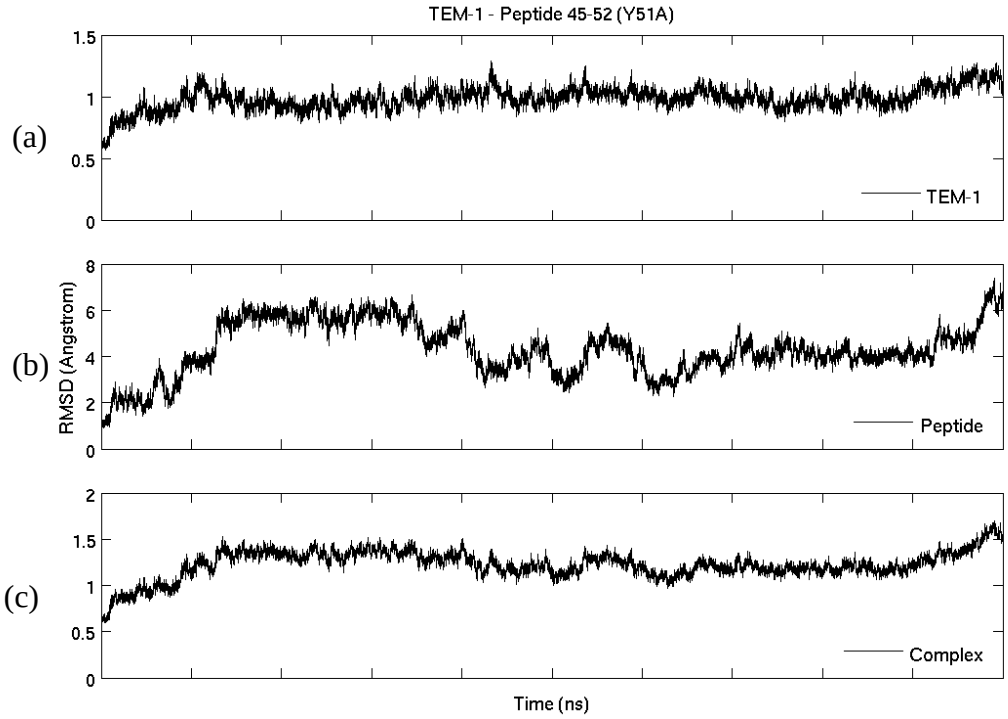

Figure 4.4. RMSD of beta-lactamase, peptide and complex in TEM-1 – Peptide 45-52 (Y51A) simulation.

According to the RMSD profile of P4 (Figure 4.4b), P4 reach equilibrium in 1.5 ns but while simulation reaching 4ns, deviation of P4 from TEM-1 changed. The simulation started with the distance of 8, 12, 7, 13, 11 and 10 Å between Asp49 C_α atom and C_α atoms of TEM-1 active site residues Ser70, Lys73, Ser130, Glu166, Asn170 and Lys234 respectively. After 3.5 ns peptide had started to reveal a fluctuating profile and the distances became 9, 13, 8, 14, 12, 10 Å at 3.75 ns. At the end of the simulation Asp49 deviated 10, 14, 8, 16, 14, 9 Å away from Ser70, Lys73, Ser130, Glu166, Asn170 and Lys234 respectively. The distance of N and C terminuses of P4 from Asp49 changed around 1 to 2 Å and stayed 9 Å away from Asp49 at the end of the simulation. Around 2 Å of movement away of Asp49 from the active site cavity, average deviation of P4 from TEM-1 has a RMSD value of 3.49 Å and it is close to wild type peptide (P1) deviation from TEM-1 (3.45 Å).

4.1.5. Stability of TEM-1 - Peptide 45-52 (A46W) During the Simulation

Alanine at position 46 of 45-52 loop of BLIP substituted with tryptophan which has a bulkier side chain, in order to investigate the change in binding affinity.

TEM-1 reached equilibrium in 2.5 ns in the presence of P5 (Figure 4.5a), despite TEM-1 needed a little longer time period in the presence of P5 with respect to presence of wild peptide P1, it exhibited a stable profile with little fluctuations throughout the simulation. Average deviation of TEM-1 from the initial structure is 0.68 Å (Table 4.2) which is close to deviation of TEM-1 from the initial structure in the presence of P1 which is 0.72 Å. P5 has an RMSD of 0.54 Å in TEM-1 bound form. The RMSD of complex is 0.78 Å and both peptide and complex RMSD values are less than wild type peptide (1.63 Å) and wild type TEM-1 – Peptide 45-52 complex (0.92 Å) structure.

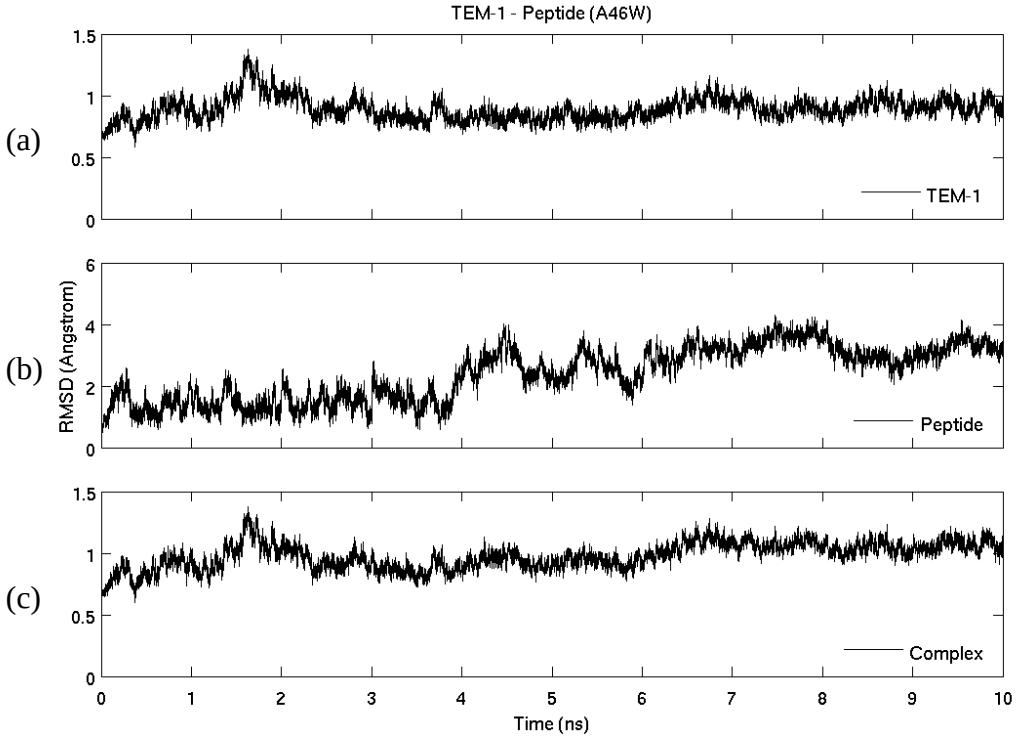

Figure 4.5. RMSD of beta-lactamase, peptide and complex in TEM-1 – Peptide 45-52 (A46W) simulation.

According to Figure 4.5 B, P5 reached equilibrium in about 0.5 ns but after 4ns its RMSD profile revealed some fluctuations. The change in distance between TEM-1 and peptide during the simulation was examined in VMD. According to that Asp49 preserved its distance from active site residues in 4ns but after 4 ns of simulation it revealed about 0 to 3 Å of changes in distance to active site pocket. N and C terminuses of the peptide revealed around 1 Å of change in distance from Asp49. However, P5 is nearly stable and

had slight mobility about active site of TEM-1 with an average deviation of 2.33 Å from TEM-1 (Table 4.2).

4.1.6. Stability of TEM-1 - Peptide 45-53 (wild type) During the Simulation

Besides BLIP 45 to 52 residues, 45 to 53 residues of it were taken to examine weather taking 45 to 53 residues is better to construct BLIP based peptide.

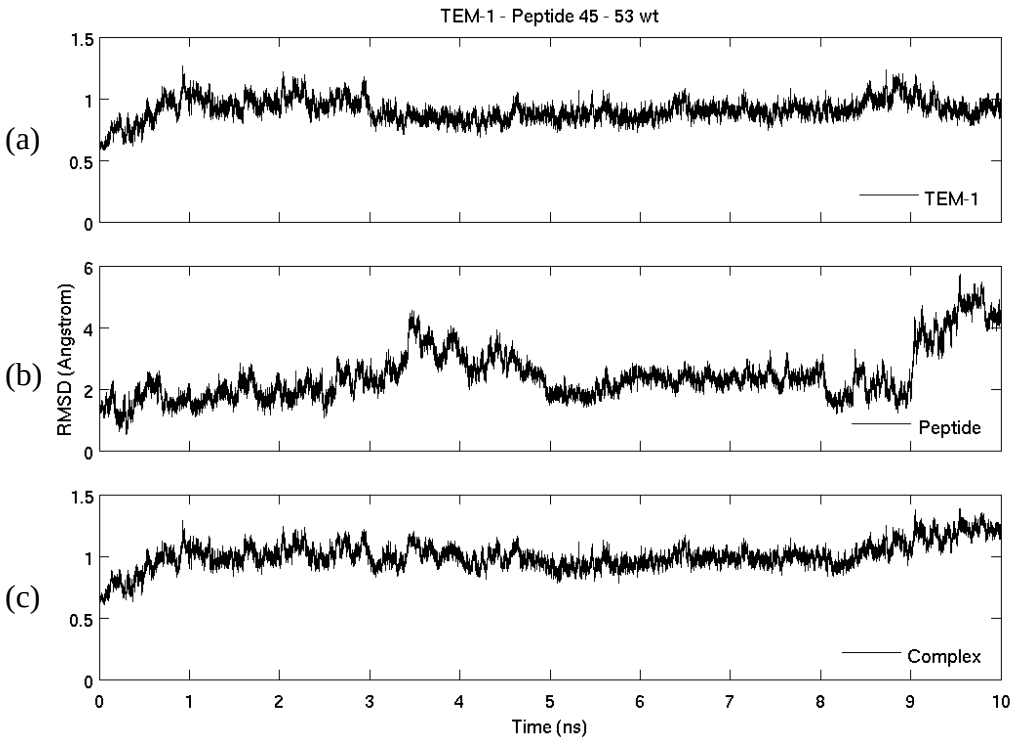

Figure 4.6. RMSD of beta-lactamase, peptide and complex inTEM-1 – Peptide 45-53 wt simulation.

According to the RMSD profile of TEM-1 in the presence of peptide 45-53 (P6), 1.5 ns was needed to reach equilibrium during 10 ns simulation (Figure 4.6a) and its average RMSD value is 0.67 Å which is less than TEM-1 in the presence of wild type P1. P6 has a RMSD of 1.18 Å with respect to its initial position and average RMSD of the complex is 0.73 Å.

The RMSD profile of P6 that was calculated after the alignment of TEM-1, revealed that P6 reached equilibrium in about 1 ns and revealed a stable profile except the

fluctuations in about 3 to 5 ns and also through the end of the simulation (Figure 4.6 b). The simulation was examined in VMD to figure out the reason of the fluctuations whether the peptide deviated away from TEM-1. According to that in the initial simulation structure the distance of Asp 49 from the active site residues Ser70, Lys73, Ser130, Glu166, Asn170 and Lys234 were 8, 12, 7, 13, 11 and 10 Å respectively as in other simulation systems. These distances became 8, 13, 7, 14, 12, 10 Å after 3ns and with the increase in distance only about 1 Å to Lys73, Glu166 and Asn170, peptide deviated away from TEM-1. Then P6 reached its initial distance again but at 9 ns it deviated again and the distance of Asp49 to active site residues became 7, 12, 7, 14, 12 and 10 Å. In other words Asp49 deviated from active site of TEM-1 about 0 to 1Å of change in distance and these deviations can be seen from the RMSD profile of peptide. Also, N and C terminuses of P6 were very flexible and changed their distances about 0.5 to 2 Å with respect to Asp49 during the simulation. Average deviation of P6 from TEM-1 has a RMSD value of 1.76 Å, which is less than the deviation of P1 from TEM-1 (3.45 Å).

Considering RMSD profiles and average RMSD values of TEM-1 beta-lactamase, peptide 45-53 and TEM-1 - Peptide 45-53 complex, 45 to 53 region of BLIP is more stable than 45 to 52.

4.1.7. Stability of TEM-1 - Peptide LLIIL-45-53 during the Simulation

A previous study on peptides indicates that hydrophobic N-terminus is important for peptide uptake. This previous study was done on pVEC which is a cell-penetrating peptide that was derived from the murine endothelial-cadherin protein. pVEC has a N- terminus with hydrophobic residue sequence that correspond to LLIIL, the rest of the peptide charged and the C-terminus residues are hydrophilic. According to that study substitution of any of the five hydrophobic residues to alanine resulted in significant drop of cellular uptake (Elmquist *et al.*, 2006). Based on the previous study it was thought that LLIIL residues can be used in the delivery of BLIP based peptides into the cells to increase its cellular upateke. In order to include LLIIL residues to peptide, 40 to 53 residues of BLIP were taken into consideration and residues 40, 41 and 44 mutated to leucine and also 42 and 43 substituted with isoleucine to generate LLIIL at the N-terminus of peptide 45-53. In this case the question was whether this addition to peptide decreased its binding affinity to

TEM-1. In order to investigate the change in binding affinity, 10ns of TEM-1 – Peptide LLIIL-45-53 simulation was performed.

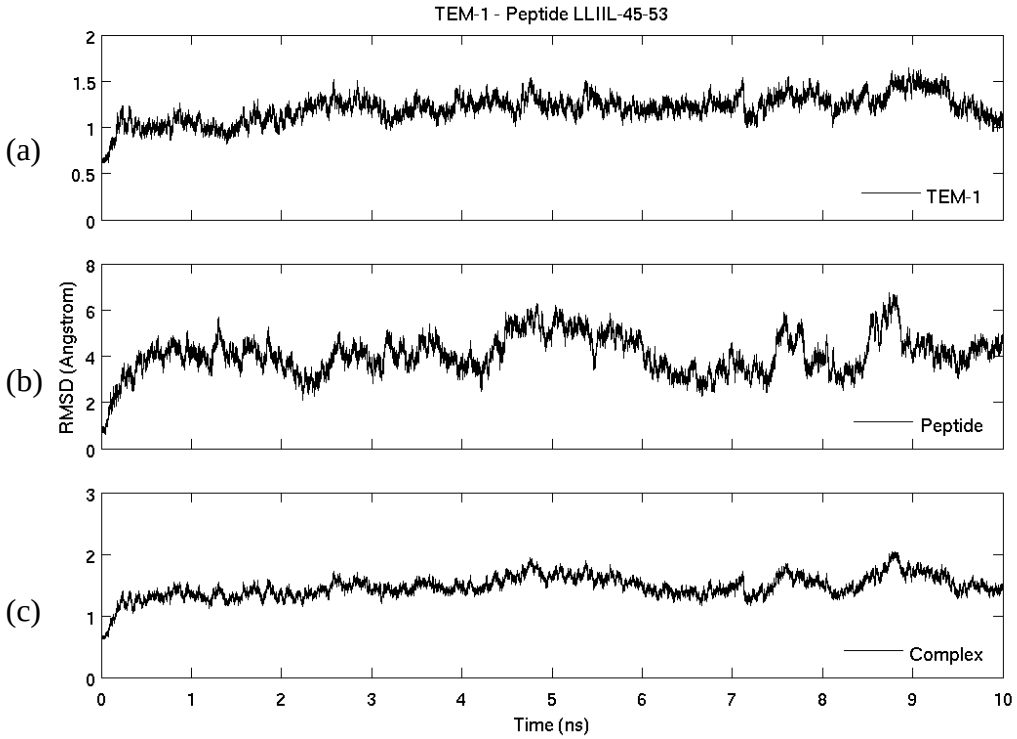

Figure 4.7. RMSD profile of beta-lactamase, peptide and complex in TEM-1 - Peptide - LLIIL-45- 53 simulation.

After addition of LLIIL residues to wild type peptide 45-53 (P7), TEM-1 reached equilibrium in about 2 ns (Figure 4.7a) and its RMSD value is 1.10 Å which is slightly more than TEM-1 in complex with wild type peptide 45-53 but it revealed a stable profile as TEM-1 in the presence of wild type P6. Average simulation structure of P7 deviated by 1.30 Å from its initial position and TEM-1 – Peptide LLIIL-45-53 complex has a RMSD of 1.28 Å. Asp49 of P7 deviated from the active site of TEM-1 with 0 to 1Å of change in distance and N and C terminuses of P7 were very flexible and changed their distances around 2 Å with respect to Asp49 during the simulation. These deviations can be seen from the RMSD profile of P7 as fluctuations (Figure 4.7b) and P7 deviated from TEM-1 with 3.33 Å of average RMSD value (Table 4.2).

4.1.8. TEM-1 - Peptide 45-53 (G48F) Complex

As mentioned in the introduction part, BLIP inserts its two loops, one from each domain, into the active site pocket of TEM-1 beta-lactamase to block substrate binding. Besides importance of Asp49 from the first domain, Phe142 from the second domain is also important and make some critical interactions with TEM-1 beta-lactamase (Petrosino *et al.*, 1998). In this study in order to create BLIP based peptides only 45 to 52 or 45 to 53 residues were taken, so interactions from Phe142 was lost. A previous study has suggested that substitution of the glycine at position 48 with an amino acid that has bulkier side chain could help to fill in the region that is occupied by Phe142 (Strynadka *et al.*, 1996). Considering this, glycine at position 48 mutated to phenylalanine and a docking server called Rosetta FlexPepDock (London *et al.*, 2011, Raveh *et al.*, 2010) was used to dock the peptide in the most suitable conformation to TEM-1 in order to gain back the position and the function of the side chain of Phe142 on binding.

According to the 10 ns simulation of TEM-1 - Peptide 45-53 (G48F) complex, TEM-1 needed nearly 3 ns to reach equilibrium (Figure 4.8a). Average RMSD value of TEM-1 is 1.04 Å in the presence of peptide 45-53 (G48F) (P8) whereas the RMSD value of TEM-1 is 0.67 in the presence of wild type P6.

The RMSD profile of P8 was calculated after the alignment of beta-lactamase on the initial simulation structure of beta-lactamase to observe its deviation from TEM-1 and the RMSD profiles shows that P8 needed about 2 ns to reach equilibrium. According to the Figure 4.8 B, mutation at position 48 led more stable RMSD profile of peptide with respect to wild type peptide. Nevertheless, average deviation of P8 from TEM-1 has a RMSD value of 4.18 Å while wild type peptide (P6) deviated with 1.76 Å of RMSD value. Also the deviation of P8 from the initial position of itself has an average RMSD value of 1.93 whereas P6 deviated with 1.18 Å of RMSD value.

In the same manner, with 1.27 Å of average RMSD value, TEM-1 - Peptide 45- 53 (G48F) complex has higher RMSD value than wild type TEM-1 - Peptide 45- 53 (0.73 Å).

The simulation was examined in VMD to observe the peptide especially behaviors of Asp49 and Phe48 residues. While Asp49 inserting itself to active site pocket of TEM-1 and became in contact with active site residues Ser70, Lys73, Ser130, Glu166, Asn170 and Lys234, the side chain of Phe48 inserted through the cavity that Glu104, Tyr105, Asn170, Ala237, Gly238 and Glu240 are located the residues which are known to interact with Phe142 of BLIP (Petrosino et al., 1998). The TEM-1 – Peptide (G48F) structure aligned on the TEM-1 – BLIP structure based on the C_α atoms of TEM-1 in order to compare the positions of Phe142 of BLIP and Phe48 of peptide. Despite the 7 Å of distance between the C_α atom of Phe142 and Phe48, both inserted their side chains through the cavity to occupy the same place.

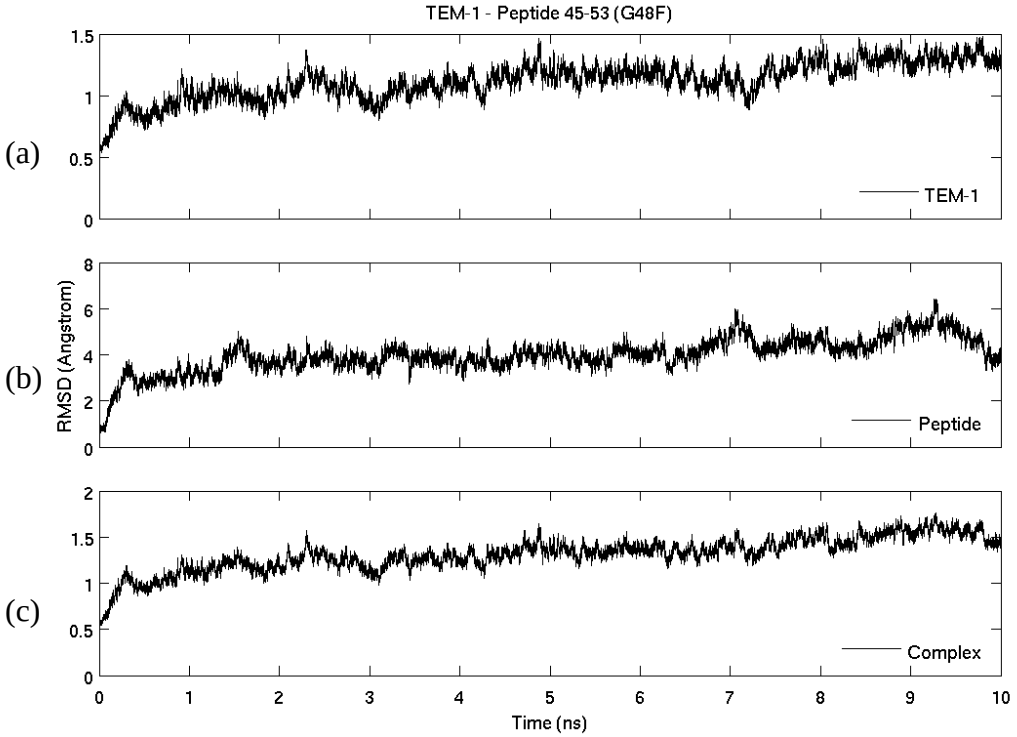

Figure 4.8. RMSD profile of beta-lactamase, peptide and complex in TEM-1 - Peptide 45-53 (G48F) simulation.

At the beginning of the simulation Asp49 is 8, 12, 7, 13, 11, 10 Å away from the active site residues Ser70, Lys73, Ser130, Glu166, Asn170 and Lys234 respectively and the distance of Phe48 to Glu104, Tyr105, Asn170, Ala237, Gly238 and Glu240 is 9, 7, 12, 6, 7, 13 Å respectively. Their distance did not change during the simulation with little fluctuations at the active site pocket of TEM-1 so peptide did not move away from TEM-1.

Nevertheless, high flexible N and C terminuses revealed high mobility during the simulation and this led to increase in average RMSD value of P8 which is deviated from TEM-1 with 4.18 Å of RMSD value. Also the bulkier side chain of Phe48 with respect to Gly48 in the wild type might have led to high RMSD value.

4.1.9. TEM-1 - Peptide 45-53 (G48F, Y50A) Complex

As mentioned before, a previous experimental study on TEM-1 – BLIP suggests that Y50A mutation on BLIP increases binding affinity for TEM-1 by 50-fold (Zhang and Palzkill, 2003). Considering this finding Y50A mutation was used besides G48F mutation and a double mutant peptide was constructed based on 45 to 53 of BLIP in order to increase binding affinity. FlexPepDock (Raveh et al., 2010; London et al., 2011) was used to dock the peptide in the most suitable conformation to TEM-1 to provide the function of F142 of BLIP by G48F of P9.

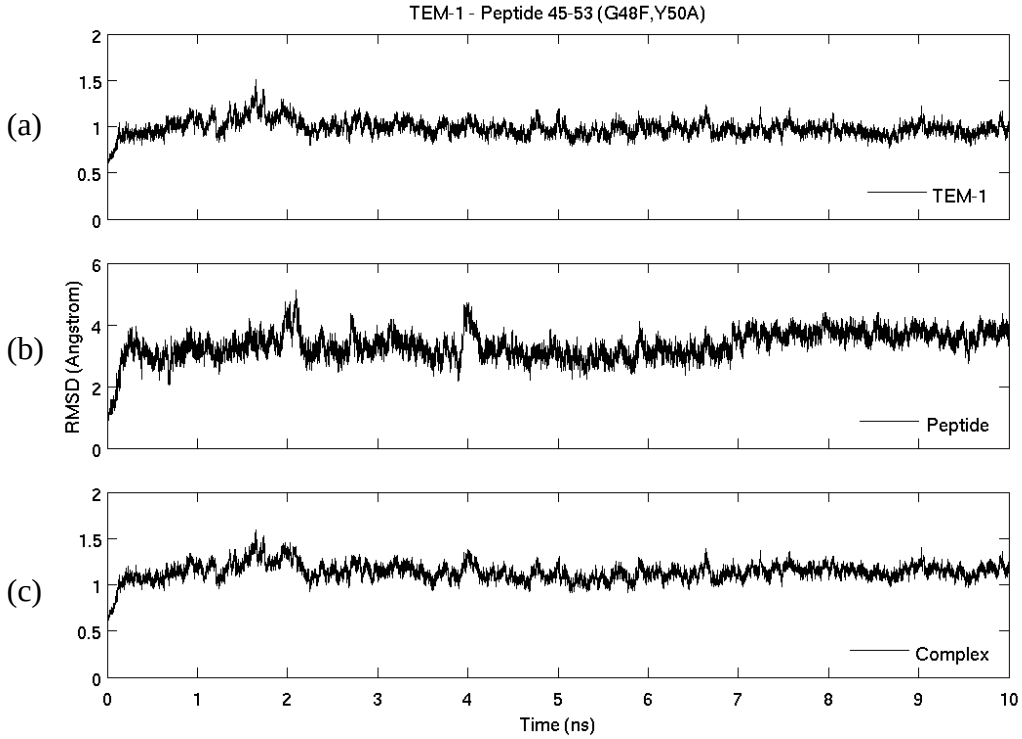

Figure 4.9. RMSD profile of beta-lactamase, peptide and complex in TEM-1 - Peptide 45-53 (G48F Y50A) simulation.

According to the Figure 4.9a TEM-1 in the presence of P9 reached equilibrium in 2 ns with a 0.81 Å of average deviation from the initial structure. RMSD of P9 was

calculated after the alignment of average simulation structure to its initial structure with a RMSD value of 1.01 Å (Table 4.2) and also alignment was performed on the initial simulation structure of TEM-1 to examine P9 deviation from TEM-1 the RMSD profile of which revealed in Figure 4.9b.

P9 has a stable RMSD profile although some fluctuations occurred in 2^{nd} and 4^{th} ns (Figure 4.9b). The examination of the simulation structure in VMD showed that, the double mutated peptide P8 was docked with 9, 13.5, 7, 14.5, 12.5, 10 Å of distance between Asp49 of P8 and TEM-1 active site residues Ser70, Lys73, Ser130, Glu166, Asn170 and Lys234 respectively. Except Ser130 and Lys234, the distances are 1 to 1.5 Å more than the initial distance between Asp49 and TEM-1 active site residues in wild type (8, 12.5, 7, 13, 11, 10). The distance of Asp49 from active site residues revealed a change about 0 to 2.5 Å at 2^{nd} and 4^{th} ns of the simulation but at the end of the simulation the peptide stayed 8, 12, 7.5, 14, 13, 7.5 Å away from Ser70, Lys73, Ser130, Glu166, Asn170 and Lys234 respectively. The distance of Phe48 from Glu104, Tyr105, Asn170, Ala237, Gly238 and Glu240 that in contact with is 10, 8, 10, 5, 7 and 12 Å at initial simulation structure. Although Phe48 preserved its distance throughout the simulation, at 2^{nd} and 4^{th} ns 1Å of movement away from them was observed. According to these findings it can be concluded that P9 deviated away from TEM-1 in 2^{nd} and 4^{th} ns of the simulation but mostly fluctuates in the same distance from TEM-1 with 3.24 Å of average deviation from TEM-1.

4.2. Mobility of TEM-1 - Peptide Simulation Systems

As previously mentioned peptides were created based on 45 to 52 or 45 to 53 loop of BLIP including the mutations A46W, D49A, Y50A, Y51A, G48F and G48FY50A. In order to investigate mobility of each simulation system, mean square fluctuations (MSF) were calculated which give fluctuations about the average structure. Table 4.3 shows residue averaged MSF values of TEM-1 and peptides as well as their complexes.

According to the Table 4.3 mobility of TEM-1 changes around 0.37 $Å^2$ in different simulation system. However mobility of peptide in each simulation system varies between 0.11 and 2.74 $Å^2$. Peptide gained high mobility due D49A mutation in which interaction

between residue 49 of BLIP and TEM-1 active site residues lost. Wild type peptide 45-52 (1.52 $Å^2$) displayed a more fluctuating profile than wild type peptide 45-53 (1.23 $Å^2$). LLIIL residues did not change mobility of peptide 45-53 significantly also mobility of TEM-1 binding to it. Peptides P5, P8 and P9 are significantly less mobile than other peptides; cyclic side chain structure of tryptophan (W) and phenyalanine (F) might have restricted the mobility of these peptides. Including Y50A mutation besides G48F, peptide 45-53 did not reveal a significant change with respect to the simulation system that has only G48F mutation.

Table 4.3 Mean Square Fluctuations of TEM-1, peptide, TEM-1 – Peptide Complex.

Simulation	**TEM-1 - Peptide Complex**	**MSF ($Å^2$)**		
		Beta-Lactamase	**Ligand**	**Complex**
P1	TEM-1 - Peptide 45 to 52 wt	0.41	1.52	0.78
P2	TEM-1 - Peptide 45 to 52 (D49A)	0.42	2.74	1.01
P3	TEM-1 - Peptide 45 to 52 (Y50A)	0.40	1.44	0.55
P4	TEM-1 - Peptide 45 to 52 (Y51A)	0.36	1.38	0.62
P5	TEM-1 - Peptide 45 to 52 (A46W)	0.32	0.11	0.38
P6	TEM-1 - Peptide 45 to 53 wt	0.38	1.23	0.58
P7	TEM-1 – Peptide LLIIL-45-53	0.38	1.33	0.70
P8	TEM-1 - Peptide 45 to 53 (G48F)	0.34	0.50	0.37
P9	TEM-1 - Peptide 45 to 53 (G48F Y50A)	0.32	0.43	0.32

In spite of the fact that average mobility of TEM-1 in each simulation system did not change remarkably, important regions of TEM-1 revealed some variety due to the mutations on peptide. All the mobility changes in beta-lactamase features depending on the peptide binding to it were examined in detail and mentioned in the following parts.

4.2.1. Mobility of TEM-1 Beta-Lactamase In The Presence of Wild Type Peptide 45-52 (P1) or 45-53 (P6) and The Effect of LLIIL Addition to Peptide 45-53 on TEM-1.

MSF values were calculated by using Matlab and the script in Appendix B. Simulation trajectory file that comprises whole motion of the beta-lactamase throughout the equilibrium period of the simulation was used as the input. After the alignment of the

time averaged beta-lactamase structure from the simulation on the initial simulation structure of beta-lactamase based on C_α atoms, MSF values of each residue on beta-lactamase were calculated. Then MSF graphs that reveal MSF value of each residue were gained. From the MSF graph, MSF values of TEM-1 residues in the presence of peptide 45-52 (P1) (Figure 4.10a) and peptide 45-53 (P6) (Figure 4.10b) and also their difference by subtracting residue based MSF values of P6 bound TEM-1 from P1 bound TEM-1 (ΔMSF) (Figure 4.10c) can be seen.

Average mobility of TEM-1 is nearly the same with 0.41 $Å^2$ and 0.38 $Å^2$ of MSF values in the presence of P1 and P6 respectively. On the other hand, important regions of TEM-1 responded differently depending on the peptide type (Figure 4.10).

H10 helix (218 to 230) of TEM-1 is significantly more mobile in the presence of P1 with 1.35 $Å^2$ of MSF value whereas MSF value of H10 helix is 0.63 $Å^2$ in the presence of P6 (Table 4.4). Also H9-H10 region (201 to 230) is more mobile in the presence of P1 (0.91 $Å^2$) due to the high flexible H10 helix while the mobility of H9-H10 is 0.65 $Å^2$ when TEM-1 bound to P6. On the other hand Asp214 on the loop connecting H9 helix (201 to 212) to H10 helix is significantly more mobile when TEM-1 bound to P6. Also, Leu198 which is close to N-terminus of H9 helix (201 to 212) is more mobile in the presence of P6 too.

Omega loop (161 to 179) is the low mobile feature of TEM-1 beta-lactamase with respect to other regions and in the presence of P1 its mobility is 0.33 $Å^2$ which is less than the mobility of omega loop in the presence of P6 (0.49 $Å^2$). Also omega loop flexible part (174-176) is less mobile when TEM-1 in complex with P1 with MSF value of 0.93 $Å^2$ while its MSF values is 1.32 $Å^2$ in TEM-1 – P6 complex. Moreover, Gly156 on the loop connecting omega loop to H6 helix (145 to 154) is less mobile in the presence of P1.

Asp252 located on the loop connecting B4 (243 to 251) and B5 (259 to 266) beta-strands, is more mobile when TEM-1 bound to P1.

While mobility of H9-H10 and omega loop of TEM-1 revealed differences depending on the peptide type, 99-112 loop has mobility around 0.50 $Å^2$ in the presence of either P1 or P6.

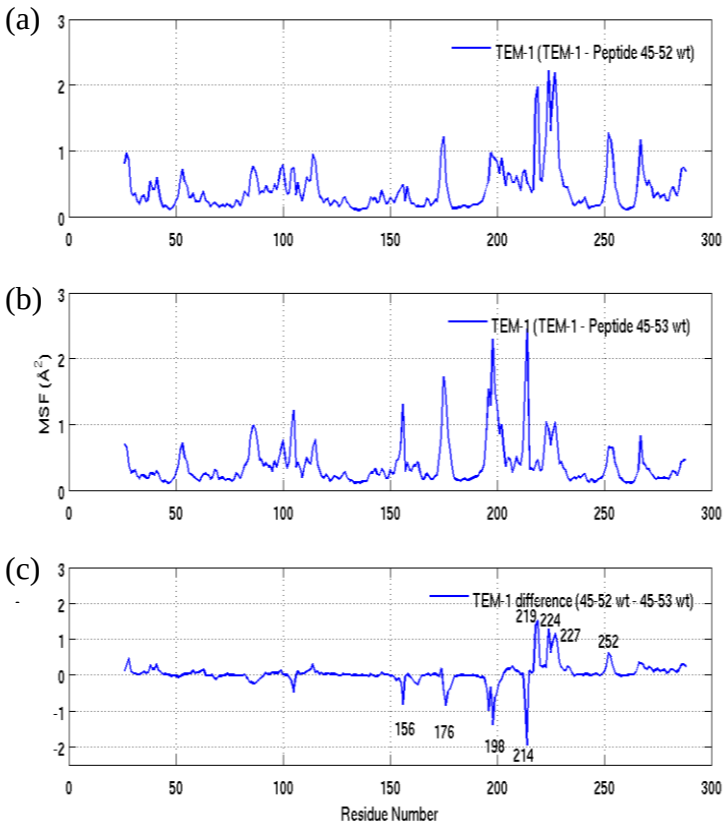

Figure 4.10. Residue based MSF of TEM-1 in the presence of peptide 45-52 (a) and peptide 45-53 (b) and difference between peptide 45-52 bound TEM-1 and peptide 45-53 bound TEM-1 (c).

TEM-1 structures were colored according to the MSF value of each residue in the presence of P1 and P6 (Figure 4.11). In order to generate colored structure figure, residue based MSF value data obtained by the Matlab script in Appendix B was used and the MSF values were mapped onto the structure in VMD by using the Tcl script in Appendix A. In the structure figure color scale varying blue to green to red which correspond to low to high MSF values.

According to the Figure 4.11, H10 is the most fluctuating part of TEM-1 in the presence of Peptide 45-52 while residues near the N and C terminuses of H9 helix and also omega loop flexible part are high mobile regions in the presence of Peptide 45-53.

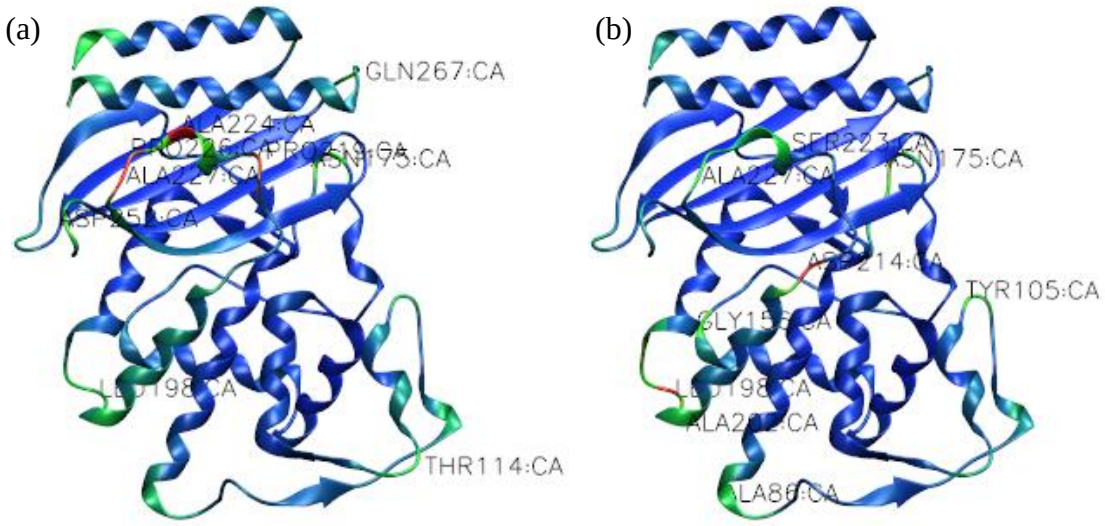

Figure 4.11. TEM-1 structure colored by residue based MSF values in TEM-1- Peptide 45-52 complex (a) and in TEM-1 – Peptide 45-53 complex (b).

TEM-1 in TEM-1 – Peptide LLIIL-45-53 complex was compared with TEM-1 in wild type complex structure (Figure 4.12) in order to evaluate the change in mobility of TEM-1 due to LLIIL addition to peptide.

Average mobility of TEM-1 did not change after the addition of LLIIL residues to peptide 45-53 and MSF value of TEM-1 is 0.38 $Å^2$ in both P6 and P7 bound forms (Table 4.4). However, some regions revealed change in mobility due to LLIIL.

Mobility of H9-H10 region (201 to 230) of TEM-1 decreased to 0.49 $Å^2$ from 0.65 $Å^2$ after addition of LLIIL to peptide 45-53. Also 99-112 loop of TEM-1 lost mobility and its MSF value decreased to 0.39 $Å^2$ from 0.52 $Å^2$ (Table 4.4). Besides, Leu198 near the N-terminus of H9 helix (201 to 212) and Gly156 on the loop near the omega loop lost mobility. On the other hand, omega loop (161 to 179) gained mobility after LLIIL addition to peptide 45-53 and its MSF value increased from 0.49 Å in P6 bound structure to 0.62 Å in P7 bound structure.

According to the TEM-1 structure colored by residue based MSF value (Figure 4.12d), the most flexible residues of TEM-1 correspond to residues of omega loop especially its flexible tip in the presence of P7 with 1.48 $Å^2$ of MSF value.

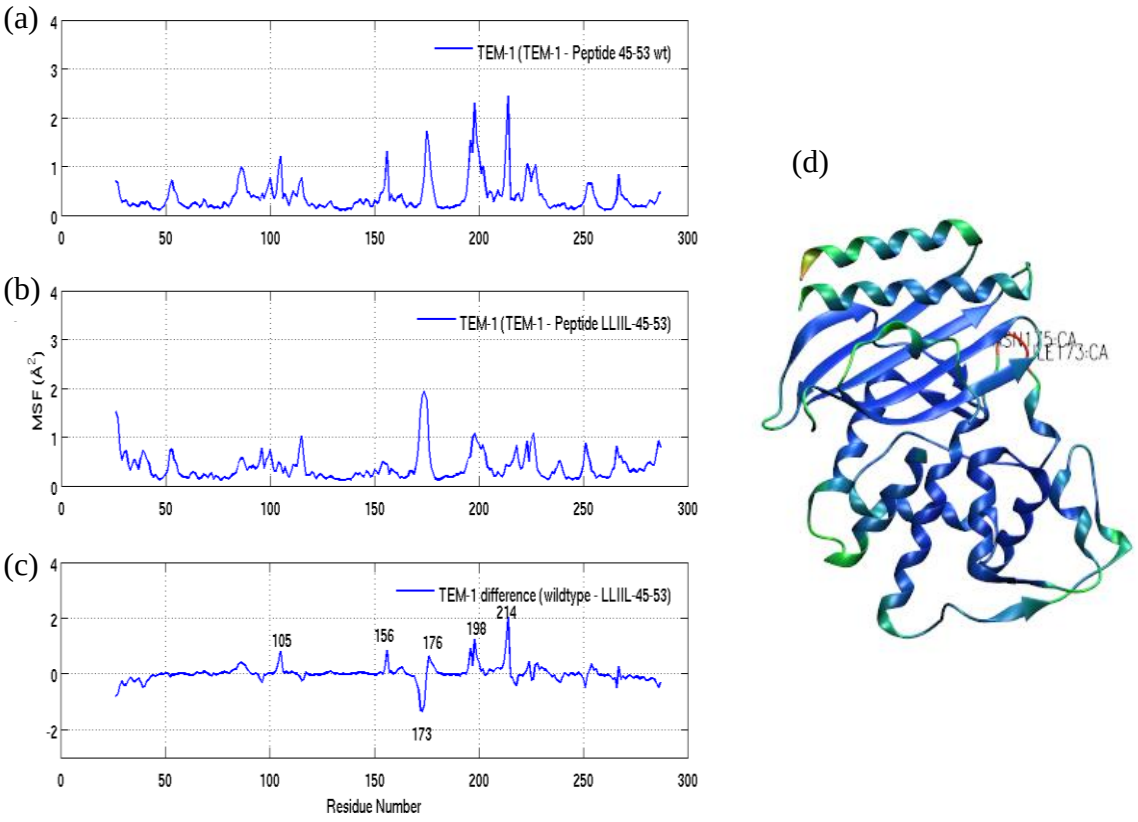

Figure 4.12. MSF of TEM-1 in the presence of peptide 45-53 (a), peptide LLIIL-45-53 (b), their mobility difference (c), TEM-1 structure colored by residue based MSF values in the presence of peptide LLIIL-45-53 (d).

4.2.2. Mobility of TEM-1 Beta-Lactamase Binding to Peptide 45-52 with D49A Mutation

TEM-1 in TEM-1 – Peptide 45-52 (D49A) complex was compared with TEM-1 in wild type complex structure (Figure 4.13) in order to evaluate the effect of D49A mutation on mobility of TEM-1.

According to the average MSF value of TEM-1 in the presence of peptide 45-52 (D49A) (P2), mutation of catalytically important residue Asp49 to alanine did not change average mobility of TEM-1 (0.42 $Å^2$) but the peptide itself affected due to mutation and revealed an increase in mobility from 1.52 $Å^2$ in wild type to 2.74 $Å^2$ in P2. In spite of the fact that, no change in the average mobility of TEM-1, the important regions of TEM-1 revealed some changes due to mutation.

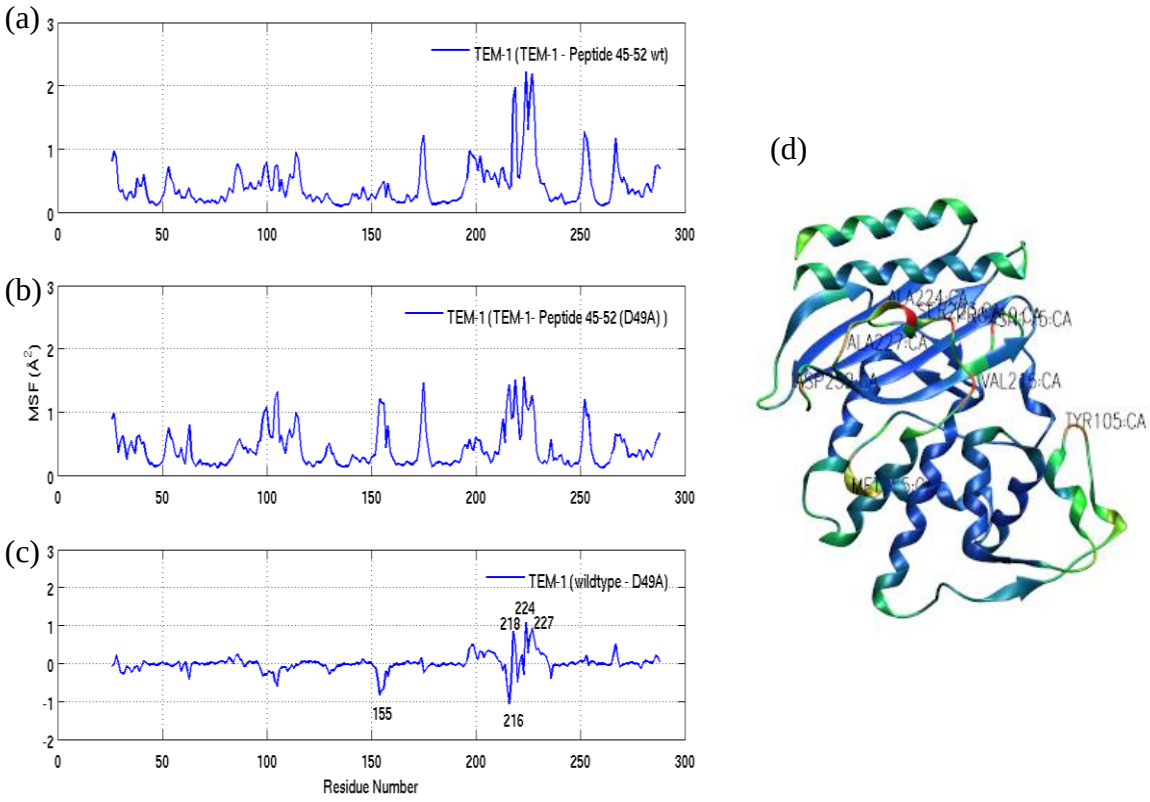

Figure 4.13. MSF of TEM-1 in the presence of peptide 45-52 (a), peptide 45-52 (D49A) (b), their mobility difference (c), TEM-1 structure colored by residue based MSF value in the presence of peptide 45-52 (D49A).

H10 helix (218 to 230) of TEM-1 lost mobility due to D49A mutation on peptide and decreased to 0.95 $Å^2$ from 1.35 $Å^2$ in wild type. Conversely, 99-112 loop gained mobility and its MSF value increased to 0.74 $Å^2$ from 0.51 $Å^2$ in wild type. Also Met155, located on the loop near the N- terminus of omega loop (161 to 179), and Val216 on the loop connecting H9 and H10 helixes gained mobility after D49A mutation.

TEM-1 structure colored by residue based MSF value indicates most flexible parts of TEM-1 that correspond to H10 helix, omega loop flexible part and 99-112 loop in the presence of P2 (Figure 4.13d).

4.2.3. Mobility of TEM-1 Beta-Lactamase Binding to Peptide 45-52 with Y50A Mutation

TEM-1 in TEM-1 – Peptide 45-52 (Y50A) complex was compared with TEM-1 in wild type complex structure (Figure 4.14) in order to evaluate the effect of Y50A mutation on mobility of TEM-1.

Considering the Table 4.4, after tyrosine at position 50 mutated to alanine, average mobility of TEM-1 did not reveal a change. On the other hand, due to Y50A mutation on peptide, mobility of H10 helix (218 to 230) decreased to 0.92 $Å^2$ from 1.35 $Å^2$ in wild type, while mobility of 99-112 loop increased to 0.73 $Å^2$ from 0.51 $Å^2$ in wild type. Mobilities of Gly196 and Ala213, at the N and C terminuses of H9 helix (201 to 212) respectively, increased due to Y50A mutation too (Figure 4.14c).

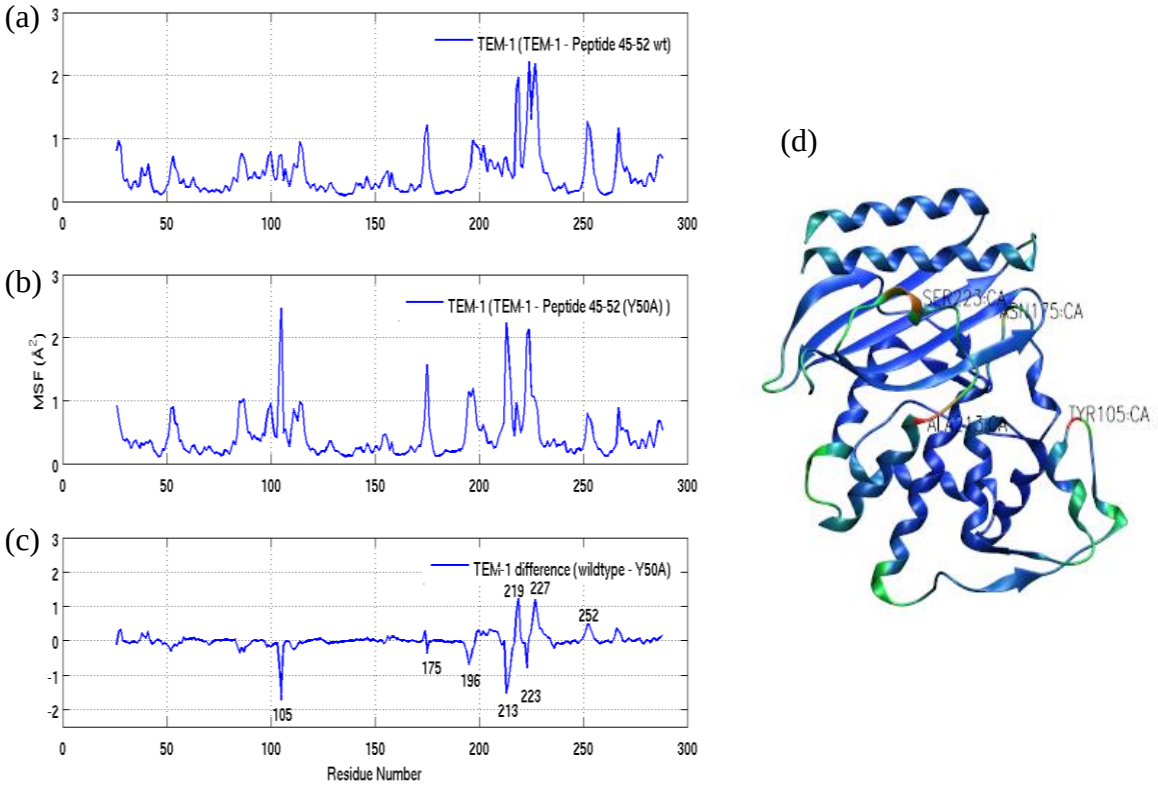

Figure 4.14. MSF of TEM-1 in the presence of peptide 45-52 (a), peptide 45-52 (Y50A) (b), their mobility difference (c), TEM-1 structure colored by residue based MSF value in the presence of peptide 45-52 (Y50A).

TEM-1 structure colored by residue based MSF value reveals the most flexible regions of TEM-1 in the presence of P3. According to that, despite the decrease in mobility of H10 helix with respect to wild type structure still H9-H10 region is very mobile, also 99-112 loop and omega loop flexible part are very mobile regions of TEM-1 in the presence of P3 (Figure 4.14d).

4.2.4. Mobility of TEM-1 Beta-Lactamase Binding to Peptide 45-52 with Y51A Mutation

The effect of Y51A mutation on TEM-1 mobility was examined by comparing TEM-1 in TEM-1 – Peptide 45-52 (Y51A) complex with TEM-1 in wild type complex structure (Figure 4.15). According to that mutation of tyrosine at position 51 to alanine in peptide 45-52, decreased average mobility of TEM-1 to 0.36 $Å^2$ in P4 bound structure from 0.41 $Å^2$ in wild type P1 bound structure.

According to the Figure 4.15, due to Y51A mutation mobility of H9-H10 region (201 to 230) decreased especially H10 helix (218 to 230) revealed significant decrease in mobility to 0.56 $Å^2$ from 1.35 $Å^2$ in wild type . Also, mobility of Asp252 on the loop connecting B4 and B5 beta strands decreased. However, residues from 146 to 154 located on the H6 helix (145 to 154) which is very close to N-terminus of omega loop (161 to 179) increased their mobility due to Y51A mutation of peptide 45-52.

Despite the increase in mobility of H9-H10 region, 99-112 loop and omega loop did not reveal change in mobility due to mutation.

TEM-1 structure colored by residue based MSF value reveals the most flexible regions of TEM-1 in the presence of P4. Omega loop flexible tip and H6 helix (145 to 154) which is very close to N-terminus of omega loop (161 to 179) are pretty mobile regions of TEM-1 in the presence of P4. Moreover, Asp115 on the loop connecting 99-112 loop to b3 strand (115 to 118) is a mobile residue of TEM-1 in P4 bound structure (Figure 4.15 D).

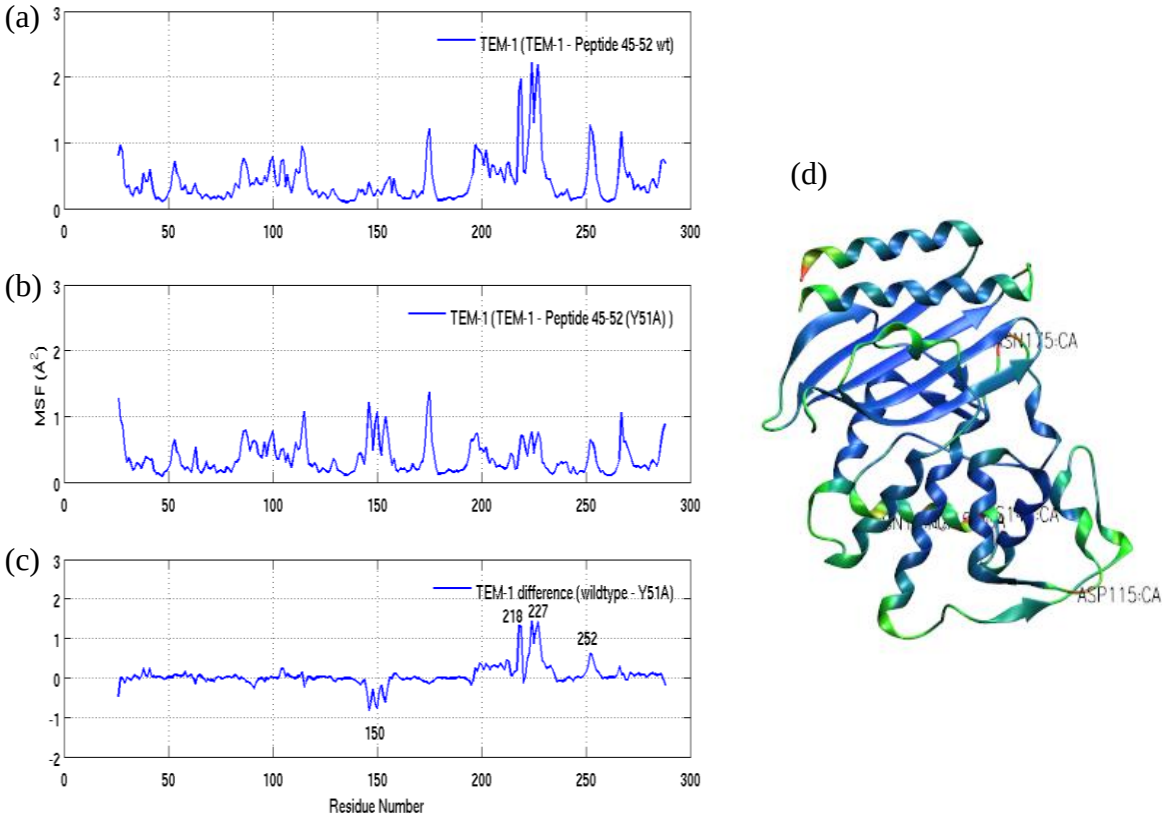

Figure 4.15. MSF of TEM-1 in the presence of peptide 45-52 (a), peptide 45-52 (Y51A) (b), their mobility difference (c), TEM-1 structure colored by residue based MSF value in the presence of peptide 45-52 (Y51A).

4.2.5. Mobility of TEM-1 Beta-Lactamase Binding to Peptide 45-52 with A46W Mutation

Ala46 of peptide 45-52 was mutated to tryptophan and TEM-1 – Peptide 45-52 (A46W) complex was simulated for 10ns with MD simulation. This substitution at position 46 decreased average mobility of TEM-1 to 0.32 $Å^2$ from 0.41 $Å^2$ in wild type. Also mobility of the important regions of TEM-1 revealed some changes due to mutation.

Mobility of H10 helix (218 to 230) decreased significantly to 0.46 $Å^2$ from 1.35 $Å^2$ in wild type (Table 4.3). On the other hand, Gly156 on the loop connecting omega loop (161 to 179) to H6 (145 to 154) gained some mobility despite the mobility of omega loop did not change due to mutation. Moreover, the loop connecting H2 helix (69 to 84) to b2 strand (94 to 97) gained some mobility due to mutation (Figure 4.16c).

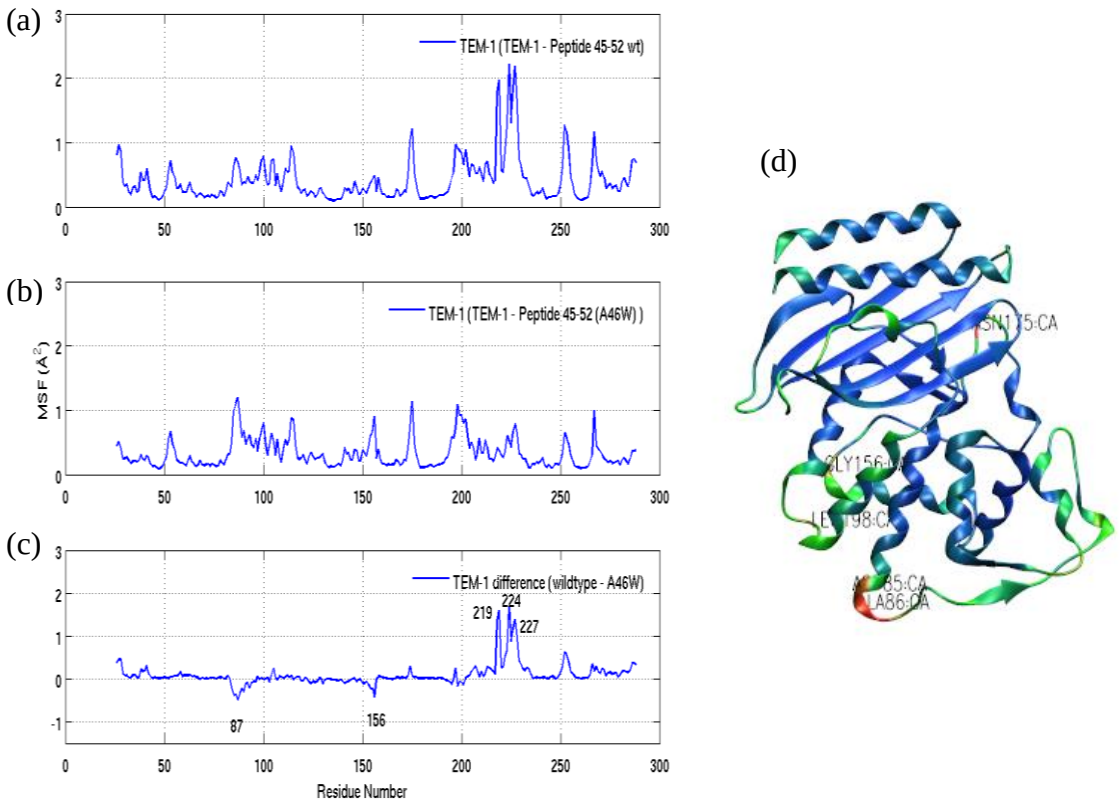

Figure 4.16. MSF of TEM-1 in the presence of peptide 45-52 (a), peptide 45-52 (A46W) (b), their mobility diffrence (c), TEM-1 structure colored by residue based MSF value in the presence of peptide 45-52 (A46W).

TEM-1 structure colored by residue based MSF value reveals the most flexible regions of TEM-1 in the presence of P5, that are omega loop flexible part and the loop which connecting H2 helix (69 to 84) to b2 strand (94 to 97).

4.2.6 Mobility of TEM-1 Beta-Lactamase Binding to Peptide 45-53 with G48F Mutation

Glycine at position 48 of peptide 45-53 mutated to phenylalanine to fulfill the role of side chain of Phe142 in BLIP on binding. G48F mutation on BLIP led slight decrease in average MSF value of TEM-1 to 0.34 $Å^2$ from 0.38 $Å^2$ in wild type complex. Also mobility of the important regions of TEM-1 revealed some changes due to mutation.

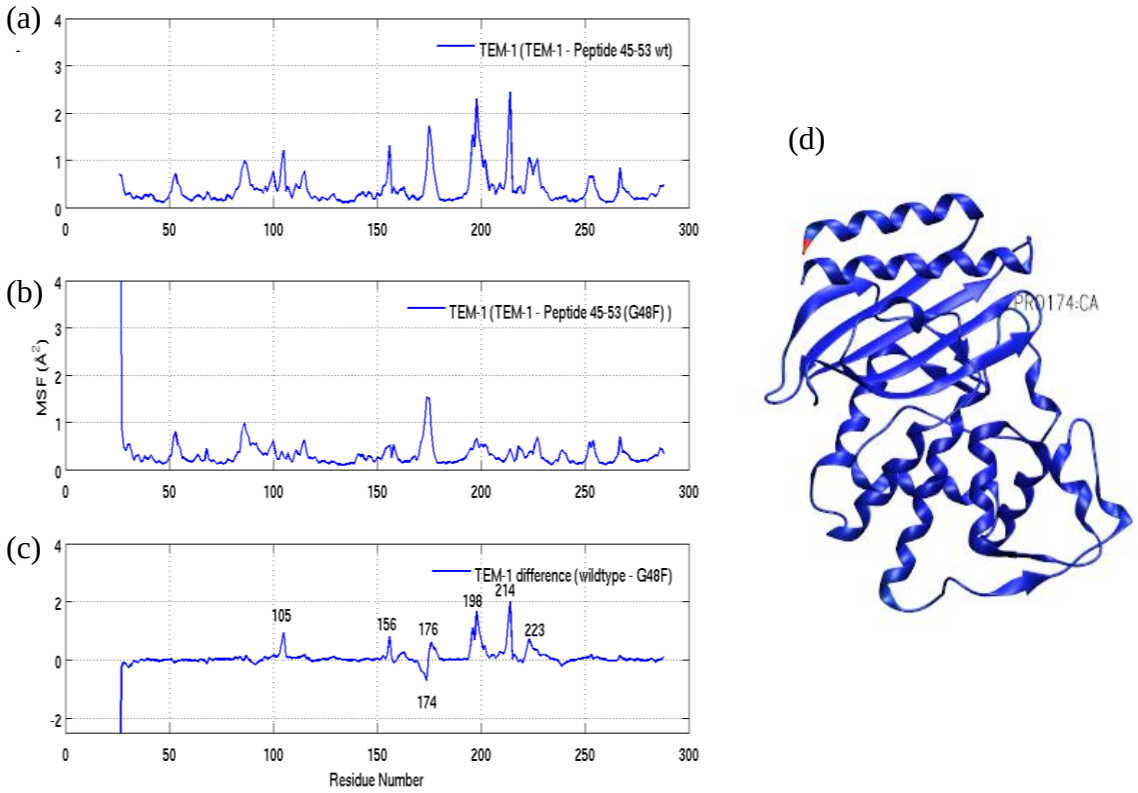

Figure 4.17. MSF of TEM-1 in the presence of peptide 45-53 (a), peptide 45-53 (G48F) (b), their mobility difference (c), TEM-1 structure colored by residue based MSF value in the presence of peptide 45-53 (G48F).

H9-H10 region (201 to 230) of TEM-1 affected mostly due to the G48F mutation on peptide (Figure 4.17). MSF value of H9-H10 decreased to 0.34 $Å^2$ while it is 0.65 $Å^2$ in TEM-1 – Peptide 45-53 wild type complex (Table 4.4). Also, mobility of Leu198 which is near the N-terminus of H9 helix decreased due to G48F mutation on peptide (Figure 4.17c). Moreover 99-112 loop became less mobile with 0.32 $Å^2$ of MSF value, while its MSF value is 0.52 $Å^2$ in wild type.

On the other hand, omega loop (161 to 179) and its flexible tip did not reveal significant change in mobility due to G48F mutation.

TEM-1 structure colored by residue based MSF value; reveals the most flexible regions of TEM-1 in the presence of P8 (Figure 4.17d). Based on the TEM-1 structure, mobility of the beta-lactamase decreased in the presence of P8 and revealed nearly rigid

structure (blue) except the omega loop flexible tip whose MSF value is 1.28 $Å^2$ which is close to MSF value of it in wild type structure (Table 4.4).

4.2.6. Mobility of TEM-1 Beta-Lactamase Binding to Peptide 45-53 with G48F and Y50A Mutations

In this simulation system, both G48F and Y50A mutations were done on the purpose of increasing the binding affinity of peptide 45-53 to TEM-1. Average mobility of TEM-1 in the presence of P9 did not change with respect to TEM-1 in the presence of P8 but mobility of TEM-1 decreased to 0.32 $Å^2$ with respect to TEM-1 in the presence of wild type peptide P6 (0.38 $Å^2$). Also mobility of the important regions of TEM-1 revealed some changes due to mutation with respect to wild type.

Mobility of H9-H10 region (201 to 230) decreased to 0.41 $Å^2$ in TEM-1-P9 complex while its mobility is 0.65 $Å^2$ when TEM-1 bound to wild type peptide P6 (Table 4.4). Also, mobility of Leu198 which is near the N-terminus of H9 helix decreased due to G48F and Y50A mutations on peptide.

Furthermore, 99-112 loop revealed some decrease in mobility to 0.33 $Å^2$ from 0.52 $Å^2$ in wild type (Table 4.4). While mobility of omega loop did not change with respect to wild type structure, its flexible tip became less mobile (0.93 $Å^2$) due to mutations.

TEM-1 structure colored by residue based MSF value; reveals the most flexible regions of TEM-1 in the presence of P9 (Figure 4.18). Considering the TEM-1 structure in P9 bound form, the most flexible part is omega loop flexible tip as in TEM-1 when bound to P8 but in TEM-1 structure bound to P9, some loops and turns (green) have more flexibility with respect to TEM-1 in P8 bound form, nearly whole of which was highlighted with blue that reveals somewhat rigidity except omega loop flexible part (Figure 4.18).

The important regions of TEM-1 that are thought to have importance in binding and the mobilities of these regions in each simulation system tabulated in Table 4.4. Also RMSD values for these regions were calculated and tabulated in the parenthesis.

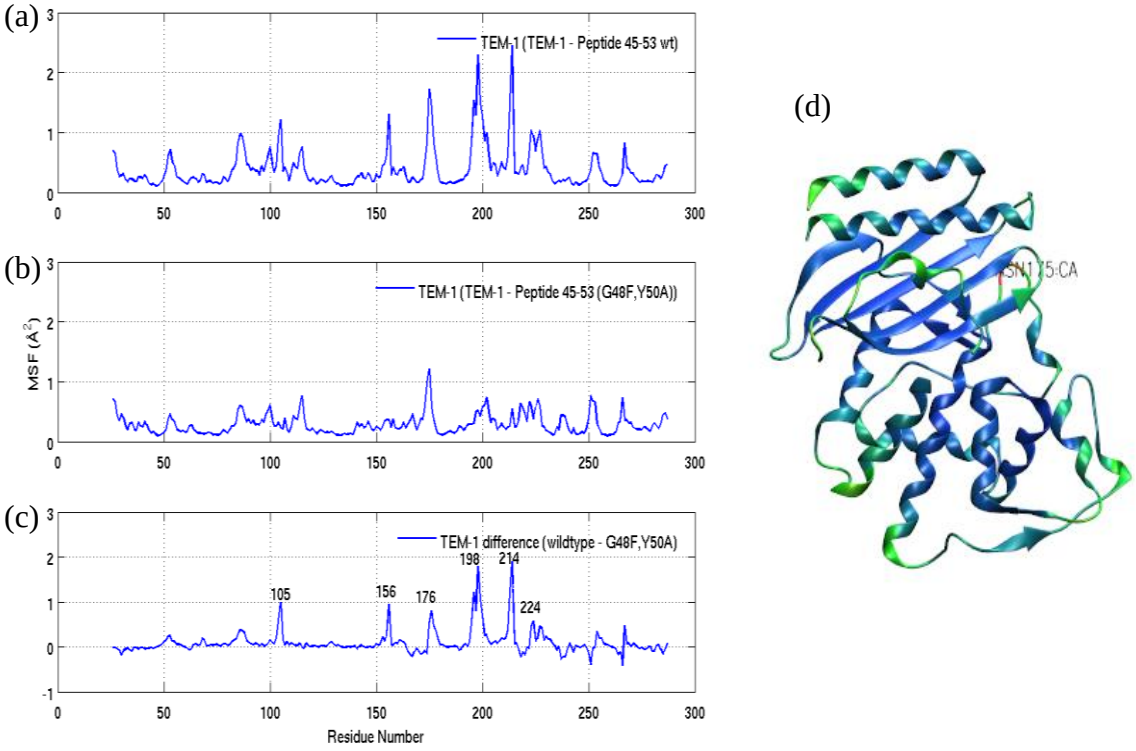

Figure 4.18. MSF of TEM-1 in the presence of peptide 45-53 (a) and peptide 45-53 (G48F Y50A) (b), their mobility difference (c), structure of TEM-1 in the presence of peptide 45-52 (G48F Y50A).

According to the Table 4.4, H10 helix is the most influenced region of TEM-1 beta-lactamase depending on the peptide binding to it. H10 helix is very mobile when TEM-1 bound to wild type peptide 45-52 (P1) but its mobility decreased when bound to wild type peptide 45-53 (P6). Also, mutations on peptide decreased the mobility of H10 helix; in the presence of P8 H10 helix of TEM-1 became least mobile with 0.39 $Å^2$ of MSF value.

The mobility of 99-112 loop was also affected depending on the peptide type. In the presence of P2 and P3 it became very mobile about 0.70 $Å^2$ of MSF value. On the other hand in the presence of P8 or P9 it became low flexible with around 0.30 $Å^2$ of MSF value. Other important regions of TEM-1 revealed similar flexibilities that did not change significantly due to the peptide binding to it. Nevertheless, addition of LLIIL residues to peptide 45-53 increased mobility of omega loop, especially mobility of its flexible tip to 0.62 $Å^2$ from around 0.40 $Å^2$.

Table 4.4. Mean square fluctuations of important regions on TEM-1 beta-lactamase, RMSD values are in parenthesis.

Simulation	H10	H9-H10	99-112 loop	Ω loop	Ω loop flexible part
P1 (1.5-10ns)	1.35 (0.93)	0.91 (0.97)	0.51 (0.72)	0.33 (0.74)	0.93 (1.13)
P2 (2.5-10ns)	0.95 (1.43)	0.73 (1.57)	0.74 (1.40)	0.35 (0.71)	1.02 (0.85)
P3 (2.5-10ns)	0.92 (2.01)	0.78 (1.63)	0.73 (0.92)	0.34 (0.60)	0.97 (1.02)
P4 (1.5-10ns)	0.56 (1.40)	0.41 (1.53)	0.46 (0.76)	0.38 (0.69)	1.04 (1.19)
P5 (2.5-10ns)	0.46 (1.24)	0.42 (1.03)	0.46 (0.87)	0.30 (0.52)	0.84 (0.77)
P6 (1.5-10ns)	0.63 (1.20)	0.65 (0.97)	0.52 (0.90)	0.49 (0.66)	1.32 (0.91)
P7 (2-10ns)	0.58 (1.56)	0.49 (1.63)	0.39 (1.18)	0.62 (1.65)	1.48 (3.06)
P8 (3-10ns)	0.39 (1.26)	0.34 (1.60)	0.32 (1.25)	0.47 (1.15)	1.28 (2.25)
P9 (2-10ns)	0.48 (1.29)	0.41 (1.09)	0.33 (1.16)	0.41 (0.87)	0.93 (1.45)

A comparison of the change in mobilities of important regions of TEM-1 due to the peptide binding to it revealed the reasons of some differences between average mobilities of TEM-1 due to the peptide binding to it.

When TEM-1 bound to P2, D49A mutation on peptide decreased mobility of H10 helix while it increased mobility of 99-112 loop with respect to those in TEM-1 in the presence of wild type P1. So TEM-1 has the same average MSF value both in TEM-1 – P1 (0.41 $Å^2$) and TEM-1 – P2 (0.42 $Å^2$) structures. Also Y50A mutation has similar effect on TEM-1 by decreasing H10 helix mobility while increasing 99-112 loop mobility that led to the same average MSF value of TEM-1in the presence of P3 (0.40 $Å^2$) with TEM-1 in the wild type structure (0.41 $Å^2$) (Table 4.3).

However in TEM-1 – P4 complex Y51A mutation and in TEM-1 – P5 complex A46W mutation decreased mobility of H10 helix significantly while mobilities of 99-112 loop and omega loop stayed nearly the same with respect to wild type. This decrease in

mobility of H10 helix, decreased the average mobility of TEM-1 in the presence of P4 (0.36 $Å^2$) or P5 (0.32 $Å^2$) when compared with TEM-1 in the wild type complex (0.41 $Å^2$).

TEM-1 in the presence of P6 or P7 has approximate average MSF value (with 0.38 $Å^2$) with TEM-1 in the presence of P1. This is because TEM-1 in complex with P6 or P7 has less flexible H10 helix while it has more flexible omega loop flexible tip with respect to those in TEM-1 in the presence of P1.

On the other hand TEM-1 has low average MSF value when in complex with P8 (0.34 $Å^2$) or P9 (0.32 $Å^2$) with respect to TEM-1 in the presence of either wild type peptides P1 (0.41 $Å^2$) or P6 (0.38 $Å^2$). This is mainly arising from the very low mobile H10 helix due to the G48F mutation in TEM-1 – P8 complex and due to the G48F and Y50A mutations in TEM-1 – P9 complex.

According to these findings H10 helix is a very important region of TEM-1 beta-lactamase that revealed change in mobility due to the peptide binding to TEM-1. The response of H10 helix may be the main reason of binding affinity differences between TEM-1 and different peptide types.

4.3. Intermolecular Interaction Energy

Intermolecular interaction energy between the beta-lactamase and the peptide was calculated from the simulation trajectory file and the structure file for each simulation system by using NAMD Energy Plugin of VMD. At the end of the calculation an output file that comprises interaction energy in every 0.1 ns of time step was gained for each simulation system. These data files were loaded to Matlab and figures that reveal intermolecular interaction energy profiles of each system were drawn. Examination of energy profiles can give a clue about binding affinity of peptide to beta-lactamase and also their behaviors during the simulation whether the beta-lactamase and the peptide move away from each other or they come close to each other throughout the simulation.

The energy profiles show electrostatic (Figure 4.19 and Figure 4.22) and vdW (Figure 4.20 and Figure 4.23) interaction energies for each simulation system and these

two kinds of energy compose non-bonded interaction energy (Figure 4.21 and Figure 4.24) between beta-lactamase and the peptide for each simulation system.

According to the energy profiles vdW interaction is less effective whereas electrostatic interaction is the major contribution to the non-bonded interaction energy between beta-lactamase and the peptide.

Each peak to upward indicates that beta-lactamase and peptide moves away from each other and the peaks to downward indicates they come close thus the interaction between them gain strength. If energy profile is compared with RMSD profile of peptide respective which was calculated after the alignment of average structure of TEM-1 to the initial simulation structure of TEM-1, both figures reveal the movements of peptide with respect to TEM-1.

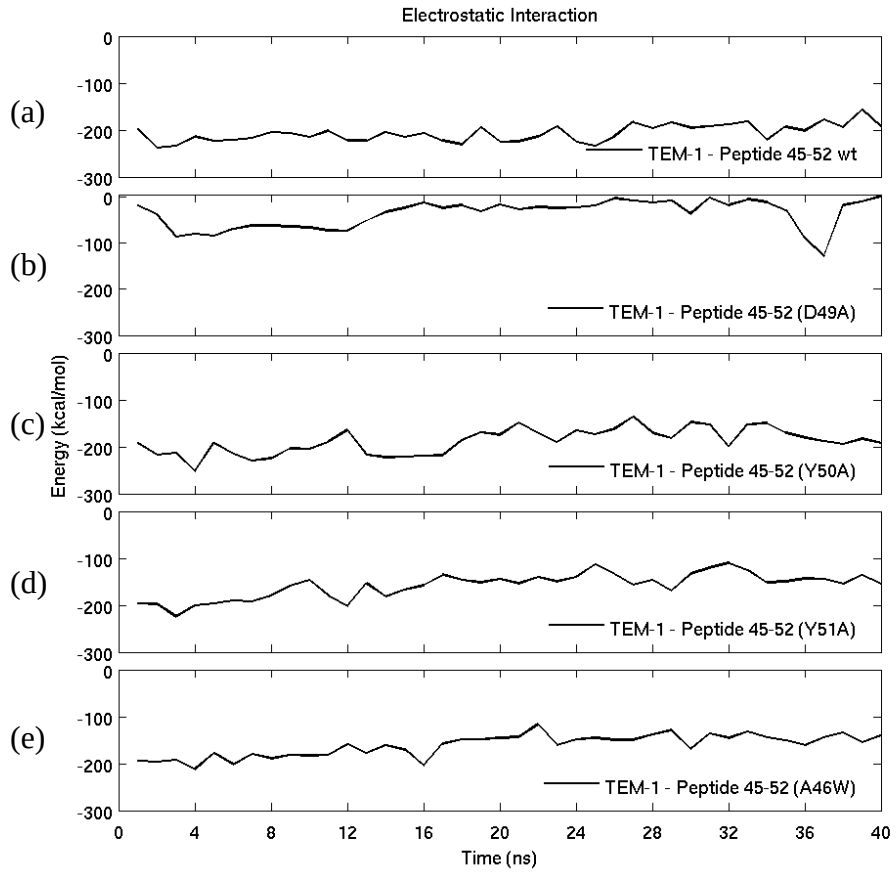

Figure 4.19. Electrostatic interaction energy between TEM-1 and wild type or mutated peptides corresponds to 45-52 region of BLIP.

According to the Figure 4.19 electrostatic interaction energy value range between -120 and -260 kcal/mol for each simulation system except TEM-1 – Peptide 45-52 (D49A) complex in which electrostatic energy ranges between 1 and -150 kcal/mol. Electrostatic energy profiles reveals fluctuations of peptides without significant change in distance to TEM-1, while electrostatic energy profile of TEM-1 – Peptide 45-52 (D49A) reveals peptide 45-52 (D49A) movements from TEM-1 or towards to TEM-1 (Figure 4.19b). Also electrostatic energy profile of TEM-1 – Peptide 45-52 (D49A) was compared with RMSD profile of peptide 45-52 (D49A) that shows its deviation with respect to TEM-1 (Figure 4.2b). This comparison revealed that after 3 ns peptide moved away from TEM-1 therefore electrostatic energy strength between TEM-1 and peptide decreased. Between 7^{th} at 8^{th} ns of simulation peptide moved towards to TEM-1 some, consequently the electrostatic interactions between them increased for a short time as Figure 4.19b shows. Also the increase in electrostatic interactions due to the movement of peptide towards TEM-1 after 9 ns can be seen from the figure.

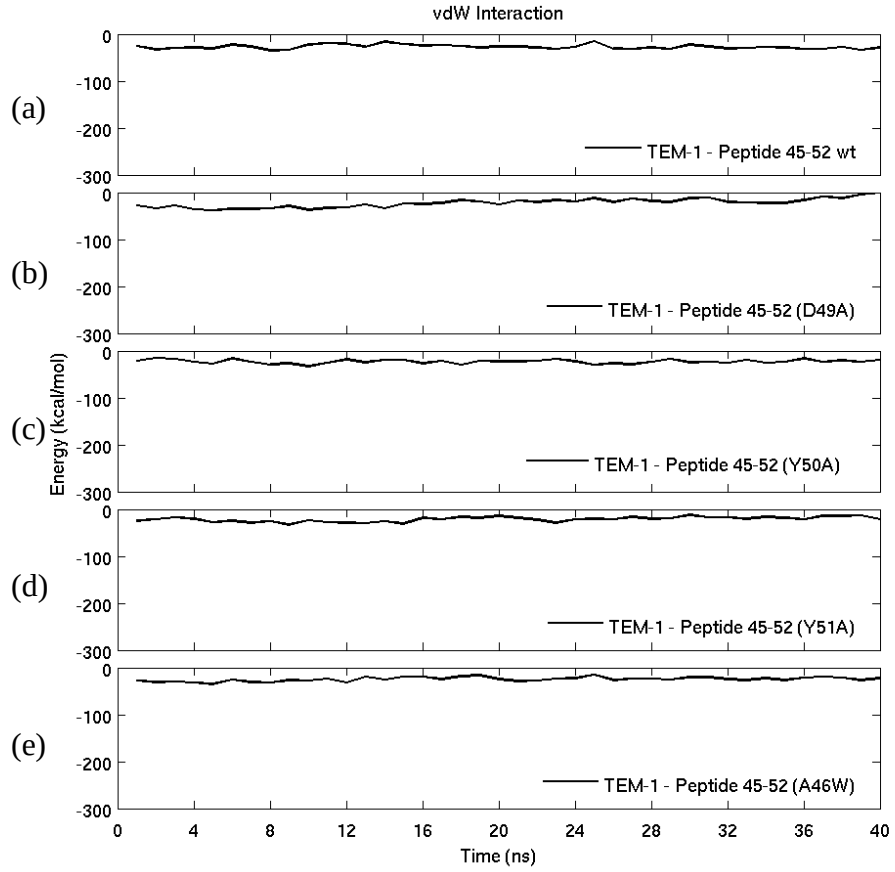

Figure 4.20. vdW interaction energy between TEM-1 and wild type or mutated peptides corresponds to 45-52 region of BLIP.

While electrostatic interactions range between 1 to -260 for different simulation systems, vdW interaction energy range between -1 to -40 (Figure 4.20) therefore vdW interaction has a minor contribution to total energy. Also vdW interaction profiles of complexes are more stable than electrostatic interaction profiles.

According to the interaction energy of TEM-1 – Peptide 45-52 wt, electrostatic energy which is the major contribution to non-bonded energies ranges between -150 to -240 kcal/mol, while vdW energy ranges between -15 to -35 kcal/mol. The total of these two energies that correspond to non-bonded interaction energy, changes from -190 to -280 kcal/mol while peptide fluctuates during the simulation. The interaction energy profile of complex reveals that throughout the simulation the peptide fluctuates without moving away from TEM-1. The average intermolecular energy of TEM-1 – Peptide 45-52 wt is -233.79 kcal/mol.

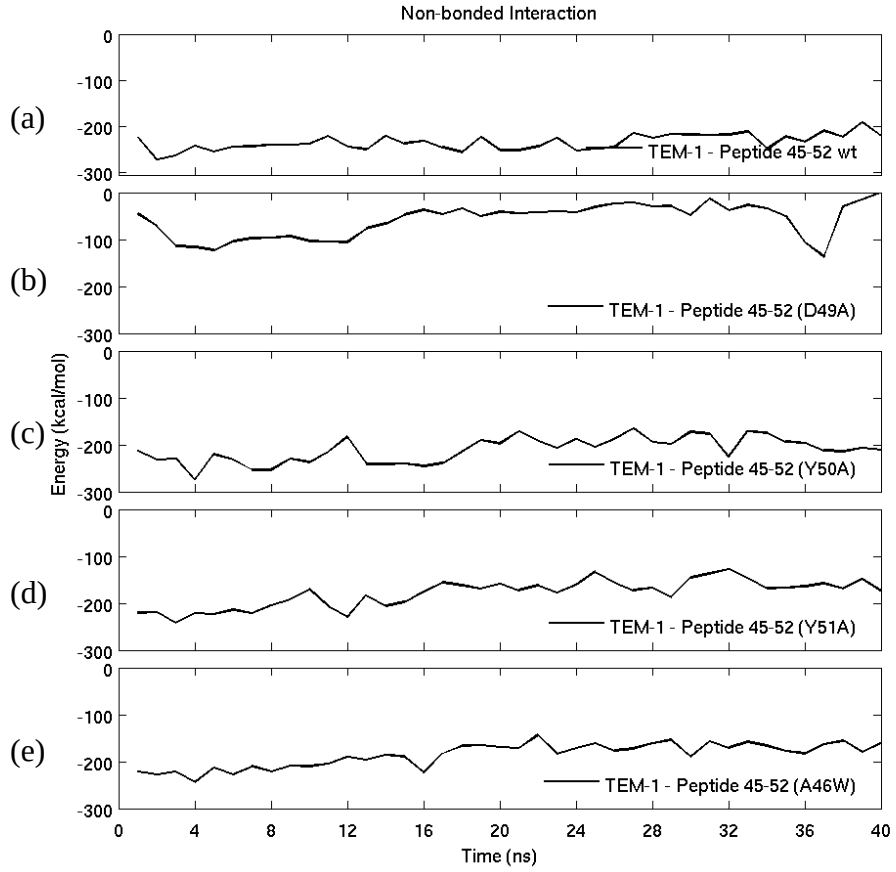

Figure 4.21. Non-bonded interaction energy between TEM-1 and wild type or mutated peptides corresponds to 45-52 region of BLIP.

The non- bonded interaction energy of TEM-1 – Peptide (D49A) complex ranging between 0 and -140 kcal/mol. Electrostatic interactions ranging between 1 and -150 while vdW interactions vary between -1 and -40 kcal/mol respectively. Intermolecular interaction between TEM-1 and peptide 45-52 (D49A) is low with -59.32 kcal/mol average non-bonded energy value.

Intermolecular interaction energy ranges between -170 and -280 kcal/mol in TEM-1 – Peptide (Y50A) complex, -120 to -250 kcal/mol in TEM-1 – Peptide (Y51A) complex and -140 to -250 kcal/mol in TEM-1 – Peptide (A46W) complex. Electrostatic interaction is the major contribution to intermolecular interaction energy for each complex likewise in wild type TEM-1 – Peptide 45-52 complex. The average non-bonded interaction energy values are -210, -179 and -184 kcal/mol for the complexes of TEM-1 with Y50A, Y51A and A46W mutated peptides respectively.

Intermolecular interaction energy profiles between TEM-1 and wild type or mutated peptides corresponds to 45-53 region of BLIP were shown; Figure 4.22 reveals electrostatic interactions, Figure 4.23 reveals vdW interactions and Figure 4.24 reveals total non-bonded interactions.

According to the intermolecular interaction energy profile of TEM-1 – Peptide 45-53 wt complex non-bonded interaction energy value ranges between -100 and -250 (Figure 4.24a). The major contribution to the energy comes from electrostatic interactions that energy value ranges between -60 and -230 kcal/mol (Figure 4.22a). vdW interactions are not effective as electrostatic interactions with energy values change between -15 and -35 during the simulation (Figure 4.23a).

The energy profile of TEM-1 – Peptide LLIIL-45-53 complex did not reveal a significant difference from wild type complex but the interaction between TEM-1 and peptide increased some with addition of LLIIL. The non-bonded interaction energy value ranges between -120 and -310 kcal/mol which reveal stronger interaction with respect to wild type. Nevertheless, at about 9 ns a decrease in electrostatic energy value occurred that indicates the movement of peptide from TEM-1 for a short time as the RMSD profile of

peptide indicates in Figure 4.7b. The average non-bonded interaction energy value for TEM-1 – Peptide LLIIL-45-53 is -245 kcal/mol.

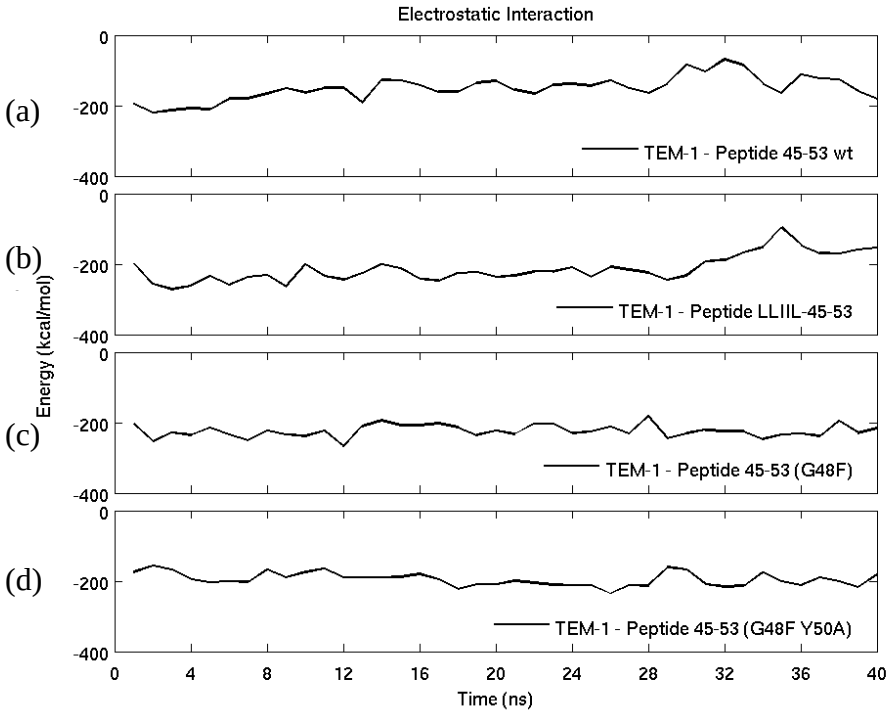

Figure 4.22. Electrostatic interaction energy between TEM-1 and wild type or mutated peptides corresponds to 45-53 region of BLIP.

Both TEM-1 – Peptide 45-53 (G48F) and TEM-1 – Peptide 45-53 (G48F Y50A) complexes have quite stable energy profiles so it can be deduced that peptides P8 and P9 preserve their distances from TEM-1 during the simulations. The main contribution to energy came from electrostatic interaction whose energy value ranges between -180 to -270 kcal/mol in TEM-1 – P8 and -150 to -220 in TEM-1 – P9 complex while total non-bonded interaction energy ranges between -240 to -310 kcal/mol in TEM-1 – P8 and -180 to -265 kcal/mol in TEM-1 – P9. The average non-bonded interaction energy values are -265 kcal/mol and -216 kcal/mol when TEM-1 bound to P8 and P9 respectively.

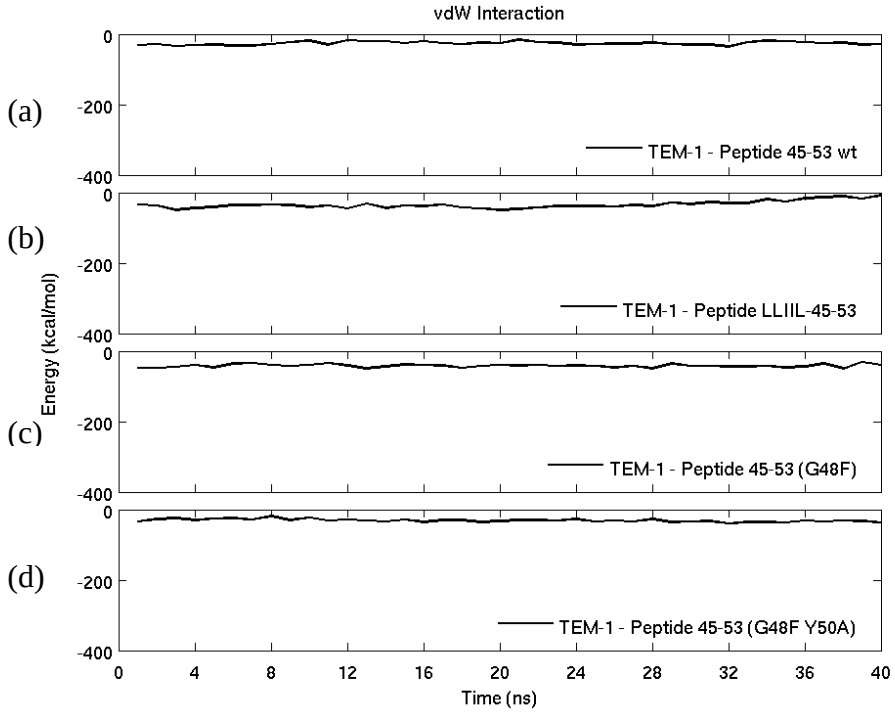

Figure 4.23. vdW interaction energy between TEM-1 and wild type or mutated peptides corresponds to 45-53 region of BLIP.

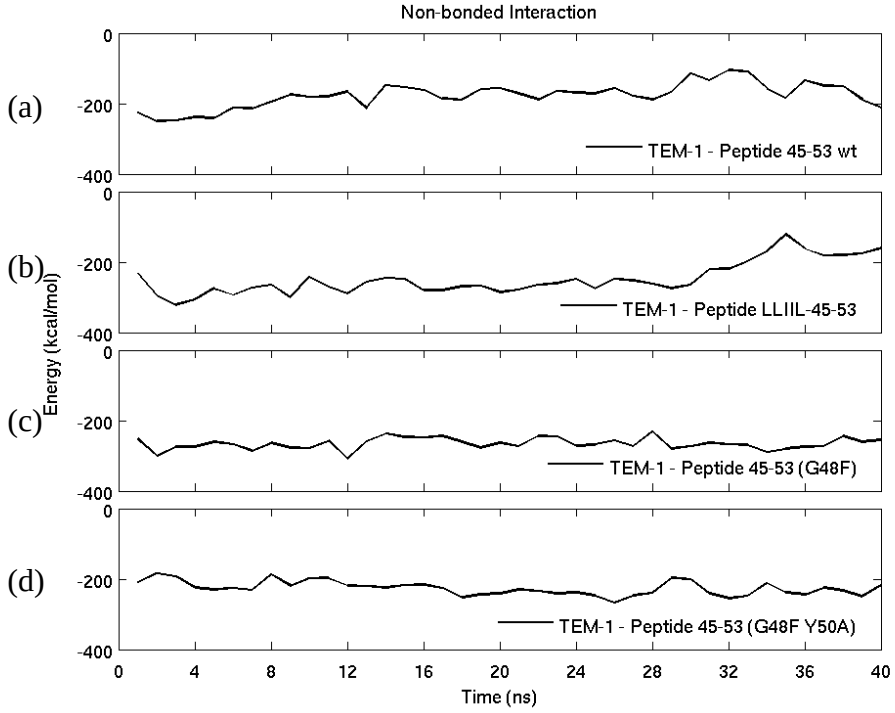

Figure 4.24. Non-bonded interaction energy between TEM-1 and wild type or mutated peptides corresponds to 45-53 region of BLIP.

4.4. Binding Free Energy Calculations

MM-PBSA (Molecular Mechanics-Poisson Boltzmann Surface Area) method was used in order to calculate binding free energy of each simulation system in order to gain an idea about tightness of binding. In MM-PBSA, MM represents average molecular mechanical gas-phase energies (electrostatic, van der Waals and bonded interaction energy) that were calculated in VMD with a Tcl script in Appendix A, PB represents polar solvation energy that was calculated by APBS (Baker et al., 2001) and SA is for non-polar salvation energy that was calculated by using MSMS program (Sanner et al., 1996). Binding free energy of each simulation system can be seen from the Table 4.5, also energy contributions to binding free energy were tabulated. Binding free energy for each simulation system was calculated by subtracting entropy contributions (-TΔS) from Δ MMPBSA. Δ Energy represents change in related energy term due to the binding calculated by subtracting the beta-lactamase and ligand energy terms from energy term of the complex.

According to Table 4.5 the main contribution to binding free energy for each simulation system comes from the change in electrostatic energy due to binding. Polar and non-polar solvation energies have minor contribution also entropy contributions are slight with respect to other energy types.

Table 4.5. Binding free energy (kcal/mol) of simulation systems and energy contributions to binding free energy.

Energy Term (kcal/mol)	TEM-1 – P1	TEM-1	P1	Δ Energy
$E_{electrostatic}$	-6537	-6262	-70	-205
E_{vdW}	-1200	-1178	5	-27
E_{bonded}	4178	4068	112	-2
E_{MM}	-3559	-3372	46	-232
Gpb	-1569	-1486	-111	28
Gsa	66	65	7	-6
MMPBSA	-5061	-4793	-58	-210
Entropy (T×S)	521	495	21	5
G	-5583	-5289	-79	-215

Energy Term (kcal/mol)	TEM-1 – P2	TEM-1	P2	Δ Energy
$E_{electrostatic}$	-6336	-6313	7	-30
E_{vdW}	-1171	-1163	11	-19
E_{bonded}	4158	4058	99	1
E_{MM}	-3350	-3419	118	-49
Gpb	-1529	-1472	-88	31
Gsa	68	65	7	-4
MMPBSA	-4811	-4826	38	-23
Entropy(T×S)	502	468	26	8
G	-5313	-5294	12	-31

Energy Term (kcal/mol)	TEM-1 – P3	TEM-1	P3	Δ Energy
$E_{electrostatic}$	-6634	-6400	-50	-184
E_{vdW}	-1205	-1182	-2	-21
E_{bonded}	4159	4064	98	-3
E_{MM}	-3680	-3518	46	-208
Gpb	-1527	-1428	-110	11
Gsa	65	64	7	-6
MMPBSA	-5142	-4882	-57	-203
Entropy(T×S)	491	465	21	5
G	-5634	-5348	-77	-209

Energy Term (kcal/mol)	TEM-1 – P4	TEM-1	P4	Δ Energy
$E_{electrostatic}$	-6478	-6285	-45	-148
E_{vdW}	-1205	-1184	1	-22
E_{bonded}	4142	4049	98	-5

Table 4.5. Binding free energy (kcal/mol) of simulation systems and energy contributions to binding free energy (cont.).

E_{MM}	-3542	-3421	54	-175
Gpb	-1568	-1471	-126	29
Gsa	66	65	7	-6
MMPBSA	-5044	-4827	-65	-152
Entropy(T×S)	523	494	22	7
G	-5567	-5321	-87	-159

Energy Term (kcal/mol)	**TEM-1 – P5**	**TEM-1**	**P5**	**Δ Energy**
$E_{electrostatic}$	-6470	-6237	-83	-150
E_{vdW}	-1188	-1169	2	-21
E_{bonded}	4164	4045	125	-6
E_{MM}	-3494	-3361	44	-177
Gpb	-1595	-1493	-109	7
Gsa	66	65	7	-6
MMPBSA	-5024	-4790	-58	-176
Entropy(T×S)	446	468	12	-34
G	-5470	-5258	-70	-142

Energy Term (kcal/mol)	**TEM-1 – P6**	**TEM-1**	**P6**	**Δ Energy**
$E_{electrostatic}$	-6548	-6333	-81	-134
E_{vdW}	-1183	-1170	13	-26
E_{bonded}	4178	4047	128	3
E_{MM}	-3553	-3456	60	-157
Gpb	-1586	-1459	-122	-4
Gsa	67	64	8	-5
MMPBSA	-5072	-4851	-54	-166
Entropy(T×S)	507	478	23	6
G	-5579	-5329	-77	-172

Energy Term (kcal/mol)	**TEM-1 – P7**	**TEM-1**	**P7**	**Δ Energy**
$E_{electrostatic}$	-6529	-6273	-54	-202
E_{vdW}	-1203	-1166	-6	-31
E_{bonded}	4262	4047	220	-5
E_{MM}	-3470	-3392	160	-238
Gpb	-1536	-1423	-136	23
Gsa	69	65	11	-7

Table 4.5. Binding free energy (kcal/mol) of simulation systems and energy contributions to binding free energy (cont.).

MMPBSA	-4937	-4750	35	-222
Entropy(T×S)	514	473	36	5
G	-5450	-5222	-1	-227

Energy Term (kcal/mol)	**TEM-1 – P8**	**TEM-1**	**P8**	**Δ Energy**
$\mathbf{E_{electrostatic}}$	-6516	-6225	-72	-219
$\mathbf{E_{vdW}}$	-1198	-1174	16	-40
$\mathbf{E_{bonded}}$	4219	4067	154	-2
$\mathbf{E_{MM}}$	-3495	-3332	98	-261
Gpb	-1604	-1530	-104	30
Gsa	67	66	8	-7
MMPBSA	-5033	-4797	2	-238
Entropy(T×S)	464	442	16	6
G	-5497	-5239	-14	-244

Energy Term (kcal/mol)	**TEM-1 – P9**	**TEM-1**	**P9**	**Δ Energy**
$\mathbf{E_{electrostatic}}$	-6523	-6268	-58	-197
$\mathbf{E_{vdW}}$	-1190	-1171	13	-32
$\mathbf{E_{bonded}}$	4179	4047	133	-1
$\mathbf{E_{MM}}$	-3534	-3392	88	-230
Gpb	-1520	-1432	-118	30
Gsa	66	64	8	-6
MMPBSA	-4988	-4760	-22	-206
Entropy(T×S)	480	459	15	6
G	-5468	-5219	-37	-212

The tightest binding occurred in TEM-1 – Peptide 45-53 (G48F) complex with a binding free energy of -244 kcal/mol. Substitution of glycine with phenylalanine in peptide almost took the role of the side chain of Phe142 of BLIP on binding and increased tightness of binding when compared to wild type TEM-1 – Peptide 45-53 complex in which binding free energy value is -172 kcal/mol (Table 4.6).

Table 4.6. Binding free energy (kcal/mol) of simulation systems and change in binding free energy due to mutation.

Simulation System	**Δ G (kcal/mol)**	**Δ Δ G[a] (kcal/mol)**
TEM-1 – P1	-215	0
TEM-1 – P2	-31	184
TEM-1 – P3	-209	6
TEM-1 – P4	-156	59
TEM-1 – P5	-142	73
TEM-1 – P6	-172	43
TEM-1 – P7	-227	-12
TEM-1 – P8	-244	-29
TEM-1 – P9	-212	3

[a] $\Delta\Delta G = \Delta G_{mutant} - \Delta G_{wildtype(P1)}$

When two wild type complexes TEM-1 – P1 and TEM-1 – P6 were compared it was found that Tyr53 in P6 decreased the binding affinity according to the increase in binding free energy from -215 in TEM-1 – P1 complex to -172 in TEM-1 – P6 complex.

Binding of D49A, Y50A, Y51A and A46W mutated peptides to TEM-1 revealed different binding affinities with respect to each other and also to wild type peptide 45-52. Among P2, P3, P4 and P5 peptides P3 has tightest binding with binding free energy value of -209 kcal/mol which is very close to binding free energy value of wild type P1 (-215 kcal/mol). Due to the loss of interactions between active site pocket of TEM-1 and Ala49 of peptide, D49A mutation decreased binding affinity of P2 to TEM-1 and binding free energy became -31 kcal/mol. Also Y51A and A46W mutations decreased binding affinity of P4 and P5 to TEM-1 and binding free energy values became -159 kcal/mol for TEM-1 – peptide 45-52 (Y51A) complex and -142 kcal/mol for TEM-1 – Peptide 45-52 (A46W) complex.

Mutations on 45-53 loop increased binding affinity with respect to wild type peptide 45-53. LLIIL addition did not decrease binding affinity conversely it increased the tightness of binding for TEM-1 with -227 kcal/mol binding free energy value which is significantly lower than binding free energy value of wild type complex (-172 kcal/mol). Peptide with G48FY50A mutations (P9) revealed tighter binding to TEM-1 with respect to wild type P6 and TEM-1 – P9 complex has a binding free energy of -212 kcal/mol.

5. CONCLUSIONS AND RECOMMENDATIONS FOR FUTURE STUDIES

5.1. Conclusions

In this study MD simulations of TEM-1 and SHV-1 beta-lactamases in apo forms and in complex with BLIP and BLIP (D49A), TEM-1 W229A mutant in apo form and in complex with BLIP and also free BLIP and BLIP (D49A) were performed to examine the interaction of beta-lactamase with beta-lactamase inhibitory protein BLIP. The features that lead to affinity difference of BLIP to TEM-1 and SHV-1 beta-lactamases were investigated. The role of the H10 helix region in TEM-1 that corresponds to residues 218 to 230 was examined with W229A mutation on TEM-1 to evaluate its possible contribution to binding. In addition to this, TEM-1 binding to peptides designed based on the BLIP residues 45 to 52 or 45 to 53, including the catalytically important Asp49 residue, was examined by MD simulations to investigate their inhibition potential. Besides the wild type peptides, binding of peptides with A46W, D49A, Y50A, Y51A, G48F and G48FY50A mutations were investigated.

For each simulation system, the stability of the simulation was assessed by calculating root mean square deviation (RMSD) of beta-lactamase, ligand and complex with respect to their initial simulation structure. In addition, RMSD of important regions of beta-lactamase that were thought to have effects on binding were also calculated. The flexibility and mobility of beta-lactamase, its important regions, and of the ligand and the complex were evaluated by calculating mean square fluctuations (MSF) that gives fluctuations about the average structure.

In order to investigate interaction energy between the beta-lactamase and the ligand, intermolecular interaction energy that represents total non-bonded interactions between beta-lactamase and ligand was calculated for each simulation system. Moreover, binding free energy was calculated to evaluate binding affinity of beta-lactamase and ligand in each simulation system.

According to the binding free energy calculations; binding free energy of TEM-1 – BLIP complex is -407 kcal/mol while it is -383 kcal/mol in SHV-1 – BLIP complex. The difference in binding affinity that BLIP exhibits to TEM-1 and SHV-1 beta-lactamases may be related to the difference in flexibility of the omega loop (residues 161 to 179) especially its flexible tip (residues 174 to 176) in the two beta-lactamases.

Residue 175 located at the tip of the omega loop is asparagine with a bulkier side chain in TEM-1, and glycine in SHV-1. Both in unbound and BLIP bound forms of TEM-1, Asn175 has a MSF value of 1.10 $Å^2$ while Gly175 of SHV-1 increased from 1.00 to 1.74 $Å^2$ after BLIP binding. The significant increase in mobility of Gly175 in SHV-1 leads to the high mobility of the omega loop in SHV-1 – BLIP structure (0.59 $Å^2$) unlike the low mobility omega loop in TEM-1 - BLIP simulation (0.29 $Å^2$). The difference between amino acid type at position 175 of omega loop in TEM-1 (Asn175) and SHV-1 (Gly175) may cause the higher in binding affinity of BLIP to TEM-1 compared to SHV-1.

Another region that displays differential mobility between TEM-1 and SHV-1 is the H10 helix. TEM-1 has a highly flexible H10 helix and BLIP binding decreases its flexibility. On the other hand, apo SHV-1 has a less flexible H10 helix with respect to apo TEM-1 but BLIP binding to SHV-1 increases the flexibility of H10 helix. Also the conformation of H10 helix may contribute to the binding affinity difference. In the apo form, H10 helix of SHV-1 has an alternate conformation compared to its conformation in TEM-1 and in BLIP bound form. When BLIP binds to SHV-1, H10 helix conformation changes and becomes similar to the H10 helix conformation in both unbound and BLIP bound forms of TEM-1. The alternative conformation of H10 observed in apo SHV-1 is due to the presence of detergent at this site. Studies on other beta-lactamases have shown that this site is the binding site for allosteric inhibitors.

In order to further investigate the effect of H10 on binding, simulations were repeated with TEM-1 W229A mutant. W229 residue on H10 is in stacking arrangement with P226 and P252. The H10 helix deviates more from its initial structure but is less flexible in the W229A mutant compared to the wild type form. Other important regions of beta-lactamase did not reveal a significant change with respect to wild type. The change in

conformation and the decrease in flexibility of H10 helix suggest that H10 helix is allosterically affected by BLIP binding.

Simulation of TEM-1 – BLIP (D49A) and SHV-1 – BLIP (D49A) complexes show that Asp49 on BLIP is an important residue and its substitution with alanine disfavors binding by increasing binding free energy around 120 kcal/mol with respect to wild type. Asp49 in the wild type aligns itself in the active site and forms four strong hydrogen bonds with four catalytic residues (Ser130, Lys234, Ser235, Arg244). However, BLIP (D49A) reveals some movement of Ala49 towards to 99-112 loop during the simulation and this movement leads to the loss of these interactions consequently tightness of binding decreases. In the BLIP (D49A) bound form, mobility of H10 helix decreases in TEM-1, while its mobility increases in SHV-1. On the other hand mobility of omega loop flexible tip increases in TEM-1 whereas it decreases in SHV-1 in the BLIP (D49A) bound form.

TEM-1 – peptide simulations were examined to find a peptide inhibitor with binding potential. Peptides based on BLIP 45-52 loop region structure were used in the simulations. The peptide corresponding to the 45-53 region of BLIP with G48F mutation (P8) has the tightest binding affinity with -244 kcal/mol of binding free energy. G48F mutation was done to fulfill the role of residue F142 of BLIP on binding. Phenylalanine at position 48 of the peptide inserts its side chain into the cavity formed by Glu104, Tyr105, Asn170, Ala237, Gly238 and Glu240. Phenylalanine 142 of BLIP inserts its side chain into this cavity in TEM-1 – BLIP complex. The interactions achieved by Phe48 of peptide (P8) made the binding to TEM-1 tighter with respect to wild type complex (TEM-1 – P6) in which the binding free energy is -172 kcal/mol. Also addition of LLIIL residues to 45-53 region of BLIP (P7) increased the binding affinity to -227 kcal/mol from -172 kcal/mol in wild type.

5.2. Recommendations for Future Studies

MD simulations of SHV-1 W229A mutant in unbound and BLIP bound forms can be performed for the examination of H10 helix behavior and also for the comparison with TEM-1 W229A mutant.

Peptide inhibitors have the advantage of their small size in the delivery as a prospective drug. Peptide 45-53 (G48F) which has a favorable binding affinity to TEM-1 compared to other peptides can be used as a starting point to optimize the inhibition potential of the peptide by performing mutations to different residues in order to enhance the binding affinity to TEM-1.

LLIIL residues, which correspond to the first five residues of the cell penetrating peptide pVEC, can increase cellular uptake of peptides. The present study showed that binding affinity of peptide to TEM-1 increased with the addition of LLIIL residues to peptide 45-53. These residues also can be added to peptide 45-53 (G48F) to improve both binding affinity and cellular uptake.

The peptides that have shown binding potential can be tested for their inhibitory and binding properties by kinetics experiments in vitro. The growth properties of bacteria in the presence of the peptide can be examined by in vivo studies.

APPENDIX A: TCL SCRIPTS USED IN VMD

Average Simulation Structure for RMSD Calculation

```
mol load pdb TEMBLIP_10ns.pdb dcd TEMBLIP_10ns.dcd
mol load pdb TEMBLIP_10ns.pdb
set protein [atomselect 0 "chain A"]
set avg [atomselect 1 "chain A"]
$avg set {x y z} [measure avpos $protein first 15500 last
40000]
```

Coloring the Beta-lactamase Structures by Residue Based MSF

```
puts "Enter MSf_color {{molid top} {data_file color.dat}
{selection \"name CA\"} \n"
puts "For Example: \nMSf_color color.dat \"name CA\"\n"
proc MSf_color {{molid top} {data_file color.dat} {selection
"name CA"}} {
if {$molid=="top"} {set molid [molinfo top]}
mol top $molid
mol rename top "MSF_color_dist"
set sel [atomselect $molid $selection]
set fp [open $data_file "r"]
set data [read $fp]
$sel set beta $data
mol modstyle 0 $molid NewCartoon .2 50 4.5 1
mol modcolor 0 $molid Beta
}
```

MM Calculation for MMPBSA

```
puts "namd_energy {{outputfile \"\"} {skip 100} {selection
protein}}"
puts "For example: \nnamd_energy TEM 100 protein \n"
proc namd_energy {{outputfile ""} {skip 100} {selection
protein}} {
set sel [atomselect top $selection]
namdenergy -sel $sel -vdw -elec -par /home/
Applications/toppar/par_all27_prot_lipid.prm -skip $skip -
ofile "nonbond_${outputfile}"
```

```
namdenergy -sel $sel -bond -angle -dihe -par /home/Applications/toppar/par_all27_prot_lipid.prm -skip $skip -ofile "bond_${outputfile}"
}
```

APPENDIX B: MATLAB SCRIPTS

Mean MSF Calculation

```
X=readdcd ('CA_chainA_temblip.dcd', 1:263);
x=bestfit(X);
r=findrmsd(x);
figure; plot(r);
size(x)
y=x(15500:end,:);
y=bestfit(y);
figure;msf=findmsf(y,26:288);
mean(msf)

%H10 H9-H10 99-112 omega omega_flexible
mean(msf(193:205))
mean(msf(176:205))
mean(msf(74:87))
mean(msf(136:154))
mean(msf(149:151))


%active side residue[70 73 130 166 170 234]
mean(msf([45 48 105 141 145 209]))


%TEM clusters
mean(msf([105 209 210 218]))
mean(msf([79 80 145]))
mean(msf([74 75]))
mean(msf([78 142 143]))
mean(msf([104 191]))
mean(msf([85]))

%chain B
X=readdcd ('CA_chainB_temblip.dcd', 1:165);
x=bestfit(X);
r=findrmsd(x);
size(x)
y=x(15500:end,:);
y=bestfit(y);
msf=findmsf(y);
mean(msf)

%protein
X=readdcd ('CA_protein_temblip.dcd', 1:428);
x=bestfit(X);
```

```
r=findrmsd(x);
size(x)
y=x(15500:end,:);
y=bestfit(y);
msf=findmsf(y);
mean(msf)
```

Residue Based MSF Calculation and MSF Graph

```
X1=readdcd ('CA_unboundTEM.dcd', 1:263);
x1=bestfit(X1);
size(x1)
y1=x1(16500:end,:);
y1=bestfit(y1);
figure;msf_unbound=findmsf(y1,26:288);


X2=readdcd ('CA_TEMBLIP.dcd', 1:263);
x2=bestfit(X2);
size(x2)
y2=x2(15500:end,:);
y2=bestfit(y2);
figure;msf_bound=findmsf(y2,26:288);


msf_difference=msf_unbound-msf_bound;

figure;
subplot(3,1,1);msf_unbound=findmsf(y1,26:288);

subplot(3,1,2);msf_bound=findmsf(y2,26:288);

subplot(3,1,3);plot(26:288, msf_difference)
```

Correlation

```
X=readdcd ('CA_protein_temblip.dcd', 1:428);
x=bestfit(X);
y=x(15500:end,:);
y=bestfit(y);
a=corres_20jan(y);
mean(mean(a([1:263] , [264:428])))
correlation_complex(a, 0.5, 'outputname')
```

corres_20jan(y) input for correlation

```
function rr = corres(X, rlim, res, z)

%
% Finds the correlation between the residues taking only the
r, distance
% from the average, into consideration.
% Blue -> Anticorrelatted
% Red -> Correlatted
%
% I/O format: r = corres(X, rlim, res)
%
% where     X     is the matrix of dimensions, samples x (3 x
res no.)
%           rlim (default = 0.2) is the lower threshold value
for
%          correlation
%          res (default = 1 : n) is the residue numbers
%

if nargin < 3 | isempty(res)
    res = 1 : size(X, 2)/3;
else
    res = res(:)';
end

nofres = length(res);

if nargin < 2 | isempty(rlim)
    rlim = .05;
end

[m, n] = size(X);
X = mncn(X);
C    = zeros(n/3, n/3);
Cnew = zeros(n/3, n/3);

X = reshape(X', [3 n/3 m]);

for i = 1 : m
    x = squeeze(X(:, :, i));
    Cnew = x'*x;
    C = C + Cnew;
end

C = C / (m-1);

D = diag(C);
```

```
r = C ./ sqrt(D*D');
rr=r;

% ind1 = find(r < -0.30);%yellow
% ind2 = find(r < -0.15);%light grey
% ind3 = find(r < -0.05);%white
% ind4 = find(r < 0.05);%dark grey
% ind5 = find(r < 0.15);%red
% ind6 = find(r < 0.25);%dark red
% ind7 = find(r < 0.45);%blue
% ind8 = find(r <= 1);%black
% r(ind1)= -.2;
% r(setdiff(ind2, ind1)) = -.15;
% r(setdiff(ind3, ind2)) = -0.05;
% r(setdiff(ind4, ind3)) = 0.05;
% r(setdiff(ind5, ind4)) = 0.15;
% r(setdiff(ind6, ind5)) = 0.25;
% r(setdiff(ind7, ind6)) = 0.45;
% r(setdiff(ind8, ind7)) = 1;
%
indresX = ones(nofres, 1) * res;
indresY = indresX';
%
colormap(    [0 0 0;0 0 1;0 0 1;0 0 1;0 0 1;0 0 1;0 0 1;0 0 1;0 0
1;0 0 1;0 0 1;0 0 1;0 0 1;0 0 1;0 0 1;0 1 1;0 1 1;0 1 1;0 1 1;0 1
1;0 1 1;0 1 0.1098;0 1 0.0915;0 1 0.0732;0 1 0.0549;0 1
0.0366;0 1 0.0183;0 1 0;1 1 1;1 1 1;1 1 1;1 1 1;1 1 1;1 1 1;1 1 1;1
1 1;1 1 1;1 1 1;1 1 1;1 1 1;1 1 1;1 1 1;1 1 1;1 0 1;1 0 1;1 0
1;1 0 1;1 0 1;1 0 1;1 0 0;1 0 0;1 0 0;1 0 0;1 0 0;1 0 0;1 0
0;0.8471 0.1608 0;0.8471 0.1608 0;0.8471 0.1608 0;0.8471
0.1608 0;0.8471 0.1608 0;0.8471 0.1608 0;0.8471 0.1608
0;0.8471 0.1608 0;0.8471 0.1608 0;0.8471 0.1608 0;0.8471
0.1608 0;0 0 0]);
pcolor(indresX, indresY, r),
 caxis([-1 1])
shading('interp')


% function createfigure(ZData1, CData1)
% %CREATEFIGURE(ZDATA1,CDATA1)
% %  ZDATA1:  surface zdata
% %  CDATA1:  surface cdata
%
% %  Auto-generated by MATLAB on 20-Jan-2010 17:03:05
%
% % Create figure
% figure1 = figure('Colormap',...
%     [0 0 0;0 0 1;0 0 1;0 0 1;0 0 1;0 0 1;0 0 1;0 0 1;0 0
1;0 0 1;0 0 1;0 0 1;0 0 1;0 0 1;0 0 1;0 1 1;0 1 1;0 1 1;0 1 1;0 1
1;0 1 0.1098;0 1 0.0915;0 1 0.0732;0 1 0.0549;0 1 0.0366;0 1
```

```
0.0183;0 1 0;1 1 1;1 1 1;1 1 1;1 1 1;1 1 1;1 1 1;1 1 1;1 1 1;1 1 1;1 1 1;1 1 1;1 1 1;1 1 1;1 1 1;1 1 1;1 1 1;1 0 1;1 0 1;1 0 1;1 0 1;1 0 1;1 0 1;1 0 0;1 0 0;1 0 0;1 0 0;1 0 0;1 0 0;0.8471 0.1608 0;0.8471 0.1608 0;0.8471 0.1608 0;0.8471 0.1608 0;0.8471 0.1608 0;0.8471 0.1608 0;0.8471 0.1608 0;0.8471 0.1608 0;0.8471 0.1608 0;0.8471 0.1608 0;0.8471 0.1608 0;0 0 0]);
%
% % Create axes
% axes1 = axes('Parent',figure1,'CLim',[-1 1]);
% % Uncomment the following line to preserve the X-limits of the axes
% % xlim([1 263]);
% % Uncomment the following line to preserve the Y-limits of the axes
% % ylim([1 263]);
% box('on');
% hold('all');
%
% % Create surface
%
surface(ZData1,'Parent',axes1,'FaceColor','interp','EdgeColor','none',...
%     'CData',CData1);

colorbar

%xlabel('Residue no.')
%ylabel('Residue no.')

%set(gcf, 'Color', 'w')
```

APPENDIX C: CONFIGURATION FILE FOR NAMD SIMULATIONS

```
#############################################################
## JOB DESCRIPTION                                         ##
#############################################################

# Minimization and Equilibration of
# TEM1BLIP


#############################################################
## ADJUSTABLE PARAMETERS                                   ##
#############################################################


structure          temblip_ionized.psf
coordinates        temblip_ionized.pdb
set temperature    300
set outputname     output_TEMBLIP
set init_temp      50
firsttimestep      0



#############################################################
## SIMULATION PARAMETERS                                   ##
#############################################################

# Input
paraTypeCharmm     on
parameters         par_all27_prot_lipid.prm
temperature         $init_temp


# Force-Field Parameters
exclude             scaled1-4
1-4scaling          1.0
cutoff              12.
switching           on
switchdist          10.
pairlistdist        13.5


# Integrator Parameters
timestep            1.0  ;# 1fs/step
rigidBonds          all  ;# needed for 2fs steps
```

```
nonbondedFreq       1
fullElectFrequency  2
stepspercycle       10


# Constant Temperature Control
langevin            on    ;# do langevin dynamics
langevinDamping      5     ;# damping coefficient (gamma) of
5/ps
langevinTemp         $init_temp
langevinHydrogen     off    ;# don't couple langevin bath to
hydrogens


# Periodic Boundary Conditions
cellBasisVector1     75.60599899291992    0.   0.
cellBasisVector2     0.   71.5979995727539   0.
cellBasisVector3     0.    0.   87.64800262451172
cellOrigin              5.691157341003418 1.2810559272766113
32.50239944458008
margin               3
wrapAll              on


# PME (for full-system periodic electrostatics)
PME                 yes
PMEGridSizeX        80
PMEGridSizeY        72
PMEGridSizeZ        90


# Constant Pressure Control (variable volume)
useGroupPressure      yes ;# needed for rigidBonds
useFlexibleCell       no
useConstantArea       no

langevinPiston        on
langevinPistonTarget  1.01325 ;#  in bar -> 1 atm
langevinPistonPeriod  100.
langevinPistonDecay   50.
langevinPistonTemp    $init_temp


# Output
outputName          $outputname

restartfreq         500     ;# 500steps = every 1ps
dcdfreq             250
xstFreq             250
outputEnergies      100
```

```
outputPressure      100
#####################################################################
## EXTRA PARAMETERS                                                ##
#####################################################################

constraints on
consexp 2
consref      temblip_ionized.pdb
conskfile    constrain_temblip.pdb
conskcol B
constraintScaling 5

#####################################################################
## EXECUTION SCRIPT                                                ##
#####################################################################
# turn off until later

#langevinPiston         off


# Minimization

minimize            1000
output mini.cons5

constraintScaling 3

minimize            1000

output mini.cons3

constraintScaling 0

minimize            1000

output mini.all

reinitvels      $init_temp
run            4000
for  {  set  TEMP  [expr  ($init_temp  +  10)]  }  {  $TEMP  <
$temperature } { incr TEMP 10
} {
    langevinTemp          $TEMP
    LangevinPistonTemp   $TEMP
    run                   4000
}

langevinTemp          $temperature
#LangevinPistonTemp   $TEMP
run                   1000000
```

APPENDIX D: RUBY FILES FOR MMPBSA CALCULATION

APBS Calculation

```
#!/usr/bin/env ruby

########################## APBS calculation ########################
system("clear")
energy=""

File.open("apbs_energy.ods",    'a+')    {|f|    f.write("apbs
calculation") }
File.open("apbs_energy.ods", 'a+') {|f| f.write("\n") }
File.open('framelist.ods',   'r+')   do   |f1|   #pdb   lerin
isimlerinin alt alta listelendiği txt file ından isimler tek
tek okunuyor

#while frameno = f1.gets.chomp

while line5 = f1.gets
 frameno2=line5.split(//)

 i=0
frameno=""
  while number = frameno2[i]
    if number=="\n"
      number=""
    end
    frameno<<number
    i=i+1
  end


@pdbname = @name= ARGV[0]
# @pathway= ARGV[1]
 @pathway= "/home/asligul/Applications/"

system("wordom  -f  "+frameno+"  -itrj  "+@name+".dcd  -imol
"+@name+".pdb -omol "+@name+"_"+frameno+".pdb") #wordom dan
frame extract ettik
@name=@name.to_s+"_"+frameno
system("cp      "+@name+".pdb      "+@pathway+"pdb2pqr-1.5/.")
#pdb2pqr-1.5 ın olduğu path i koy
system("python "+@pathway+"pdb2pqr-1.5/pdb2pqr.py --ff=charmm
-v   --apbs-input   "+@pathway+"/pdb2pqr-1.5/"+@name+".pdb"+"
"+@name+".pqr ") #pdb2pqr-1.5 in pdb nin olduğu path leri koy
```

```
system("apbs "+@name+".in > "+@name+".apbsout")
sum=0
mynumber="" #boş string oluşturuldu

  File.open(@name+'.apbsout', 'r') do |f2| # apbs run ından
elde edilen .out file ından istenen enerji çekilcek
  while line = f2.gets
  puts line
  mynumber=""
  if line =~ /net energy/ then #pattern match
  line2=line.split(//)   #net   energy   nin   geçtiği   line
parçalandı
  i=0
  while i<=line2.length do  # seçilen line daki her bir char
ın number mı letter mı olduğu kontrol ediliyor
  if line2[i] =~ /[0123456789.+E]/ then
  mynumber<<line2[i]  #bulunan  rakamlar  mynumber  stringime
ekleniyor
  end
  i=i+1
  end
  end
mynumber2=mynumber.split(//)
mynumber2.delete_at(0)
i=0

while number = mynumber2[i]
energy<<number
i=i+1
end
end
puts @pdbname
# system("rm "+@pdbname+"_*") #hesaplandıktan sonra gereksiz
dosyaların silinmesi
File.open("apbs_energy.ods", 'a') {|f| f.write(energy) }
File.open("apbs_energy.ods", 'a') {|f| f.write("\n") } # tüm
frame lerin apbs değerleri apbs_energy.ods file ına yazıldı
energy=""
end
end
end
```

SASA Calculation

```
#################### Surface Area Calculation ####################
system("clear")
gama=0.00542
beta=0.92
```

```
myline=""
counter=1
counter2=100
File.open("sasa_energy.ods",    'a+')    {|f|    f.write("sasa
calculation") }
puts "I am here"
File.open('framelist.ods',   'r+')   do   |f1|   #pdb   lerin
isimlerinin alt alta listelendiği txt file ından isimler tek
tek okunuyor
puts "and now here"
while frameno = f1.gets.chomp
 @pdbname = @name= ARGV[0]
 @pathway= "/home/asligul/Applications/"
puts frameno
 system("wordom  -f  "+frameno+"  -itrj  "+@name+".dcd  -imol
"+@name+".pdb -omol "+@name+"_"+frameno+".pdb")
 #wordom dan frame extract ettik
 @name=@name.to_s+"_"+frameno
 # msms.x86_64Linux2.2.6.1
 system("cp                                        "+@name+".pdb
"+@pathway+"msms/.")#msms_i86_64Linux2_2.6.1 pathini koy

 system("pdb_to_xyzr     "+@pathway+"msms/"+@name+".pdb     >
"+@name+".xyzr") #msms_i86_64Linux2_2.6.1 path ini koy
 system("msms -if "+@name+".xyzr -of "+@name+" -probe_radius
1.4 -surface ases > "+@name+".out")
 number=""
 # msms den çıkan sonuçlar .out file ına yazıldı
 File.open(@name+'.out', 'r+') do |f2| #pdb lerin isimlerinin
alt alta listelendiği txt file ından isimler tek tek okunuyor
 while line = f2.gets
  if line =~ /ANALYTICAL SURFACE AREA/ # /../ arasındaki
kelimenin geçtiği line bulundu
  line= f2.gets
  line= f2.gets
  words = line.split
  File.open("junk1.ods", 'a+') {|f| f.write(words[6]) }
  File.open("sasa_energy.ods", 'a+') {|f| f.write("\n") }
  File.open("sasa_energy.ods",          'a+')          {|f|
f.write(Float(words[6])*gama+beta)} #yukarda tanımlanan gama
ve  beta  değerleriyle  sırasıyla  çarpıldı  toplandı  ve
sasa_energy.ods file ına yazıldı
counter=counter+1
puts counter
  end
counter2=counter2+100
puts counter2
 end
end
end
```

```
end
```

Entropy Calculation

```
system("rm  mass_avg.pdb")  #hesaplandıktan  sonra  gereksiz
dosyaların silinmesi
system("junk.pdb")
system("rm qentr1-*")
system("rm average.pdb")
system("rm final.pdb")
system("rm tclfile")
File.open("entropy_energy.ods",  'a')  {|f|  f.write("entropy
calculation") }
@name= ARGV[0]
#@pathway= ARGV[1]
@first= ARGV[1]
@last=ARGV[2]

File.open("tclfile", 'a+') {|f| f.write(@name+'.pdb') }
File.open("tclfile", 'a+') {|f| f.write("\n") }
File.open("tclfile", 'a+') {|f| f.write(@name+'.dcd') }
File.open("tclfile", 'a+') {|f| f.write("\n") }
File.open("tclfile", 'a+') {|f| f.write(@first) }
File.open("tclfile", 'a+') {|f| f.write("\n") }
File.open("tclfile", 'a+') {|f| f.write(@last) }

system("vmd -dispdev text -e avg.tcl")
system("awk    -f    put_mass_in_pdb.awk    average.pdb    >
mass_avg.pdb")


i=0
aFile=File.open("mass_avg.pdb", 'r+') do |f1|
while line = f1.gets
puts i
if i>4080   # A dan B ye geçiş olmasını istediğin line ın
numarasını yaz,hepsi A olcaksa da yüksek bi sayı yazabilirsin
line.sub!("      N","      B")
line.sub!("      H","      B")
line.sub!("      O","      B")
line.sub!("      C","      B")
i=i+1
else
line.sub!("      N","      A")
line.sub!("      H","      A")
line.sub!("      O","      A")
line.sub!("      C","      A")
```

```
i=i+1
end

File.open('final.pdb', 'a+') {|f| f.write(line) }
end
File.open("entropy_energy.ods", 'a') {|f| f.write("\n") }
end
system("wordom   -iA   entropy   -imol   final.pdb   -itrj
"+@name+".dcd -beg "+@first+" -end "+@last+"")
number=""
File.open('qentr1-eigval.txt', 'r+') do |f2|
line = f2.gets
mynumber2=line.split(//)
puts line
i=6
while i<19
number<<mynumber2[i]
i=i+1
end
end
File.open("entropy_energy.ods", 'a') {|f| f.write(number) } #
tüm frame lerin entropy değerleri entropy_energy.ods file ına
yazıldı
```

Input Files for Entropy Calculation

avg.tcl

```
set fid [open tclfile "r"]
set data [read $fid]
close $fid
set pdbname [lindex $data 0]
set dcdname [lindex $data 1]
set first [lindex $data 2]
set last [lindex $data 3]
mol load pdb $pdbname
mol addfile $dcdname type dcd first $first last $last waitfor
all
set sel [atomselect top all]
$sel writepdb junk.pdb
mol load pdb junk.pdb
set avg [atomselect top all]
$avg set {x y z} [measure avpos $sel]
set sel [atomselect top all]
$sel writepdb average.pdb
```

```
exit
```

put_mass_in_pdb.awk

```
BEGIN{
while(getline<"/home/asligul/Applications/toppar/top_all27_pr
ot_lipid.inp"){
if($1=="MASS"){mass[$3]=$4}
if($1=="RESI"){res=$2}
if($1=="PRES"&&($2=="NTER"||$2=="CTER")){res=""}

if($1=="ATOM"){type[res,$2]=$3}
}
}
$1!="ATOM"{print}
$1=="ATOM"{
 if(($4,$3) in type){
  printf"%s                                                %5.2f
%s\n",substr($0,1,60),mass[type[$4,$3]],$NF;
 }else{
  printf"%s                                                %5.2f
%s\n",substr($0,1,60),mass[type["",$3]],$NF;
}
}
```

Entropy

```
BEGIN entropy
--TITLE qentr1
--SELE /A/*/CA
--TEMP 300
END
```

REFERENCES

Albeck, S. and G. Schreiber, 1999, "Biophysical characterization of the interaction of the beta-lactamase TEM-1 with its protein inhibitor BLIP", *Biochemistry*, Vol. 38, No. 2, pp. 11-21.

Allen, M.P., 2004, "Introduction to Molecular Dynamics Simulation", *NIC Series*, Vol. 23, No. 1, pp. 1-28.

Ambler, R.P., 1980, "The structure of beta-lactamases", *Philosophical Transactions of the Royal Society B: Biological Sciences*, Vol. 289, No. 1036, pp. 321-331.

Babic, M., A.M. Hujer and R.A. Bonomo, 2006, "What's new in antibiotic resistance? Focus on beta-lactamases", *Drug Resistance Updates*, Vol. 9, No. 3, pp. 142-156.

Baker, N.A., D. Sept, S. Joseph, M.J. Holst and J.A. McCammon, 2001, "Electrostatics of nanosystems: application to microtubules and the ribosome", *Proceedings of the National Academy of Sciences of the United States*, Vol. 98, No. 18, pp. 10037-10041.

Bos, F. and J. Pleiss, 2009, "Multiple molecular dynamics simulations of TEM beta-lactamase: dynamics and water binding of the omega-loop", *Biophysical Journal*, Vol. 97, No. 9, pp. 2550-2558.

Brasseur, L., P. Desgieux and F. Guirimand, 1999, "Update on the pharmacologic approach to pain", *Therapie*, Vol. 54, No. 1, pp. 111-116.

Brown, N.G., S. Shanker, B.V. Prasad and T. Palzkill, 2009, "Structural and biochemical evidence that a TEM-1 beta-lactamase N170G active site mutant acts via substrate-assisted catalysis", *The Journal of Biological Chemistry*, Vol. 284, No. 48, pp. 33703-33712.

Bush, L.M., J. Calmon and C.C. Johnson, 1995, "Newer penicillins and beta-lactamase inhibitors", *Infectious Disease Clinics of North America*, Vol. 9, No. 3, pp. 653-686.

Buynak, J.D., 2007, "Cutting and stitching: the cross-linking of peptidoglycan in the assembly of the bacterial cell wall", *ACS Chemical Biology*, Vol. 2, No. 9, pp. 602-605.

Campanera, J.M. and R. Pouplana, 2010, "MMPBSA decomposition of the binding energy throughout a molecular dynamics simulation of amyloid-beta (Abeta(10-35)) aggregation", *Molecules*, Vol. 15, No. 4, pp. 2730-2748.

Chen, C.C., T.J. Smith, G. Kapadia, S. Wasch, L.E. Zawadzke, A. Coulson and O. Herzberg, 1996, "Structure and kinetics of the beta-lactamase mutants S70A and K73H from Staphylococcus aureus PC1", *Biochemistry*, Vol. 35, No. 38, pp. 12251-12258.

Diaz, N., T.L. Sordo, K.M. Merz Jr and D. Suarez, 2003, "Insights into the acylation mechanism of class A beta-lactamases from molecular dynamics simulations of the TEM-1 enzyme complexed with benzylpenicillin", *Journal of the American Chemical Society*, Vol. 125, No. 3, pp. 672-684.

Doran, J.L., B.K. Leskiw, S. Aippersbach and S.E. Jensen, 1990, "Isolation and characterization of a beta-lactamase-inhibitory protein from Streptomyces clavuligerus and cloning and analysis of the corresponding gene", *The Journal of Bacteriology*, Vol. 172, No. 9, pp. 4909-4918.

Elmquist, A., M. Hansen and U. Langel, 2006, "Structure-activity relationship study of the cell-penetrating peptide pVEC", *Biochimica et Biophysica Acta*, Vol. 1758, No. 6, pp. 721-729.

Fisette, O., S. Morin, P.Y. Savard, P. Lague and S.M. Gagne, 2010, "TEM-1 backbone dynamics-insights from combined molecular dynamics and nuclear magnetic resonance", *Biophysical Journal*, Vol. 98, No. 4, pp. 637-645.

Ghuysen, J.M., P. Charlier, J. Coyette, C. Duez, E. Fonze, C. Fraipont, C. Goffin, B. Joris and M. Nguyen-Disteche, 1996, "Penicillin and beyond: evolution, protein fold, multimodular polypeptides, and multiprotein complexes", *Microbial Drug Resistance*, Vol. 2, No. 2, pp. 163-175.

Gretes, M., D.C. Lim, L. de Castro, S.E. Jensen, S.G. Kang, K.J. Lee and N.C. Strynadka, 2009, "Insights into positive and negative requirements for protein-protein interactions by crystallographic analysis of the beta-lactamase inhibitory proteins BLIP, BLIP-I, and BLP", *Journal of Molecular Biology*, Vol. 389, No. 2, pp. 289-305.

Hanes, M.S., K.A. Reynolds, C. McNamara, P. Ghosh, R.A. Bonomo, J.F. Kirsch and T.M. Handel, 2011, "Specificity and cooperativity at beta-lactamase position 104 in TEM-1/BLIP and SHV-1/BLIP interactions", *Proteins*, Vol. 79, No. 4, pp. 1267-1276.

Heritage, J., F.H. M'Zali, D. Gascoyne-Binzi and P.M. Hawkey, 1999, "Evolution and spread of SHV extended-spectrum beta-lactamases in gram-negative bacteria", *Journal of Antimicrobial Chemotherapy*, Vol. 44, No. 3, pp. 309-318.

Huang, W., J. Petrosino, M. Hirsch, P.S. Shenkin and T. Palzkill, 1996, "Amino acid sequence determinants of beta-lactamase structure and activity", *Journal of Molecular Biology*, Vol. 258, No. 4, pp. 688-703.

Humphrey, W., A. Dalke and K. Schulten, 1996, "VMD: visual molecular dynamics", *Journal of Molecular Graphics and Modelling*, Vol. 14, No. 1, pp. 33-38.

Jelsch, C., L. Mourey, J.M. Masson and J.P. Samama, 1993, "Crystal structure of Escherichia coli TEM1 beta-lactamase at 1.8 A resolution", *Proteins*, Vol. 16, No. 4, pp. 364-383.

Jensen, S.E., D.W. Westlake, R.J. Bowers, L. Lyubechansky and S. Wolfe, 1986, "Synthesis of benzylpenicillin by cell-free extracts from Streptomyces clavuligerus", *The Journal of Antibiotics* Vol. 39, No. 6, pp. 822-826.

Jerne, N.K., 1974, "Towards a network theory of the immune system", *Annales D Immunologie*, Vol. 125C, No. 1-2, pp. 373-389.

Kale, L. and S. Krishnan, 1993, "CHARM++: a portable concurrent object oriented system based on C++", *ACM SIGPLAN Notices*, Vol. 28, No. 10, pp. 91-108.

Kale, L., R. Skeel, M. Bhandarkar, B. R., A. Gursoy, N. Krawetz, J. Phillips, A. Shinozaki, K. Varadarajan and K. Schulten, 1999, "NAMD2: Greater Scalability for Parallel Molecular Dynamics", *Journal of Computational Physics*, Vol. 151, No.5, pp. 283-312.

Karplus, M., 2002, "Molecular dynamics simulations of biomolecules", *Nature Structural & Molecular Biology*, Vol. 35, No. 6, pp. 321-323.

Kollman, P.A., I. Massova, C. Reyes, B. Kuhn, S. Huo, L. Chong, M. Lee, T. Lee, Y. Duan, W. Wang, O. Donini, P. Cieplak, J. Srinivasan, D. Case, T. Cheatham, 2000, "Calculating structures and free energies of complex molecules: combining molecular mechanics and continuum models", *Accounts of Chemical Research*, Vol. 33, No. 12, pp. 889-897.

Kuzin, A.P., M. Nukaga, Y. Nukaga, A.M. Hujer, R.A. Bonomo and J.R. Knox, 1999, "Structure of the SHV-1 beta-lactamase", *Biochemistry*, Vol. 38, No. 18, pp. 5720-5727.

Laitinen, T., J.A. Kankare and M. Perakyla, 2004, "Free energy simulations and MM-PBSA analyses on the affinity and specificity of steroid binding to antiestradiol antibody", *Proteins*, Vol. 55, No. 1, pp. 34-43.

Laitinen, T., J. Rouvinen and M. Perakyla, 2003, "MM-PBSA free energy analysis of endo-1,4-xylanase II (XynII)-substrate complexes: binding of the reactive sugar in a skew boat and chair conformation", *Organic and Biomolecular Chemistry*, Vol. 1, No. 20, pp. 3535-3540.

Lee, K.Y., J.D. Hopkins, T.F. O'Brien and M. Syvanen, 1991, "Gly-238-Ser substitution changes the substrate specificity of the SHV class A beta-lactamases", *Proteins*, Vol. 11, No. 1, pp. 45-51.

London, N., B. Raveh, E. Cohen, G. Fathi and O. Schueler-Furman, 2011, "Rosetta FlexPepDock web server--high resolution modeling of peptide-protein interactions", *Nucleic Acids Research*, Vol. 39, No.1, pp. 249-253.

MacKerell, A.D., D. Bashford, Bellott, R. Dunbrack, J. Evanseck, S. Fisher, H. Guo, S. Ha, D. Joseph-McCarthy, L. Kuchnir, F. Lau, C. Mattos, T. Ngo, D. Nguyen, B. Prodhom, W. Reiher, B. Roux, M. Schlenkrich, J. Smith, J. Straub, M. Watanabe, J. Wiorkier-Kuczera, D. Yin, M. Karplus, 1998, "All-Atom Empirical Potential for Molecular Modeling and Dynamics Studies of Proteins†", *The Journal of Physical Chemistry B*, Vol. 102, No. 18, pp. 3586-3616.

MacKerell, A.D., Jr., N. Banavali and N. Foloppe, 2000, "Development and current status of the CHARMM force field for nucleic acids", *Biopolymers*, Vol. 56, No. 4, pp. 257-265.

Majiduddin, F.K., I.C. Materon and T.G. Palzkill, 2002, "Molecular analysis of beta-lactamase structure and function", *International Journal of Medical Microbiology*, Vol. 292, No. 2, pp. 127-137.

Matagne, A., J. Lamotte-Brasseur and J.M. Frere, 1998, "Catalytic properties of class A beta-lactamases: efficiency and diversity", *Biochemical Journal*, Vol. 330 (Pt 2), No., pp. 581-598.

Matthew, M., R.W. Hedges and J.T. Smith, 1979, "Types of beta-lactamase determined by plasmids in gram-negative bacteria", *The Journal of Bacteriology*, Vol. 138, No. 3, pp. 657-662.

Medeiros, A.A. and J. Crellin, 1997, "Comparative susceptibility of clinical isolates producing extended spectrum beta-lactamases to ceftibuten: effect of large inocula", *The Pediatric Infectious Disease Journal*, Vol. 16, No. 3, pp. S49-55.

Meroueh, S.O., J.F. Fisher, H.B. Schlegel and S. Mobashery, 2005, "Ab initio QM/MM study of class A beta-lactamase acylation: dual participation of Glu166 and Lys73 in a concerted base promotion of Ser70", *Journal of the American Chemical Society*, Vol. 127, No. 44, pp. 15397-15407.

Nordlund, K., 2007, *Maximally simplified molecular dynamics algorithm*, http://en.wikipedia.org/wiki/Molecular_dynamics.

Parker, R.H. and M. Eggleston, 1987, "Beta-lactamase inhibitors: another approach to overcoming antimicrobial resistance", *American Journal of Infection Control*, Vol. 8, No. 1, pp. 36-40.

Petrosino, J., C. Cantu, 3rd and T. Palzkill, 1998, "beta-Lactamases: protein evolution in real time", *Trends in Microbiology*, Vol. 6, No. 8, pp. 323-327.

Petrosino, J., G. Rudgers, H. Gilbert and T. Palzkill, 1999, "Contributions of aspartate 49 and phenylalanine 142 residues of a tight binding inhibitory protein of beta-lactamases", *The Journal of Biological Chemistry*, Vol. 274, No. 4, pp. 2394-2400.

Petrosino, J.F. and T. Palzkill, 1996, "Systematic mutagenesis of the active site omega loop of TEM-1 beta-lactamase", *The Journal of Bacteriology*, Vol. 178, No. 7, pp. 1821-1828.

Phichith, D., S. Bun, S. Padiolleau-Lefevre, A. Guellier, S. Banh, M. Galleni, J.M. Frere, D. Thomas, A. Friboulet and B. Avalle, 2010, "Novel peptide inhibiting both TEM-1 beta-lactamase and penicillin-binding proteins", *FEBS Journal*, Vol. 277, No. 23, pp. 4965-4972.

Phillips, J.C., R. Braun, W. Wang, J. Gumbart, E. Tajkhorshid, E. Villa, C. Chipot, R.D. Skeel, L. Kale and K. Schulten, 2005, "Scalable molecular dynamics with NAMD", *Journal of Computational Chemistry*, Vol. 26, No. 16, pp. 1781-1802.

Potapov, V., D. Reichmann, R. Abramovich, D. Filchtinski, N. Zohar, D. Ben Halevy, M. Edelman, V. Sobolev and G. Schreiber, 2008, "Computational redesign of a protein-protein interface for high affinity and binding specificity using modular architecture and naturally occurring template fragments", *Journal of Molecular Biology*, Vol. 384, No. 1, pp. 109-119.

Raveh, B., N. London and O. Schueler-Furman, 2010, "Sub-angstrom modeling of complexes between flexible peptides and globular proteins", *Proteins*, Vol. 78, No. 9, pp. 2029-2040.

Reichmann, D., M. Cohen, R. Abramovich, O. Dym, D. Lim, N.C. Strynadka and G. Schreiber, 2007, "Binding hot spots in the TEM1-BLIP interface in light of its modular architecture", *Journal of Molecular Biology*, Vol. 365, No. 3, pp. 663-679.

Reichmann, D., Y. Phillip, A. Carmi and G. Schreiber, 2008, "On the contribution of water-mediated interactions to protein-complex stability", *Biochemistry*, Vol. 47, No. 3, pp. 1051-1060.

Reichmann, D., O. Rahat, S. Albeck, R. Meged, O. Dym and G. Schreiber, 2005, "The modular architecture of protein-protein binding interfaces", *Proceedings of the National Academy of Sciences of the United States*, Vol. 102, No. 1, pp. 57-62.

Reynolds, K.A., M.S. Hanes, J.M. Thomson, A.J. Antczak, J.M. Berger, R.A. Bonomo, J.F. Kirsch and T.M. Handel, 2008, "Computational redesign of the SHV-1 beta-lactamase/beta-lactamase inhibitor protein interface", *Journal of Molecular Biology*, Vol. 382, No. 5, pp. 1265-1275.

Reynolds, K.A., J.M. Thomson, K.D. Corbett, C.R. Bethel, J.M. Berger, J.F. Kirsch, R.A. Bonomo and T.M. Handel, 2006, "Structural and computational characterization of the SHV-1 beta-lactamase-beta-lactamase inhibitor protein interface", *The Journal of Biological Chemistry*, Vol. 281, No. 36, pp. 26745-26753.

Roccatano, D., G. Sbardella, M. Aschi, G. Amicosante, C. Bossa, A. Di Nola and F. Mazza, 2005, "Dynamical aspects of TEM-1 beta-lactamase probed by molecular dynamics", *Journal of Computer-Aided Molecular Design*, Vol. 19, No. 5, pp. 329-340.

Roy, C., A. Foz, C. Segura, M. Tirado, C. Fuster and R. Reig, 1983, "Plasmid-determined beta-lactamases identified in a group of 204 ampicillin-resistant Enterobacteriaceae", *Journal of Antimicrobial Chemotherapy*, Vol. 12, No. 5, pp. 507-510.

Rudgers, G.W., W. Huang and T. Palzkill, 2001, "Binding properties of a peptide derived from beta-lactamase inhibitory protein", *Antimicrobial Agents and Chemotherapy*, Vol. 45, No. 12, pp. 3279-3286.

Ryckaert, J.-P., G. Ciccotti and H.J.C. Berendsen, 1977, "Numerical integration of the cartesian equations of motion of a system with constraints: molecular dynamics of n-alkanes", *Journal of Computational Physics*, Vol. 23, No. 3, pp. 327-341.

Sanner, M.F., A.J. Olson and J.C. Spehner, 1996, "Reduced surface: an efficient way to compute molecular surfaces", *Biopolymers*, Vol. 38, No. 3, pp. 305-320.

Savard, P.Y. and S.M. Gagne, 2006, "Backbone dynamics of TEM-1 determined by NMR: evidence for a highly ordered protein", *Biochemistry*, Vol. 45, No. 38, pp. 11414-11424.

Saves, I., O. Burlet-Schiltz, P. Swaren, F. Lefevre, J.M. Masson, J.C. Prome and J.P. Samama, 1995, "The asparagine to aspartic acid substitution at position 276 of TEM-35 and TEM-36 is involved in the beta-lactamase resistance to clavulanic acid", *The Journal of Biological Chemistry*, Vol. 270, No. 31, pp. 18240-18245.

Seeber, M., M. Cecchini, F. Rao, G. Settanni and A. Caflisch, 2007, "Wordom: a program for efficient analysis of molecular dynamics simulations", *Bioinformatics*, Vol. 23, No. 19, pp. 2625-2627.

Sitkoff, D., K.A. Sharp and B. Honig, 1994, "Correlating solvation free energies and surface tensions of hydrocarbon solutes", *Biophysical Chemistry*, Vol. 51, No. 2-3, pp. 397-403; discussion 404-399.

Strynadka, N.C., H. Adachi, S.E. Jensen, K. Johns, A. Sielecki, C. Betzel, K. Sutoh and M.N. James, 1992, "Molecular structure of the acyl-enzyme intermediate in beta-lactam hydrolysis at 1.7 A resolution", *Nature*, Vol. 359, No. 6397, pp. 700-705.

Strynadka, N.C., S.E. Jensen, P.M. Alzari and M.N. James, 1996, "A potent new mode of beta-lactamase inhibition revealed by the 1.7 A X-ray crystallographic structure of the TEM-1-BLIP complex", *Nature Structural & Molecular Biology*, Vol. 3, No. 3, pp. 290-297.

Vorontsov, II and O. Miyashita, 2011, "Crystal molecular dynamics simulations to speed up MM/PB(GB)SA evaluation of binding free energies of di-mannose deoxy analogs with P51G-m4-Cyanovirin-N", *Journal of Computational Chemistry*, Vol. 32, No. 6, pp. 1043-1053.

Wang, J., T. Palzkill and D.C. Chow, 2009, "Structural insight into the kinetics and DeltaCp of interactions between TEM-1 beta-lactamase and beta-lactamase inhibitory protein (BLIP)", *The Journal of Biological Chemistry*, Vol. 284, No. 1, pp. 595-609.

Wiedemann, B., C. Kliebe and M. Kresken, 1989, "The epidemiology of beta-lactamases", *Journal of Antimicrobial Chemotherapy*, Vol. 24, No., pp. 1-22.

Yribarren, A.S., D. Thomas, A. Friboulet and B. Avalle, 2003, "Selection of peptides inhibiting a beta-lactamase-like activity", *European Journal of Biochemistry*, Vol. 270, No. 13, pp. 2789-2795.

Zhang, Z. and T. Palzkill, 2003, "Determinants of binding affinity and specificity for the interaction of TEM-1 and SME-1 beta-lactamase with beta-lactamase inhibitory protein", *The Journal of Biological Chemistry*, Vol. 278, No. 46, pp. 45706-45712.

Zhang, Z. and T. Palzkill, 2004, "Dissecting the protein-protein interface between beta-lactamase inhibitory protein and class A beta-lactamases", *The Journal of Biological Chemistry*, Vol. 279, No. 41, pp. 42860-42866.